BOOK OF ABSTRACTS

IN²UB ANNUAL MEETING 2021

VIRTUAL MEETING
14th October 2021

Institut de Nanociència i Nanotecnologia

Universitat de Barcelona

BOOK OF ABSTRACTS

IN²UB ANNUAL MEETING

2021

VIRTUAL MEETING
14th October 2021

Editorial Board and Scientific Management: IN²UB
Graphic Design and Layout: Cris M. Idoate -- www.idoate.com --

FOREWORD

Dear researchers,

I have the honor of welcoming you to the Annual Workshop of the IN²UB, 2021.

In this booklet, you can browse through the program of this year's IN²UB workshop.

Every annual workshop is somehow unique. The current one is special because it follows a year when it was forcefully suspended. The content of the scientific program for the Workshop 2021 witnesses on the fact that despite the difficulties, the activity and dynamism of the Institute has remain intact.

Even if the incertitude forced us to maintain this workshop on-line, the amount of contributions have made it a success. With an internationally prestigious Plenary contribution, four ART Lectures, six high-level selected Oral Presentations (among many submissions) and more than fifty papers in Poster format, we are happy to present a top scientific program reflecting on the richness and diversity of research at IN²UB.

I personally thank all of you that have enthusiastically contributed to make this event a great success.

I encourage all of you to meet in this virtual celebration, in the hope that next year we will recover the personal contact.

With my best regards,

Guillem Aromí
Director of the Institute of Nanoscience and Nanotechnology
of the University of Barcelona (IN²UB)

CONTENTS INDEX

NanoMagnetics

NanoPhotoElectro

NanosMat

NanoEnergy

PROGRAM

9.30.h - 9.45h. **ENTERING ZOOM**

9.45h. – 10.00h. **WELCOME**
G. Aromí, Director of Institute of Nanoscience and Nanotechnology (IN²UB) / Department of Inorganic and Organic Chemistry, Faculty of Chemistry, Universitat de Barcelona (UB).

SESSION I

Chaired by: *M. Duocastella*, IN²UB, Department Applied Physics, Faculty of Physics (UB).

10.00h. - 10.25h. **2019-ART GRANTEE (ART1)**
LASER ACTIVATION OF SMART NANOSYSTEMS FOR PHOTOTHERMAL THERAPIES
J. M. Fernández-Pradas, IN²UB, Department Applied Physics, Faculty of Physics (UB).

10.25h. - 10.50h. **2019-ART GRANTEE (ART2)**
MULTICALORIC EFFECTS IN FERROELECTRIC PLASTIC CRYSTALS
M. Romanini, IN²UB, Department Condensed Matter Physics, Faculty of Physics (UB).

10.50h. – 11.10h. **ORAL (O1)**
SYNTHESIS OF GRAPHENE/ TRANSITION METAL CARBIDES HETEROSTRUCTURES AND ELECTROCATALYTIC PROPERTIES
S. Chaitoglou. IN²UB, Department Applied Physics, Faculty of Physics (UB).

11.10h. - 11.50h. **POSTER SESSION**
Connect to each zoom link provided at the end of each poster title to visit the poster and meet the author.

SESSION II

Chaired by: *M. Estrader*. IN²UB, Department of Inorganic and Organic Chemistry, Faculty of Chemistry (UB).

11:50h. - 12:50h. **PLENARY LECTURE (PL)**
BIOLOGICAL SHAPES EMERGING FROM PHYSICS AT THE NANOSCALE
S. Contera, Professor of Biological Physics, University of Oxford.

12:50h. - 13:10h. **ORAL (O2)**
SELECTIVE CONTROL OVER THE SIZE, MORPHOLOGY, AND OXIDATION STATE OF IRON OXIDE NANOPARTICLES BY TUNING THE REAGENT AMOUNTS
M. Escoda-Torroella. IN²UB, Department Condensed Matter Physics, Faculty Physics (UB).

13:10h. - 13:30h. **ORAL (O3)**
TOWARDS ANGIOGENESIS-ON-A-CHIP
A. Noguera. IN²UB, Department Electronics and Biomedical Engineering, Faculty Physics (UB).

13:30h. - 15:00h. **BREAK**

SESSION III

Chaired by: *M.A. Busquets*. IN²UB, Department of Pharmacy and Pharmaceutical Technology and Physical-Chemistry, Faculty of Pharmacy and Food Sciences (UB).

15:00h. - 15:25h. **2020-ART GRANTEE (ART3)**
MULTITARGET APPROACH TO DEVELOP ANTIPRION DRUGS FOR TRANSMISSIBLE SPONGIFORM ENCEPHALOPATHIES (TSES)
A. Espargaró. IN²UB, Department of Pharmacy and Pharmaceutical Technology and Physical-Chemistry, Faculty of Pharmacy and Food Sciences (UB).

15:25h. - 16:05h. **POSTER SESSION**
Connect to each zoom link provided at the end of each poster title to visit the poster and meet the author.

SESSION IV

Chaired by: *G. Franzese*. IN²UB, Department Condensed Matter Physics, Faculty Physics (UB).

16:05h. - 16:25h. **ORAL (O4)**
COARSE GRAINED MODEL FOR WATER AND WATER-PROTEIN INTERFACES
L. E. Coronas. IN²UB, Department Condensed Matter Physics, Faculty of Physics (UB).

16:25h. - 16:50h. **ORAL (O5)**
DOPY: A GEMINI DIOLEYLBISPYRIDINIUM BASED AMPHIPHILE FOR EFFICIENT TRANSFECTION OF OLIGONUCLEOTIDES IN MAMMALIAN CELLS
D. Limón. IN²UB, Department of Pharmacology, Toxicology and Therapeutic Chemistry, Faculty of Pharmacy and Food Sciences (UB).

16:50h. - 17:15h. **2020-ART GRANTEE (ART4).**
SPATIAL MAPPING OF THE COLLAGEN DISTRIBUTION IN HUMAN AND MOUSE TISSUES BY FORCE VOLUME ATOMIC FORCE MICROSCOPY.
A. Caló. IN²UB, Department Electronics and Biomedical Engineering, Faculty of Physics (UB) and Molecular Cytology Core Facility, Memorial Sloan Kettering Cancer Center (NY).

17:15h. - 17:35h. **ORAL (O6)**
DEVELOPMENT OF METAL-ORGANIC FRAMEWORK (MOF) MATERIALS AS ROOM-TEMPERATURE CHEMIRESISTORS FOR GAS SENSING
I. Fort-Grandas, IN²UB, Department of Electronic and Biomedical Engineering, Faculty of Physics (UB).

17:35h. - 17:45h. **CLOSING REMARKS**
A. Romano, Secretary of IN²UB, Department of Electronic and Biomedical Engineering, Faculty of Physics (UB).

PLENARY LECTURE

PL
BIOLOGICAL SHAPES EMERGING FROM PHYSICS AT THE NANOSCALE

sonia.antoranzcontera@physics.ox.ac.uk

Sonia Contera
Clarendon Laboratory, Physics Department, University of Oxford, Parks Road, OX1 3PU Oxford, UK.

In the last 30 years we have witnessed the progressive integration of physics and biology facilitated by nanotechnology, which is leading to a revolution in computing, electronics, materials and medicine. If one looks at the history of physics in the previous century this is far from surprising. The work of Turing, Goedel, von Neumann, Onsager, Schroedinger, Shannon, de Gennes, Anderson etc. demonstrates that physicists' (and mathematician's) minds have always been occupied by the fundamental enquiry into what makes humans able to understand the universe. Physicists have always wondered what is life, what is information, why does entropy decrease in living organisms, why can we think?

The answer of these questions needs to address one central topic: what is a biological shape? The dynamic shapes of biological tissues emerge from a complex interplay of physics, chemistry and genetics (evolution), which determines--at each temporal and spatial scale--the mechanical properties that eventually form the smart structures of living organisms, able to adapt to their environments in order to survive. Shape and mechanical stability of living organisms rely on precise control in time and space of growth, which is achieved by dynamically tuning the mechanical (viscous and elastic) properties of their hierarchically built structures from the nanometer up. The nanometer scale is central, because biomolecules are nanostructures, and hence measuring and understanding physics of biological systems at the nanoscale becomes crucial for biology and physics. I use one of the main tools of nanotechnology, the atomic force microscope (AFM) to extract the physics underlying the emergence of biological shapes. It is now well-established that cellular behaviour (including stem cell differentiation) crucially depends on the mechanical properties of the cells' environment. Much attention has been directed towards the importance of the stiffness of the natural (extracellular matrix, ECM) or artificial matrices where cells grow, with the purpose of either understanding mechanotransduction, or controlling the behaviour of cells in medical applications such as tissue engineering. While stiffness (i.e. the capacity of a material to elastically store mechanical energy) has been the focus of most experimental research, neither cells nor matrices are elastic. Biological systems dissipate energy (i.e. they are viscous) and hence they do not respond to mechanical deformations instantaneously (like an ideal Hookean spring), but present different time responses at different spatial scales that characterise their responses to external stimuli. Measuring viscoelasticity (especially at the nanoscale) has remained experimentally challenging [1,2]. In my talk I will present AFM-based techniques to measure and map the viscoelasticity of living tissues, cells, membranes, collagen, ECMs, and tissue engineering matrices across the spatial and temporal scales, and chirp-based spectroscopic techniques to assess viscoelasticity from Hz to 100s kHz at the nano and micro scale developed in my lab.

Our results have uncovered that extracellular matrices of both living plants and tumours present an almost perfect linear viscoelastic behaviour that is key to understand their growth and shape. I will present our work showing how the growth and shape of the roots, leaves and hypocotyl of living Arabidopsis thaliana living plants are related to the nanoscale viscoelasticity of plant cell walls at the time scales probed by multifrequency AFM and how this can be understood using concepts and theories from non-equilibrium thermodynamics.

I will also show how this knowledge can be used to create "smart" bioinspired materials, which progressively will harness biological properties, such as adaptation, and eventually learning [3].

References
1. *Multifrequency AFM reveals lipid membrane mechanical properties and the effect of cholesterol in modulating viscoelasticity.* 2019. Z Al-Rekabi, S Contera; Proceedings of the National Academy of Sciences 115 (11), 2658-2663.
2. *Mapping nanomechanical properties of live cells using multi-harmonic atomic force microscopy.* 2011. A Raman, S Trigueros, A Cartagena, APZ Stevenson, M Susilo, E Nauman, S Contera. Nature Nanotechnology 6 (12), 809.
3 *Nano comes to life: How nanotechnology is transforming medicine and the future of biology.* Sonia Contera, Princeton University Press 2019.

ART
(AJUT A LA RECERCA TRANSVERSAL)

ART 2019 CALL

ART1
LASER ACTIVATION OF SMART NANOSYSTEMS FOR PHOTOTHERMAL THERAPIES

jmfernandez@ub.edu

J. M. Fernández-Pradas[1], J. Estelrich[2], M. A. Busquets[2], M.C. Moran[3], P. Serra[1]

[1] Departament de Física Aplicada, Universitat de Barcelona, Martí i Franquès 1, 08028 Barcelona.
[2] Departament de Farmàcia i Tecnologia Farmacéutica, i Fisicoquímica, Universitat de Barcelona, Avda. Joan XXIII, 27-31, 08028 Barcelona.
[3] Departament de Bioquímica i Fisiologia, Universitat de Barcelona, Avda. Joan XXIII, 27-31, 08028 Barcelona.

The work here presented corresponds to the results of a project granted in the ART 2019 call. The project explores the use of new composite nanoparticles that can efficiently convert laser radiation into heat in tissues. The final objective is to use them in a therapeutic strategy based on targeting the nanoparticles on non-healthy tissues and then focus laser light in them for thermally destroying the tumor with minimum side effects. Nanoparticles of magnetic iron oxide (ION), Prussian Blue (PrBN) and composite nanosystems of both compounds have been synthesized by chemical precipitation methods. The photothermal effect of nanoparticle suspensions at different concentrations was evaluated under laser radiation with a Nd:YAG laser source at 1064 nm wavelength and powers below 1.3 W. Thus, photothermal activity of the selected nanoparticles is studied in the second biological window (1000-1300 nm) where absorption of healthy tissues is low, and radiation benefits of less scattering, larger penetration depth and higher permissible doses than in the first window (700-950 nm) [1]. Results show that ION have better photothermal properties than PrBN at the selected wavelength. At maximum efficiency conditions temperature is increased up to 30oC and nanoparticles keep their photothermal activity after several irradiation cycles even at the highest dose (Figure 1) [2].

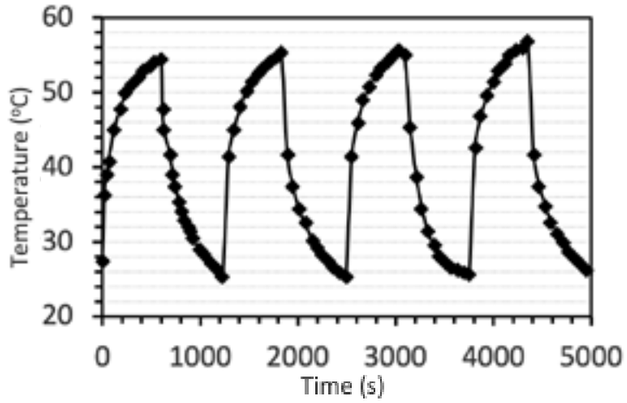

Figure1. *Plot of ION suspension temperature during on/off cycles at 1.3 W laser power.*

References
1. Cao, Y.; Wu, T.; Zhang, K.; *et al.*, ACS Nano 13 (2019) 1499-1510.
2. Busquets, M. A.; Fernández-Pradas, J. M.; Serra, P.; Estelrich, J.; Molecules 25 (2020) 5315.

ART2
MULTICALORIC EFFECTS IN FERROELECTRIC PLASTIC CRYSTALS

mromanini@ub.edu

M. Romanini[1], L. Mañosa[1], A. Planes[1], G. Aromí[2], D. Aguilà[2]

[1] Dept. Física de la Matèria Condensada, Universitat de Barcelona, Spain.
[2] Departament de Química Inorgànica i Orgànica, Universitat de Barcelona, Barcelona, Spain.

The need to replace the environmentally harmful gases used in refrigeration devices (chlorofluorocarbons, hydrofluorocarbons) has spurred intense research activity to replace these refrigerants with solid-state materials that display first order phase transitions upon application of pressure, whose latent heat and temperature change upon transition can be exploited for e.g. cooling applications without the risk of leaks as in the case of gases. The change in temperature of a material when subject to a sudden change of pressure or other external field is known as the caloric effect (barocaloric in the case of an applied pressure, electrocaloric in the case of an applied electric bias) and it is related to the change in the material's entropy when the external field is isothermally modified. There exist classes of solid state materials that exhibit a large field-driven thermal response in the vicinity of first-order phase transitions [1-4] that take place near ambient conditions, and can thus in principle be exploited in devices. The recently reported ferroelectric molecular plastic crystals, which are molecular solids displaying a plastic crystal (PC) phase at high temperature and a ferroelectric phase at low temperature [5-8], are expected to display giant barocaloric effects and possibly also electrocaloric effects, because the transition entropy is particularly large due to the dynamic disorder of the plastic crystalline phase, in which the molecules rotate almost freely about their centres of mass. These materials may represent potential non-toxic and more cost-efficient alternatives to common inorganic oxides for a wide range of applications such as solid-state refrigerants, memory elements, capacitors and sensors [9]. In a collaborative project between the Grup Transicions de Fase en Materials of the Department of Condensed Matter Physics and the Grup de Magnetisme i Molecules Funcionals (GMMF) of the Department of Inorganic and Organic Chemistry of the UB, we have synthetized and characterized two recently reported ferroelectric PC, namely quinuclidinium perrhenate [HQuin_ReO4] [8] and tetramethylammonium tetrachloroferrate [Me4N_FeCl4] [5]. I will present the results I obtained from electrocaloric and barocaloric measurements together with the characterization measurements such as DSC and X-ray powder diffraction. Dielectric spectroscopy measurements as a function of temperature have also be performed on the two substances, to elucidate whether molecular relaxation dynamics were present in the various phases of the synthesized materials.

References
1. E. Stern-Taulats *et al.*, MRS Bulletin 43, 295-299 (2018).
2. Mañosa L. and Planes A., Adv. Mater. 29, 1603607 (2017).
3. Aznar A. *et al.*, Nat. Comm. 8, 1-6 (2017).
4. Aznar A. *et al.*, Phys. Rev. Mat. 3, 044406 (2019).
5. Harada J. *et al.*, J. Am. Chem. Soc. 140, 346 (2018).
6. Lu S. *et al.*, Cryst. Eng. Comm. 20, 454 (2018).
7. Xu W. *et al.*, Chem. Comm. 54, 3347 (2018).
8. Harada J. *et al.*, Nat. Chem. 8, 946 (2016).
9. Harada J. *et al.*, J. Am. Chem. Soc. 141, 9349 (2019).

ART 2020 CALL

ART3
MULTITARGET APPROACH TO DEVELOP ANTIPRION DRUGS FOR TRANSMISSIBLE SPONGIFORM ENCEPHALOPATHIES (TSES)

aespargaro@ub.edu

A. Espargaró[2,4], A. B. Caballero[1,2], P. Gamez[1,2,3], R. Sabaté[2,4]

[1] NanoBIC, Department of Inorganic and Organic Chemistry, Faculty of Chemistry, University of Barcelona, Martí i Franquès, 1-11, 08028 Barcelona, Catalonia, Spain.
[2] Institute of Nanoscience and Nanotechnology (IN²UB), University of Barcelona, 08028 Barcelona, Catalonia, Spain.
[3] Catalan Institution for Research and Advanced Studies, Passeig Lluís Companys 23, 08010 Barcelona, Catalonia, Spain.
[4] Department of Pharmacy and Pharmaceutical Technology and Physical-Chemistry, Faculty of Pharmacy and Food Sciences, University of Barcelona, Avda. Joan XXIII, 27-31 Barcelona, Catalonia, Spain.

Since the first observation of PrPC as a copper-binding protein, many attempts have been made to understand the role of metal ions in both PrPC physiology as well as in prion pathogenesis. Interestingly, preliminary computational studies using human PrP and vole PrP suggest the presence of a druggable region around His187 residue, a copper-binding region in the globular domain. Since TSEs are linked to deposition of PrPSc accompanied by metal dyshomeostasis, wherein copper concentration could be a determinant factor, we propose the application of conceptual and experimental interdisciplinary approaches in order to identify anti-TSE drugs able to act stabilizing the PrPC structure, disfavouring the amyloid conformation and PrPSc formation, as well as reestablishing metal homeostasis. Thus, the ultimate aim of the project is to develop a new concept of anti-prion drugs that effectively cure and/or reduce the prevalence of these pernicious and fatal diseases.

ART4
SPATIAL MAPPING OF THE COLLAGEN DISTRIBUTION IN HUMAN AND MOUSE TISSUES BY FORCE VOLUME ATOMIC FORCE MICROSCOPY

annalisa.calo@ub.edu

A. Calò[1,2], Y. Romin[1], R. Srouji[1], C. P. Zambirinis[1], N. Fan[1], A. Santella[1], E. Feng[1], S. Fujisawa[1], M. Turkekul[1], S. Huang[1], A. L. Simpson[1], M. D'Angelica[1], W. R. Jarnagin[1], K. Manova-Todorova[1]

[1] Molecular Cytology Core Facility, Memorial Sloan Kettering Cancer Center, 417E 68th St, New York, NY 10065, USA.
[2] Physics Faculty, University of Barcelona (UB), Carrer de Martí i Franquès 111, 08028 Barcelona, Spain.
[3] Hepatopancreatobiliary Service, Department of Surgery, Memorial Sloan Kettering Cancer Center, 1275 York Ave, New York, NY 10065, USA.
[4] Washington University School of Medicine, 660 S. Euclid Ave, St. Louis, MO 63110, USA.
[5] Department of Surgery, Warren Alpert Medical School of Brown University, 593 Eddy street, APC4, Providence, RI 02903, USA.
[6] School of Computing, Queen's University, 557 Goodwin Hall, Kingston, ON K7L 2N8, Canada

Changes in the elastic properties of living tissues during normal development and in pathological processes are often due to modifications of the collagen component of the extracellular matrix at various length scales. Force volume AFM can precisely capture the mechanical properties of biological samples with force sensitivity and spatial resolution. The integration of AFM data with data of the molecular composition contributes to understanding the interplay between tissue biochemistry, organization and function. The detection of micrometer-size, heterogeneous domains at different elastic moduli in tissue sections by AFM has remained elusive so far, due to the lack of correlations with histological, optical and biochemical assessments. In this work, force volume AFM is used to identify collagen-enriched domains, naturally present in human and mouse tissues, by their elastic modulus. Collagen identification is obtained in a robust way and affordable timescales, through an optimal design of the sample preparation method and AFM parameters for faster scan with micrometer resolution. The choice of a separate reference sample stained for collagen allows correlating elastic modulus with collagen amount and position with high statistical significance. The proposed preparation method ensures safe handling of the tissue sections guarantees the preservation of their micromechanical characteristics over time and makes it much easier to perform correlation experiments with different biomarkers independently.

References
1. Scientific Reports **volume 10**, Article number: 15664 (2020) https://doi.org/10.1038/s41598-020-72564-9

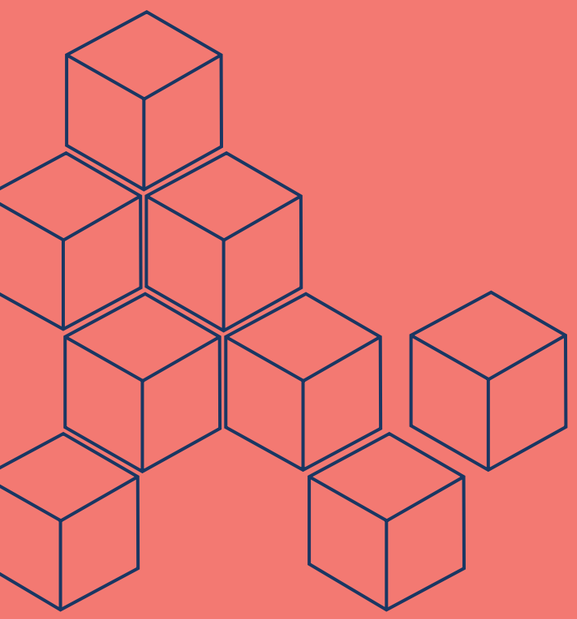

ORAL PRESENTATIONS

O1
SYNTHESIS OF GRAPHENE/ TRANSITION METAL CARBIDES HETEROSTRUCTURES AND ELECTROCATALYTIC PROPERTIES

stefanoschaitoglou@ub.edu

S. Chaitoglou[1,2], T. Giannakopoulou[1], D. Tsoutsou[1], A. Vavouliotis[3], A. Dimoulas[1]

[1] National Centre for Scientific Research "Demokritos," 15310 Athens, Greece.
[2] Departament de Física Aplicada, Universitat de Barcelona, C/Martí i Franquès 1, 08028 Barcelona, Spain.
[3] Adamant Composites Ltd, Agias Lavras & Stadiou Str., Platani-Patras, 26504, Greece.

Transition metal carbides have attracted significant attention in electrocatalysis applications, especially as electrodes in hydrogen evolution reaction (HER). In this talk, we will present results considering the controlled synthesis of ultrathin Mo2C films and graphene/Mo2C vertical heterostructures, on liquid catalysts via chemical vapor deposition. We demonstrate experimental results on the role of graphene as a diffusion barrier, resulting in the growth of Mo2C crystals with a smaller size and higher nucleation density [1]. We use Cu-based alloys, like Cu-Sn, as growth substrates, which enable the growth in reduced temperatures, with respect to pure Cu. This alloy has a lower melting point, which is an obligatory condition to enable Mo diffusion. Moreover, we present results on the enhanced HER activity of the graphene/Mo2C compounds, thanks to graphene's contribution to faster charge kinetics [2]. Then, we discuss on the increased electrocatalytic performance of the heterostructure when we apply a "flipped" transfer method which permits to reverse the vertical order of the heterostructure, allowing Mo2C to stand on the graphene and preventing the function of the latest as an electrochemical barrier [3]. Finally, we demonstrate the CVD synthesis of Mo2C films through chemical conversion of Mo foil surface, in a Cu vapor-enriched atmosphere [4].

References
1. S. Chaitoglou *et al.* Journal of Crystal Growth 495 (2018) 46–53
2. S. Chaitoglou *et al.* Nanotechnology 30 (2019) 415404
3. S. Chaitoglou *et al.* Nanotechnology 30 (2019) 125401
4. S. Chaitoglou *et al.* Appl. Surf. Sci. 510 (2020) 145516

O2
SELECTIVE CONTROL OVER THE SIZE, MORPHOLOGY, AND OXIDATION STATE OF IRON OXIDE NANOPARTICLES BY TUNING THE REAGENT AMOUNTS

mariona.escoda@ub.edu

M. Escoda-Torroella[1,2,*], C. Moya[2,3], A. Fraile Rodríguez[1,2], X. Batlle[1,2], A. Labarta[1,2]

[1] Departament de Física de la Matèria Condensada, Martí i Franquès 1, 08028 Barcelona, Spain.
[2] Institut de Nanociència i Nanotecnologia, Universitat de Barcelona, Martí i Franquès 1, 08028 Barcelona, Spain.
[3] Université libre de Bruxelles (ULB), Engineering of Molecular Nanosystems, 50 Avenue F.D. Roosevelt, 1050 Bruxelles, Belgium.

Iron oxide nanoparticles (NPs) are versatile building blocks in a variety of biomedical and environmental applications due to their good magnetic performance, ease of production and functionalization by chemical routes, and low toxicity. However, controlling the electronic and magnetic properties of iron oxide NPs remain a challenge because of their crucial dependence on composition, structure, surface chemistry, and interparticle interactions.[1,2]

In this framework, we studied the effect of the amount of both 1,2-hexadecanediol and the solvent 1-octadecene on the thermal decomposition method with iron (III) acetylacetonate. On the one hand, low amounts of either of the two reagents result in large NPs containing both Fe3O4 and FeO phases with high values of the reaction yield. On the other hand, above certain amounts of the reagents the NPs are single-phase, single-crystal Fe3O4 NPs with diameters below 10 nm, but with reaction yields slightly smaller. The hysteresis loops at room temperature for the small NPs showed the typical features of superparamagnetism: values of the saturation magnetization close to that of the bulk magnetite with no coercive field. On the contrary, larger NPs showed ferrimagnetic behavior with reduced values of the saturation magnetization, as well as shifted hysteresis loops at 5 K after field cooling the sample under 1 T. The zero-field-cool field-cool curves below 200 K for the small NPs showed a peak below room temperature corresponding to the blocking temperature, while those curves for the larger particles displayed two peaks at higher temperatures associated with the Verwey and Neel transitions of magnetite and wüstite phases, respectively. The latter was correlated with the biphasic nature of the large NPs. With this accurate monitoring of the reaction conditions we have added an extra level of optimization to the synthesis of these NPs, allowing us to tune the properties of each sample of iron oxide NPs to its specific application. [3]

The work was supported by Spanish MCIU and AEI (MAT2015-68772-P; PGC2018-097789-B-I00) and European Union FEDER funds. M.E-T. acknowledges Spanish MCIU for BES-2016-077527.

References
1. Rodríguez, A. F. *et al.* J. Mater. Chem. C **6**, 875–882 (2018).
2. Moya, C. *et al.* Phys. Chem. Chem. Phys. **17**, 13143–13149 (2015).
3. Escoda-Torroella, M. *et al.* Langmuir **37**, 35–45 (2021).

O3
TOWARDS ANGIOGENESIS-ON-A-CHIP

anoguemo21@alumnes.ub.edu

A. Noguera -Monteagudo[1,2], A. Lopez-Canosa[3,4], J. Ferrer[2,5,6], P. Barcelò[7], E. Xuriguera[7], E. Engel[8,3,4], A. Hernandez-Machado[2,5,6], O. Castaño[1,2,3,4]

[1] Electronics and Biomedical Engineering, Universitat de Barcelona (UB), 08028 Barcelona, Spain.
[2] Institute of Nanoscience and Nanotechnology, Universitat de Barcelona (UB), 08028 Barcelona, Spain.
[3] Biomaterials for Regenerative Therapies, Institute for Bioengineering of Catalonia (IBEC), The Barcelona Institute of Science and Technology (BIST), Baldiri i Reixac 10-12, 08028 Barcelona, Spain.
[4] CIBER en Bioingeniería, Biomateriales y Nanomedicina (CIBER-BBN) 28029 Madrid, Spain.
[5] Condensed Matter Physics, University of Barcelona (UB), 08028 Barcelona, Spain
[6] Centre de Recerca Matemàtica (CRM), 08193 Bellaterra, Spain.
[7] Material Science and Physical chemistry, University of Barcelona (UB), 08028 Barcelona, Spain.
[8] IMEM-BRT Group, Dept. Materials Science and Engineering, EEBE, Technical University of Catalonia (UPC), 08019 Barcelona, Spain.

The process of new blood vessel growth from existing ones is called angiogenesis. This process is essential for organ growth and repair and is very important as it is associated with a variety of health problems such as malignant disorders, inflammatory problems, ischemia, infections, and immune diseases. Currently, *in vitro* models of angiogenesis are a good option to obtain information on how this process is regulated. Advances in microfluidic technology have enabled the replication of the microenvironment *in vitro* to study the mechanism of angiogenesis. This work investigates the design and operation of a microfluidic chip to study the angiogenesis involving isolated endothelial cells. In this direction, a characterization of the used extracellular matrix in this work (fibrin hydrogel) was performed, both physically, by rheology; and micro& nano structurally, by staining the hydrogel with a covalently bound fluorophore for subsequent observation in a confocal microscope. To study the angiogenesis process under different microenvironmental conditions, the migration of endothelial cells was compared with different concentration gradients of the angiogenic signal like VEGF. In the results obtained, it was found that through the two methods used it is possible to characterize the extracellular matrix in the condition as in the cells culture at the nanoscale, which provides a piece of very interesting information. Moreover, by characterizing and controlling the physical and structural parameters of the extracellular matrix, it is possible to study the influence of these properties on angiogenesis. In terms of cellular results, it was observed that the presented design allows the generation of an angiogenic factor gradient that stimulates cell migration. In some initial experiments performed, it was observed that increasing the concentration of VEGF increases cell migration. Although more work is still needed to explore all the possibilities of the presented design for the study of angiogenesis, it has been shown that this design allows the replication of functional microenvironments with great control, allowing the study of different individual parameters in a way that only in vivo studies could do so far.

References
1. S. Chaitoglou *et al.* Journal of Crystal Growth 495 (2018) 46–53
2. S. Chaitoglou *et al.* Nanotechnology 30 (2019) 415404
3. S. Chaitoglou *et al.* Nanotechnology 30 (2019) 125401
4. S. Chaitoglou *et al.* Appl. Surf. Sci. 510 (2020) 145516

O4
COARSE GRAINED MODEL FOR WATER AND WATER-PROTEIN INTERFACES

lcoronas@ub.edu

L. E. Coronas[1,2], V. Bianco[3], O. Vilanova[1,2], G. Franzese[1,2]

[1] Departament de Física de la Matèria Condensada, Universitat de Barcelona. C. Martí i Franquès 1, 08028 Barcelona (Spain).
[2] Institute of Nanoscience and Nanotechnology (IN2UB), Universitat de Barcelona. C. Martí i Franquès 1, 08028 Barcelona (Spain).
[3] Facultad de Ciencias Químicas, Departamento de Química Física, Universidad Complutense de Madrid, Plaza de las Ciencias, 28040 Madrid (Spain).

All-atom simulations of large-size systems including proteins and explicit water come at a great computational cost. To overcome this problem, coarse-grained models aim to represent the system in a simplified manner but keeping the essential properties that are relevant for its behavior. In this talk, we present a coarse-grained model for bulk and nanoconfined water with many-body interactions, originally introduced by Franzese and Stanley (FS) [1,2]. The model is analytically tractable [3] and can be simulated by computationally-efficient (parallel) cluster Monte Carlo [4]. It allows us to equilibrate large systems at extremely low temperatures T in a wide range of pressures P [5]. Moreover, it has been extended to include proteins [6].

The phase diagram of the FS model reproduces, at least qualitatively, the experimental water phase diagram, both in confinement and in bulk [7], a prerequisite for using it as a proper solvent in protein solutions. Our results compare well with atomistic simulations and allows the analytic and numerical study of the low-density-liquid--high-density-liquid phase transition ending in a liquid-liquid critical point. They clarify fundamental properties of hydration and bulk water and are potentially useful for better understanding the effects of water thermodynamic properties on nano-bio-interactions among proteins (folding [8], aggregation [9], and design [10] in bulk, or near interfaces [11]) and other species or interfaces.

References
1. G. Franzese, and H. E. Stanley, *Liquid-liquid critical point in a Hamiltonian model for water: analytic solution*, J. Phys.: Condens. Matter **14**, pp. 2201-2209 (2002).
2. L. E. Coronas, O. Vilanova, V. Bianco, F. de los Santos, and G. Franzese, *The Franzese-Stanley Coarse Grained Model for Hydration Water*, arXiv:2004.03646 (2020).
3. G. Franzese, and H. E. Stanley, *The Widom Line of Supercooled Water*, J. Phys.: Condens. Matter **19**, p. 205126 (2007).
4. V. Bianco, and G. Franzese, *Hydrogen bond correlated percolation in a supercooled water monolayer as a hallmark of the critical region,* J. Mol. Liq. **285**, pp- 727-739 (2019).
5. V. Bianco, and G. Franzese, *Critical behavior of a water monolayer under hydrophobic confinement*, Sci. Rep. **4**, p. 4440 (2014).
6. V. Bianco, and G. Franzese, *Contribution of Water to Pressure and Cold Denaturation of Proteins*, Phys. Rev. Lett. **115**, p. 108101 (2015).
7. L. E. Coronas, V. Bianco, A. Zantop, and G. Franzese, *Liquid-Liquid Critical Point in 3D Many-Body Water Model*, arXiv:1610.00419 (2016).
8. V. Bianco, N. Pagès Gelabert, I. Coluzza, and G. Franzese, *How the stability of a folded protein depends on interfacial water properties and residue-residue interactions*, J. Mol. Liq. **245**, pp. 129-139 (2017)
9. V. Bianco, G. Franzese, and I. Coluzza, *In silico evidence that protein unfolding is as a precursor of the protein aggregation*, ChemPhysChem **21**, pp. 377-384 (2020)
10. V. Bianco, G. Franzese, C. Dellago, and I. Coluzza, *Role of Water in the Selection of Stable Proteins at Ambient and Extreme Thermodynamic Conditions*, Phys. Rev. X **7**, p. 021047 (2017).
11. D. March, V. Bianco, and G. Franzese, *Protein Unfolding and Aggregation near a Hydrophobic Interface*, Polymers **13**, p. 156 (2021)

O5
DOPY: A GEMINI DIOLEYLBISPYRIDINIUM BASED AMPHIPHILE FOR EFFICIENT TRANSFECTION OF OLIGONUCLEOTIDES IN MAMMALIAN CELLS

davidlimon@ub.edu

E. Aubets[1,4], R. Griera[2], A. J. Felix[1,4], G. Rigol[1], C. Sikorski[1], D. Limón[2,4], Chiara Mastrorosa[1], M. A. Busquets[3,4], Ll. Pérez-García[2,4], V. Noé[1,4], C. J. Ciudad[1,4]

[1] Department of Biochemistry and Physiology, School of Pharmacy and Food Sciences, University of Barcelona, 08028 Barcelona, Spain.
[2] Department of Pharmacology, Toxicology and Therapeutic Chemistry, School of Pharmacy and Food Sciences, University of Barcelona, 08028 Barcelona, Spain.
[3] Department of Pharmacy and Pharmaceutical Technology and Physical, Chemistry. School of Pharmacy and Food Sciences, University of Barcelona, 08028 Barcelona, Spain.
[4] Nanoscience and Nanotechnology Institute, IN²UB, University of Barcelona, Spain.

Nucleic acids therapeutics provide a selective and promising alternative to traditional treatments for multiple genetic diseases. A major obstacle is the development of safe and efficient delivery systems. We have synthesized a new cationic gemini amphiphile 1,3-bis[(4-oleyl-1-pyridinio)methyl]benzene dibromide (DOPY) and its transfection efficiency has been evaluated using PolyPurine Reverse Hoogsteen hairpins (PPRHs), a nucleic acid tool for gene silencing and gene repair developed in our laboratory. The interaction of DOPY with PPRHs was confirmed by gel retardation assays. Incubation of increasing amounts of DOPY with 150 ng of the PPRH resulted in a progressive disappearance of the band corresponding to the PPRH signal compared to the PPRH alone, thus demonstrating the formation of DOPY/PPRH complexes. We also demonstrated the prominent internalization of PPRHs using DOPY compared to the validated transfection agent N-[1-(2,3-Dioleoyloxy)propyl]-N,N,N-trimethylammonium methylsulfate (DOTAP) in SH-SY5Y, PC-3 and DF42 cells. In the case of hard-to-transfect SH-SY5Y cells, the percentages of fluorescent cells were 87 % using DOTAP and 71 % using DOPY, but the fluorescence mean was 4.3 times higher in DOPY transfections than that of DOTAP transfections.

We also confirmed that clathrin-mediated endocytosis was involved in DOPY/PPRHs complexes internalization. Regarding gene silencing, a specific PPRH against the survivin gene, HpsPr-C, delivered with DOPY decreased survivin protein levels and cell viability more effectively than with DOTAP in both SH-SY5Y and PC-3 cells. PC-3 cells transfected with DOTAP/HpsPr-C complexes showed a decrease in cell viability of 90 %. Similarly, cells transfected using 0.5 µg and 1 µg of DOPY showed a reduction in cell viability of 97 % and 99 %, respectively. However, in the case of SH-SY5Y cells, incubations with DOTAP/HpsPr-C complexes at standard conditions did not reduce cell viability, whereas cells treated with DOPY/HpsPr-C complexes showed a decrease in cell viability of 36 % and 84 % using 1 µg and 2 µg of DOPY, respectively. We also validate the applicability of DOPY in gene repair approaches by correcting a point mutation in the endogenous locus of the dhfr gene in DF42 cells using repair-PPRHs. DOPY transfections led to repair frequencies of 0.4 %, which represented a 2-fold increase compared to calcium phosphate frequencies. All these results indicate both an efficient entry and release of PPRHs at the intracellular level. Therefore, DOPY can be considered as a new lipid-based vehicle for the delivery of therapeutic oligonucleotides.

Acknowledgements

Work supported by grant RTI2018-093901-B-I00 from MICINN (Spain), TEC2017-85059-C3-2-R, and by Ajut a la Recerca Transversal 2018 from IN²UB. Groups holding the Quality Mention from Generalitat de Catalunya 2017-SGR-94 and 2017-SGR-1277.

References
1. Aubets *et al.* Eur J Pharm Biopharm. 2021 Aug;165:279-292.

O6
DEVELOPMENT OF METAL-ORGANIC FRAMEWORK (MOF) MATERIALS AS ROOM-TEMPERATURE CHEMIRESISTORS FOR GAS SENSING

ignfortgra_9@ub.edu

I. Fort Grandas[1,2], A. Neyra-Perez[2], A. Rodriguez-Iglesias[1], M. Moreno[1,2], Paolo Pellegrino[1,2], D. Sainz[2,3], A. Romano-Rodriguez[1,2]

[1] Electronic and Biomedical Engineering, Universitat de Barcelona, 08028, Spain.
[2] Institute of Nanoscience and Nanotechnology (IN²UB), Universitat de Barcelona, 08028, Spain.
[3] Inorganic and Organic Chemistry, Universitat de Barcelona, 08028, Spain.

The direction of sustainability and overall health concerns in which society is moving towards has brought an increasing demand of reliable and affordable new materials-based systems capable of monitoring key gas compounds of such concerns. Currently, sensitive and selective gas monitoring systems are complex, bulky and expensive and, thus, there are few of them and bound to fixed locations. To complement these systems, advanced, miniaturised, low cost and low power consuming gas sensing devices are required. Among them, sensors based on high conductivity nanostructured metal-organic frameworks (MOFs) materials, which present high porosity and specific surface area, are very interesting candidates[1].

In this work, highly conjugated triphenylene-derived ligands, namely hexahydroxytriphenylene (HHTP) or hexaiminotriphenylene (HITP), were used, together with different metal centres (Co, Cu, Ni and Zn) that yield isostructural MOFs with diverse electrical conductivity and chemical properties. The synthetic route was adapted from elsewhere[2]. and modified to obtain new MOFs and various controlled morphologies at the nanoscale. The planar nature of the coordination of the beforementioned ligands with the metallic centres yields hexagonal 2D structures with a centre pore, and the vertical arrangement, probably provided by π-π stacking, gives rise to nanostructures with dimensions from 30 to 300 nm depending on the synthetic conditions and the nature of the MOF itself.

The MOFs were dispersed in ultrapure water, sonicated for 10 minutes, and one drop (0.5 µl) of the solution has been dispersed on a glass chip with interdigitated Ti/Au electrodes (IDE). Afterwards, the chips have been heated in a furnace at 80°C for 10 minutes to allow the evaporation of the water. The remaining material contacted the IDE and allowed current to flow between them. The prepared devices were exposed to different gases (EtOH, H_2O vapor, CO_2...), where a change in the electrical resistance was observed, with responses varying as a function of both the ligand and metal used for the MOF. Furthermore, poisoning of these chemiresistors is observed as a result of their continuous use as gas sensors and regeneration strategies are required[1].

References
1. Won-Tae Koo *et al.*, Chem 5 (8), 1938-1963 (2019)
2. M.G. Campbell *et al.*, Journal of the American Chemical Society 137, 13780 (2015)

POSTERS
BY RESEARCH AREAS

NanoMet

P1
NANOPARTICLE SIZE EFFECT ON PROTEIN CORONA'S KINETICS AND COMPOSITION

amartise43@alumnes.ub.edu

A. Martinez-Serra[1], G. Franzese[2]

[1] Statistical Physics of Complex Matter, Faculty of Physics, Universitat de Barcelona, 08034 Barcelona, Spain

[2] Institute of Nanoscience and Nanotechnology (IN²UB), Universitat de Barcelona, 08034 Barcelona, Spain

Tunable drug delivery systems are one of the grand challenges of nanomedicine. When nanoparticles flow through the bloodstream, they interact with various plasma proteins, forming protein layers on the nanoparticle surface, the so-called protein corona. Experiments have shown that intrinsic properties of the nanoparticle such as size, shape, and surface properties modulate the protein corona composition. This has a clear influence on the aggregation of nanoparticles and their interactions with cell membranes, which can increase or decrease the drug delivery efficiency. Being able to do so will enable a class of adaptive nanovectors with direct use in therapeutics and theranostics.

Real biological systems, however, are too complex to obtain fundamental understanding of the mechanism of protein-nanoparticle interactions. Such understanding can be obtained from computer simulations using simplified models with a small number of parameters, reflecting the essential features of the real systems. Coarse-grained (CG) molecular simulations have proven to be a powerful tool for the study of NPs interacting with biological systems at the macromolecular scale [2].

The major challenge is to perform simulations capable of reproducing experimental results by fitting the theoretical approaches. These explain that after the corona is exposed to a multicomponent system, its composition undergoes a relaxation scenario. Fast-diffusing but weakly adsorbing proteins reach the surface first, despite being quickly replaced by strong-binding proteins.

Two stages define the formation mechanism of the protein corona on a NP. First, a bare NP enters the biological medium having contact with biomolecules that adsorb faster, forming the initial corona. Second, a protein competition takes places, evolving the corona composition until an equilibrium state.

The protein corona is usually classified as hard corona (HC) or soft corona (SC), depending on the how strong is the protein adsorption. The HC is typically made of those proteins directly adsorbed onto the NP's surface, while those at larger distances loosely bound to the surface form the SC. It is habitual to focus the studies on the HC as adsorbed proteins remain attached to the NP surface after several washing cycles, so can be better characterized in experiments.

From experiments it is apparent that NP's size affects the HC composition [3-8]. Here, we perform numerical simulations running on GPUs of a model solution made of three most abundant proteins in plasma, which are Human Serum Albumin (HSA), Transferrin (Tf) and Fibrinogen (Fib). They compete to adsorb onto a silica NP which is set to different radiuses, ranging from 10 to 80 nm. In the parallel protocol we introduce the three proteins at the same time, while in the sequential we introduce them one by one, with enough time lapse to fully precoat the NP. We demonstrate the existence of a size effect by looking how does the HC and SC composition and kinetics change depending of the radius of the NP, comparing both sequential and parallel protocols.

References

1. O. Vilanova, G. Franzese *et al.* ACS Nano 2016, 10, 10842−10850.
2. P. Vilaseca *et al.* Soft Matter 2013, 9, 6978-6985.
3. C. Moya *et al.* ACS Applied Bio Materials 2019, 2 (7), 3084-3094.
4. S. Tezner *et al.* ACS Nano 2011, 5 (9), 7155–7167.
5. H. Zhang *et al.* Proteomics 2011, 11, 4569–4577.
6. M. Lundqvist *et al.* PNAS 2008, 105 (38), 14265–14270.
7. S. Lindman *et al.* Nano letters 2007, 7 (4), 914-920.
8. M. Schäffler *et al.* Nanotechnology 2013, 24, 265103 (9pp).

P2
CHARACTERIZATION OF THIN CIGS SOLAR CELLS BY ELECTRON MICROSCOPY TECHNIQUES

mfisse@ub.edu

M. Fisse[1], L. López-Conesa[1,2,3], Ll. Yedra Cardona[1,3], F. Peiró[1,3], S. Estradé[1,3], S. Paetel[4], R. Fonoll-Rubio[5], M. Guc[5], V. Izquierdo-Roca[5]

[1] LENS-MIND, Departament d'Enginyeria Electrònica i Biomèdica, Universitat de Barcelona, 08028, Barcelona, Spain

[2] CCiTUB, Centres Científics i Tecnològics de la UB, Universitat de Barcelona, 08028, Barcelona, Spain

[3] Institute of Nanoscience and Nanotechnology (IN2UB), Universitat de Barcelona, 08028, Barcelona, Spain

[4] Zentrum für Sonnenenergie- und Wasserstoff-Forschung, Baden-Württemberg (ZSW), Meitnerstr. 1, 70563 Stuttgart, Germany.

[5] Catalonia Institute for Energy Research (IREC), Jardins de les Dones de Negre 1, 08930 Sant Adrià de Besòs-Barcelona, Spain

After the obtention of promising results from $Cu(In,Ga)Se_2$ (CIGS) solar cells in laboratory scale, achieving efficiencies as high as 23,35% [1] with heavy alkali-based post-deposition treatments (PDT) [2], the transfer of this process to a pre-industrial module level is being developed.

In this work, we deal with the structural and chemical analysis of thin film solar cells grown in a pre-industrial inline-system for the CIGS deposition. The devices consist in a stack of Mo\$MoSe_2$\CIGS\CdS\i-ZnO\ZAO grown on soda-lime glass (SLG) with a RbF Post-Deposition treatment at different source temperatures and thus rates. The solar cells show good electro-optical properties with efficiencies up to 18.0 % without antireflective coating. For the obtention of as much information as possible different samples were observed: non-complete device stopped after CIGS with RbF at 520°C (prepared by mechanical polishing and subsequent low angle ion milling for a PV observation) and three complete samples with RbF at 490°C, 520°C and 540°C respectively, prepared by FIB lift-out technique for a cross-section (XS) view.

In order to fully characterize the samples, different microscopy techniques were applied using JEM-2100 and JEM-2010F electron microscopes, equipped with X-ray detector from Oxford Instruments and EELS energy filter (Gatan) respectively. Besides atomic resolution phase contrast imaging (HRTEM) and Selected Area Electron Diffraction (SAED), Electron Energy-Loss Spectrometry (EELS) in both low-loss and core loss regimes was also applied for the analysis of composition. These observations were also supported by Energy Dispersive X-Ray analysis (EDX). Additionally, phase and grain orientation maps were obtained by precession assisted electron diffraction (PED) using the Astar system from Nanomegas. This technique allows us to study the changes in phase or orientation of different grains. In order to determine the unit cell 3D electron diffraction (3D ED) was also applied. The data acquired was processed using the eADT and PETS2 programs in order to determine the unit cell of the observed material [3].

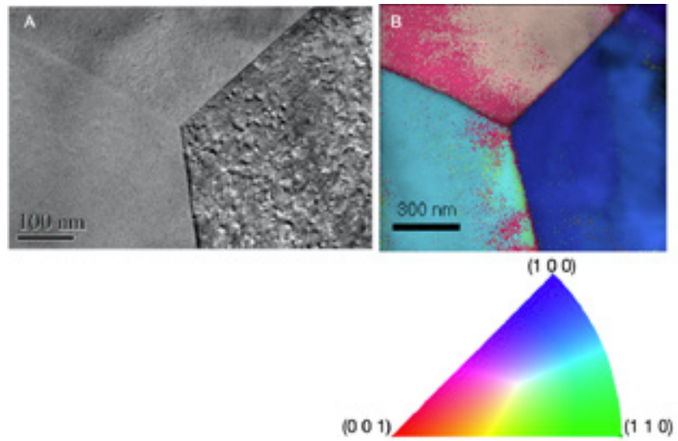

Figure1. *Data obtained from the PV 520°C. (a) Triple grain frontier and (b) Astar processed image showing orientation and reliability combination map and the corresponding crystallographic triangle*

The observation of the PV oriented sample allowed us to observe clearly the CIGS grains and how the CIGS orientation changes from one grain to another. The PED technique was used for this particular procedure, and showed, as can be seen in Fig. 1, that both the grain borders and grain orientation suffer sharp changes.

Unlike previous studies ([4]) no signal of the Cu(In,-Ga)$_3$Se$_5$ or Rb(In,Ga)Se$_2$ expected layers to be found between the CIGS and the CdS were observed in any of the complete devices nor in the EELS, the EDX or the HRTEM (Fig. 2). Also, no remnants of Rb were found in the EDX, that were expected from the RbF-PDT, but its concentration may be below the detection limit of the used microscopes.

Low-loss EELS allowed us to observe different behavior on the plasmon-peaks for all (non-complete and complete) samples, that are due to a change in the electron mean free-path.

For the SAED patters acquired what was observed was that the unit cell of the CIGS found in literature [5] did not agree with the diffraction patterns obtained for any of the samples, so, later, 3D PED was performed in order to obtain the unit cell and the lattice parameters of these samples. The 3D PED allowed to determine the unit cell, that appeared to be a tetragonal one, of the /42d space group (the same one reported in previous literature), but with different lattice parameters.

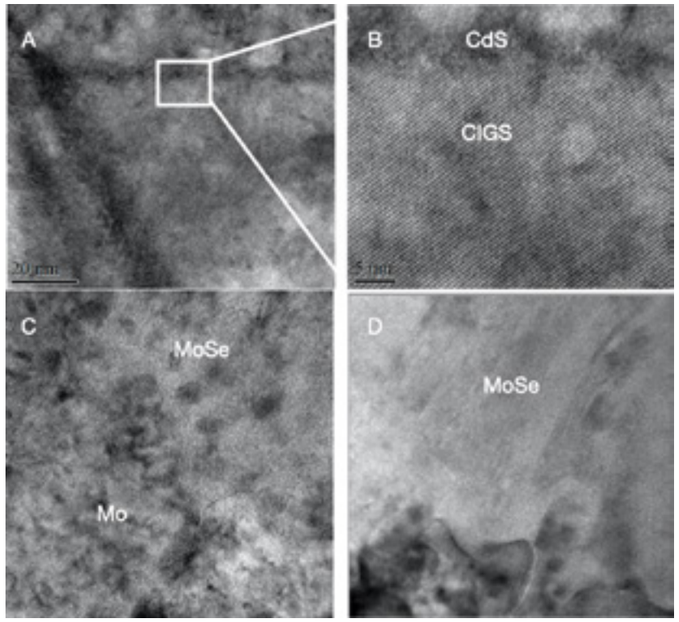

Figure2. *HRTEM images obtained in the CIGS-CdS interface*

References
1. Press-Release of Solar Frontier 17/01/2019: Solar Frontier Achieves World Record Thin-Film Solar Cell Efficiency of 23.35%.
2. T. Kodalle, T. Bertram, R. Schlatmann and C.-A. Kaufmann, "Effectiveness of an RbF Post Desposition Treatment of CIGS Solar Cells in Dependence on the Cu Content of the Absorber Layer", IEEE Journal of Photovoltaics, VOL. 9, NO.6, NOVEMBER 2016.
3. Krysiak, Y., Maslyk, M., Silva, B. N., Plana-Ruiz, S., Moura, H. M., Munsignatti, E. O., ... & Pastore, H. O. (2021). The Elusive Structure of Magadiite, Solved by 3D Electron Diffraction and Model Building. *Chemistry of Materials.*
4. L. Kronik, L. Burstein, M. Leivbovitch, Y. Saphira, D. Gal, E. Moons, J. Beier, G. Hodes, D. Cahen, D. Hariskos, R. Klenk, and H.-W. Schock, "Band diagram of the polycrystalline CdS/Cu(In,Ga)Se$_2$ heterojunction", American Institute of Physichs, 4th September 1995, **67**
5. Tinoco, T., Rincón, C., Quintero, M., & Pérez, G. S. (1991). Phase diagram and optical energy gaps for CuInyGa1− ySe2 alloys. physica status solidi (a), 124(2), 427-434.

P3
SUPPORT VECTOR MACHINES TO DETERMINE THE OXIDATION STATE IN ELECTRON ENERGY-LOSS SPECTRA (EELS)

ddelpozo@ub.edu

D. del Pozo Bueno[1,2], F. Peiró[1,2], S. Estradé[1,2]
[1] LENS-MIND, Dept. Enginyeries Electrònica i Biomèdica, Universitat de Barcelona, Barcelona, Spain.
[2] Institute of Nanoscience and Nanotechnology (IN²UB), Universitat de Barcelona, Barcelona, Spain.

Electron Energy-Loss Spectroscopy (EELS) is a powerful and functional spectroscopic technique to study the composition and properties of materials locally at a nanoscale. The technological improvement of the Scanning and Transmission Electron Microscopes (S/TEM) technique leading to higher spatial and energy resolution results in an enormous increase of the total amount of data acquired in STEM-EELS measurements. Thus, currently the EELS technique offers better energy and spatial resolutions making possible a better nanometric characterization, at the cost of producing large spectral datasets, hindering the spectra analysis for the spectroscopist.

The machine learning methods provide a large variety of tools to properly deal with these large amounts of spectral data in an automated manner, at the same time that allow for extracting valuable physical information. In this sense, a promising machine learning strategy for identifying EELS data is the Support Vector Machine (SVM) [1], in particular the soft-margin SVM, which is a supervised machine learning algorithm allowing the multiclass classification, even with non-linear data, and that can be used as a probabilistic classifier.

The soft-margin SVM algorithm has shown promising results identifying the oxidation state in transition metal (TM) oxides, manganese and iron oxides, through the study of their EELS spectra, concretely, their white lines (L3 and L2) [2]. The algorithm has been implemented in Python programming language from the library Scikit-learn [3], concretely, the LIBSVM library [4]. It has presented a performance above 90 % classifying the TM oxidation state, and additionally, it has exhibited a good performance classifying these EEL spectra considering the usual level of noise and additional instrumental energy shifts in the spectrum. This very same algorithm has been also used to identify the oxidation state using the oxygen K edge of the EELS spectra, instead of the white lines, and in this case, it has also shown an excellent performance, above 90 %, determining the oxidation state for iron oxides. Besides, it has presented a good robustness to the usual level of noise and instrumental energy shifts.

Finally, the SVM applied to EEL spectra makes the most of the simplicity (it presents few parameters to optimize) and short computation times of it to identify the oxidation state of the transition metals correctly and automatically. Furthermore, although it presents fast computing times for large spectral datasets, they can even be reduced by implementing additional algorithms, as the Stochastic Gradient Descend (SDG), which is an iterative method that optimizes, and so, accelerates model training enabling also faster parameter optimization.

References
1. C. Cortes and V. Vapnik, *Machine Learning* **20** (1995), pp. 273–297.
2. D. del Pozo Bueno, F. Peiró and S. Estradé, *Ultramicroscopy* **221** (2021), p. 113190.
3. F. Pedregosa *et al.*, *Journal of Machine Learning Research* **12** (2011), pp. 2825–2830.
4. C. C. Chang and C. J. Lin, ACM Trans. *Intell. Syst. Technol.* **2** (2011), pp. 1–39.

NanoBio

P4

BACTERIAL NANOCELLULOSE-REINFORCED TYPE I COLLAGEN HYDROGELS AS SCAFFOLDS FOR 3D CELL CULTURE

jorge.otero@ub.edu

N. Malandain[1], H. Sanz-Fraile[2], J. Otero[2,3], A. Laromaine[1], A. Roig[1], R. Farré[2,3]

[1] Institut de Ciència de Materials de Barcelona (ICMAB-CSIC), Campus Universitat Autònoma de Barcelona, Spain.
[2] Unit of Biophysics and Bioengineering, School of Medicine and Health sciences, Universitat de Barcelona, Spain.
[3] Institut de Nanociència I Nanotecnologia, Universitat de Barcelona, Spain.

In the last decade, there has been a growing interest in the development of hydrogels derived from native extracellular matrices (ECM) for 3D cell culture as they better mimic the physiological cellular microenvironment. Despite improvements in organ decellularization techniques, extracellular matrix's hydrogels obtained exhibit lower stiffness than native tissues. A common solution to overcome this problem is to mix ECM-based hydrogels with high-stiffness biomaterials, such as silk[1].

However, by incorporating micron-sized fibrous components, the structure and the properties of the hydrogel is affected and the cell behaviour can be modified. Thus, bacterial nanocellulose (BNC), due to the size and the robustness of its nanofibers, and its multiples properties (such as biocompatibility, non-cytotoxicity, high natural purity) seems a good compromise[2].

The aim of this work is to reinforce the ECM hydrogels with bacterial nanocellulose to develop a biomaterial suitable for the cell culture without micron-sized fibers. BNC fibers were produced from BNC films derived from the culture of Komagataeibacter xylinus and mixed homogeneously with high concentration of type I collagen from rat tails[3]. Laser confocal microscopy and scanning electron microscope images were used to assess the homogenous macro- and micro-distribution of the two types of fibers. Elongation capacity and rheological properties of these composite hydrogels were compared to type I collagen hydrogels and non-decellularized organs. 3D cell culture was assessed to evaluate the cell viability inside these hydrogels and their suitability for the cell culture.

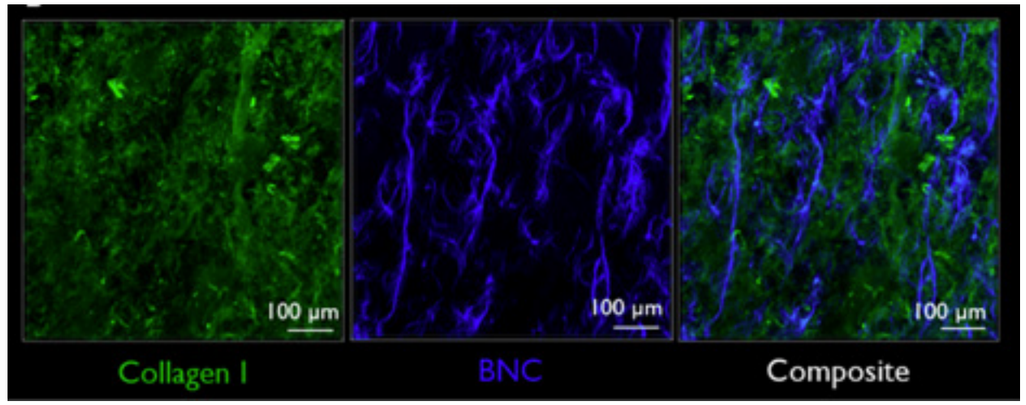

Figure 1. *Confocal microscopy images of hybrid hydrogel composed of collagen and bacterial nanocellulose*

References
1. Sanz-Fraile H., *et al.*, Tissue Engineering Part A., 358-370, 2020.
2. Anton-Sales I., *et al.*, ACS Biomaterials Science & Engineering, 6, 9, 893-4902, 2020.
3. Rajan, N., *et al.*, Nature Protocols, 1, 2753, 2006.

P5

ACTIVE WETTING DRIVES MIGRATION, ROLLING AND DUROTAXIS ON CADHERIN COATED SUBSTRATES

rsunyer@ub.edu

M. Pallarès[1], R. Sunyer[3,6], X. Trepat[1,2,3,4,5]

[1] Institute for Bioengineering of Catalonia (IBEC), Barcelona 08028, Spain.
[2] The Barcelona Institute for Science and Technology (BIST), Barcelona 08028, Spain.
[3] Facultat de Medicina, University of Barcelona, Barcelona 08036, Spain.
[4] Institució Catalana de Recerca i Estudis Avançats (ICREA), Barcelona 08028, Spain.
[5] Centro de Investigación Biomédica en Red en Bioingeniería, Biomateriales y Nanomedicina, Barcelona 08028, Spain.
[6] Institut de Nanociència i Nanotecnologia (IN2UB), Barcelona, Spain.

Directed cell migration –the ability of cells to follow environmental cues– is an essential mechanism involved in important tissue processes such as morphogenesis, wound healing and tumor metastasis. This kind of cell migration has been mainly studied when mediated by focal adhesions at the extracellular matrix (ECM) interface. However, important migratory processes during development or metastasis take place in absence of extracellular matrix. These processes are mediated by cadherins, a cell-cell adhesion protein that is essential to maintain tissue integrity, to promote coordination and establish cell polarity. In the context of cadherin mediated migration, it is unknown how migratory cells are able to orient themselves to reach their destination. In this work, we report for the first time that human epidermoid carcinoma cell clusters (A431) systematically migrate from low to high stiffness regions when seeded on a hydrogel coated with oriented E-cadherin molecules, exhibiting a migratory behavior called durotaxis. We show that E-cadherin-mediated durotaxis increases with cluster size and peaks at a certain local stiffness offset. Interestingly, we found that some A431 cell clusters migrate unexpectedly large distances by rolling, presenting a non-gaussian migratory behavior. We also found that clusters on E-cadherin-coated substrates display actin-enriched protrusions, while cluster spreading area increases with local stiffness offset. Taken together, these results suggest that durotaxis on E-cadherin-coated substrates is driven by the interplay between traction forces and contractile intercellular stresses in what is called a wetting transition. To date, durotaxis has only been described on ECM coated surfaces such as fibronectin and collagen. In this work we show that durotaxis can also be mediated through E-cadherin, and this might be key for fundamental processes such as development or tumor dissemination.

P6
POLYOXOMETALATE-DECORATED GOLD NANOPARTICLES AS B-AMYLOID INHIBITORS

mperxes@ibecbarcelona.eu

M. Perxés Perich[*2,5], S. Palma Florez[1,2], S. Goberna Ferrón[5], J. Samitier[1,2,3], P. Gómez Romero[*5], A. Lagunas Targarona[3,2*], M. Mir Llorente[1,2,3,4*]

[1] Department of Electronics and Biomedical Engineering, University of Barcelona, Martí i Franquès 1, 08028 Barcelona, Spain.
[2] Nanobioengineering Group, Institute for Bioengineering of Catalonia (IBEC) Barcelona Institute of Science and Technology (BIST), Baldiri i Reixac, 08028 Barcelona, Spain.
[3] Biomedical Research Networking Center in Bioengineering, Biomaterials, and Nanomedicine (CIBER-BBN), 28029 Madrid, Spain.
[4] Institute for Nanoscience and Nanotechnology-IN²UB, University of Barcelona, 08028 Barcelona, Spain.
[5] Catalan Institute of Nanoscience and Nanotechnology, ICN2 (CSIC-BIST) Campus UAB, Bellaterra Barcelona, E-08193, Spain.

Alzheimer's disease (AD) is characterized by progressive neurodegeneration, being loss of memory the main symptom. One of the two main hallmarks is the amyloid plaque, formed by extracellular aggregates of amyloid fibrils[1,2]. Those are associated with the β-amyloid protein, that can polymerize forming aggregates, resulting in disfunction of axons and dendrites[3]. β-amyloid aggregation has been thoroughly studied, and numerous ligands have been synthesized in order to target it and to inhibit its aggregation[4], such as the new treatment recently approved by the FDA[5].

Polyoxometalates (POMs) are early transition metal oxide inorganic anionic clusters very well known for their redox activity[6]. Its negative charge allows them to bind to the β-amyloid monomer, which lowers the concentration of free monomer and shifts the equilibrium away from fibrillization[7]. Therefore, POM-decorated gold nanoparticles (AuNPs@POM) could be used as a drug delivery system for inhibiting β-amyloid fibrillization[8,9].

In the framework of this project, gold nanospheres have been functionalized with POMs, specifically with β_2 isomer of the monolacunary 11-tungstosilicate (β_2-$K_8SiW_{11}O_{39}$), which has promising effects in β-amyloid fibrillization inhibition. To evaluate the system as a possible therapeutic agent for β-amyloid fibrillization inhibition, evaluation of AuNPs@POM cytotoxicity in neurovascular cell cultures *in vitro* was performed and it was evaluated β-amyloid fibrillization inhibition in vitro by AuNPs@POM as well as the permeability of the AuNPs@POM in the blood brain barrier (BBB) in an organ on a chip microfluidic system.

References

1. Pike, C. J., Burdick, D., Walencewicz, A. J., Glabe, C. G. & Cotman, C. W. Neurodegeneration induced by β-amyloid peptides in vitro: The role of peptide assembly state. J. *Neurosci*. **13**, 1676–1687 (1993).
2. C L Masters, G Simms, N A Weinman, G Multhaup, B L McDonald, and K. B. Amyloid plaque core protein in Alzheimer disease and Down syndrome. *PNAS* **82**, 4245–4249 (1985).
3. Selkoe, D. J. Cell biology of protein misfolding: The examples of Alzheimer's and Parkinson's diseases. *Nat. Cell Biol.* **6**, 1054–1061 (2004).
4. Stains, C. I., Mondal, K. & Ghosh, I. Molecules that target beta-amyloid. *ChemMedChem* **2**, 1674–1692 (2007).
5. Cavazzoni, P. (FDA C. for D. E. and R. FDA's Decision to Approve New Treatment for Alzheimer's Disease. *FDA* https://www.fda.gov/drugs/news-events-human-drugs/fdas-decision-approve-new-treatment-alzheimers-disease (2021).
6. Gómez-Romero, P. Polyoxometalates as photoelectrochemical models for quantum-sized colloidal semiconducting oxides. *Solid State Ionics* **101–103**, 243–248 (1997).
7. Geng, J., Li, M., Ren, J., Wang, E. & Qu, X. Polyoxometalates as inhibitors of the aggregation of amyloid β peptides associated with Alzheimer's disease. *Angew. Chemie* - Int. Ed. **50**, 4184–4188 (2011).
8. Gao, N., Sun, H., Dong, K., Ren, J. & Qu, X. Gold-nanoparticle-based multifunctional amyloid-β inhibitor against Alzheimer's disease. *Chem. - A Eur. J.* **21**, 829–835 (2015).
9. Surman, A. J. et al. Sizing and Discovery of Nanosized Polyoxometalate Clusters by Mass Spectrometry. *J. Am. Chem. Soc.* **138**, 3824–3830 (2016).

P7
PHOTOACTIVE ACTIVE NEMATIC

ivelez@ub.edu

I. Vélez-Cerón[1,2], J. Ignés-Mullol[1,2], F. Sagués Mestre[1,2]

[1] Science Materials and Physical Chemistry Department, Faculty of Chemistry, Universitat de Barcelona
[2] Institute of Nanoscience and Nanotechnology (IN2UB), Universitat de Barcelona

Active soft matter is composed of non-equilibrium self-driven entities that often develop orientational order. The main property of these systems is that each constituent is able to convert stored or ambient energy into systematic movement. Because of the interaction between the entities, these systems exhibit collective behaviour [1].

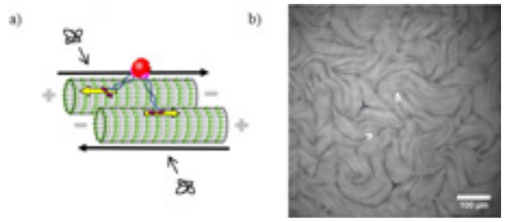

Figure 1. *Active nematic formation by in-vitro cytoskeletal reconstitutions at a water-oil interface. a) Microtubules are bundled together under the depletion force applied by PEG and crosslinked with dimeric motor clusters. b) Fluorescence microscopy image of the active nematic. Examples of semi-integer defects are highlighted (+1/2 in white and -1/2 in black)*

One of the most fascinating active matter systems is obtained by in-vitro cytoskeletal reconstitutions based on dense suspensions of microtubules [2]. The latter are bundled together under the depleting action of polyethylene-glycol (PEG), which facilitates crosslinking and internal shearing by dimeric kinesin-streptavidin motor clusters. Fuelled with adenosine triphosphate, the bundles are permanently subjected to extension and buckling (Figure 1a). This mixture arranges as an extensile active gel. However, in the presence of a bio-compatible soft and flat interface this bulk-material is condensed towards the interface driven by the depletion force. The resulting active layer, known as active nematic, adopts a characteristic long-range orientational order, continuously permeated by large-scale flows and locally interrupted by regions void of microtubules that configure semi-integer defects (Figure 1b). The chaotic dynamics of this active layer with continuous defect creation and annihilation corresponds to a state of active nematic turbulence [3].

Active nematic dynamics can be influenced by means of rheology [4], magnetic fields [5] and confinement [6]. Nevertheless, these experimental systems lack spatio-temporal control. Taking advantage of novel bioengineering, kinesin motors have been fused to optically dimerizable iLID proteins [7], offering the opportunity to include light control in the active nematic. Unlike the control strategies mentioned above, the new protocol offers a control ability that is intrinsic to the material. In the modified system, light activates reversible linking between kinesins (Figure 2), allowing the formation and spontaneous motion of the active nematic filaments, while, turning off the light, motor clusters are disengaged thus stopping active nematic movement. Employing light patterns with arbitrary spatial and temporal characteristics we intend to couple external and intrinsic length and time scales, and unveil new scenarios of spatio-temporal dynamics in active matter.

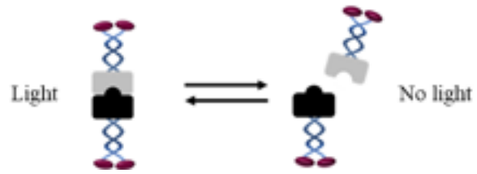

Figure 2. *Kinesin motors have been fused to optically dimerizable iLID proteins allowing the reversible linking between kinesins in the presence of light*

References

1. M. Cates and F. MacKintos, Soft Matter, 7, 3050–3051 (2011).
2. T. Sanchez, D. T. N. Chen, S. J. DeCamp, M. Heymann and Z. Dogic, Nature, 491, 431-434 (2012).
3. B. Martínez-Prat, J. Ignés-Mullol, J. Casademunt and F. Sagués, Nat. Phys., 15, 362–366 (2019).
4. P. Guillamat, J. Ignés-Mullol, S. Shankar, M. C. Marchetti and F. Sagués, Phys. Rev. E, 94, 060602 (2016).
5. P. Guillamat, J. Ignés-Mullol and F. Sagués, Proc. Natl. Acad. Sci., 113, 5498-5502 (2016).
6. J. Hardoüin, R. Hughes, A. Doostmohammadi, J. Laurent, T. Lopez-Leon, J. M. Yeomans, J. Ignés-Mullol and F. Sagués, Commun. Phys., 2, 121 (2019).
7. G. Guntas, R. A Halletta, S. P. Zimmermana, T. Williamsa, H. Yumerefendia, J. E. Bearb and B. Kuhlman, Proc. Natl. Acad. Sci. U. S. A., 112, 112–117 (2015).

P8
WATER-SOLUBLE GOLD NANOPARTICLES COATED WITH GEMINI CATIONIC AMPHIPHILES AS A NOVEL TRANSFECTING AGENT FOR CANCER GENE THERAPY

cciudad@ub.edu

D. Limón[1,2], S. Bagherpour[1,2], P. Karakitsou[3], S. Valiuska[3], R. Griera[1], S. Giraldo[1], V. Noé[2,3], C. J. Ciudad[2,3], Ll. Pérez-García[1,2]

[1] Department of Pharmacology, Toxicology and Therapeutic Chemistry, School of Pharmacy and Food Sciences, University of Barcelona, 08028 Barcelona, Spain.
[2] Nanoscience and Nanotechnology Institute, IN²UB, University of Barcelona, Spain.
[3] Department of Biochemistry and Physiology, School of Pharmacy and Food Sciences, University of Barcelona, 08028 Barcelona, Spain.

Gene therapy is a promising selective strategy for treating cancer and other genetic diseases. However, the physicochemical properties of DNA prevent its internalization in cells, and for that reason appropriate vehicles are needed[1]. We have recently designed and synthesized the cationic gemini amphiphile 1,3-bis[(4-oleyl-1-pyridinio)methyl]benzene dibromide (**DOPY**), which can interact with PolyPurine Reverse Hoogsteen hairpins (**PPRHs**) forming vesicles that are able to transfect cancerous cells, including PC3 and hard-to-transfect neuroblastoma SH-SY5Y cells[2].

In this work we show that **DOPY** can also be used to synthesize and stabilize water-soluble gold nanoparticles (**GNP.DOPY**) as a nanomaterial for gene therapy. **GNP.DOPY** show an SPR band at 536 nm and a mean diameter of 5 nm according to UV-vis absorption spectroscopy. According to electrophoretic mobility experiments, **GNP.DOPY** can interact electrostatically with PPRHs. In addition, Transmission Electron Microscopy has shown that **GNP.DOPY** can completely coat the strands of **PPRH** forming a complex (**GNP.DOPY-PPRH**), which can be successfully internalized in cancerous PC3 cells as observed by Fluorescence Microscopy.

Preliminary experiments using a **PPRH** for silencing the Survivin gene show that cancerous PC3 cells treated with **GNP.DOPY-PPRH** have decreased viability as a result of the successful transfection. These results show **GNP.DOPY** as a promising nanomaterial for gene therapy.

Acknowledgements

Work supported by grant RTI2018-093901-B-I00 from MICINN (Spain), TEC2017-85059-C3-2-R, and by Ajut a la Recerca Transversal 2018 from IN2UB. Groups holding the Quality Mention from Generalitat de Catalunya 2017-SGR-94 and 2017-SGR-1277. S. B. thanks Generalitat de Catalunya for a predoctoral FISDUR grant, and P.K. is a recipient of an Erasmus grant.

References

1. Niidome, T.; Huang, L. Gene Therapy Progress and Prospects : Nonviral Vectors. *Gene Ther*. **2002**, 9, 1647–1652. https://doi.org/10.1038/sj.gt.3301923.
2. Aubets, E.; Griera, R.; Felix, AJ.; Rigol, G.; Sikorski, C.; Mastrorosa, C.; Busquets, M.; Limon, D. Perez-García, Ll.; Noé, V and Ciudad, CJ. Synthesis and Validation of DOPY : A New Gemini Dioleylbispyridinium Based Amphiphile for Nucleic Acid Transfection. *Eur. J. Pharm. Biopharm.* **2021**, 165 (April), 279–292. https://doi.org/10.1016/j.ejpb.2021.05.016.

P9
ENZYMATIC FUNCTIONALIZATION OF BACTERIAL NANOCELLULOSE BY POLYSACCHARIDE LYTIC MONOOXYGENASES. A SUSTAINABLE APPROACH TO THE DEVELOPMENT OF NEW MATERIALS.

veronica.cabanas@ub.edu

L. V. Cabañas-Romero[1,2], C. Buruaga-Ramiro[1,2], J. Martinez[1,2], R. I. Santamaría[3], S. V. Valenzuela[1, 2]

1 University of Barcelona/ Department of Genetics, Microbiology, and Statistics/ Barcelona, Spain.
2 Institute of Nanoscience and Nanotechnology (IN²UB)/ Barcelona, Spain.
3 Institute of Functional Biology and Genomics (CSIC)/ University of Salamanca (USAL)/ Institute of Functional Biology and Genomics((IBFG)/ Salamanca, Spain.

Cellulose is the most abundant biopolymer on Earth. The biosynthesis of cellulose takes place not only in plants but, also in Bacteria. Bacterial nanocellulose (BC) is synthesized and extruded outside the cell by some microorganisms, especially from the genera *Komagataeibacter*. BC presents unique properties that make it superior for many applications. BC displays a high degree of polymerization and crystallinity, great mechanical strength, and a high water-holding capacity. BC is also biodegradable and biocompatible (Klemm *et al.*, 2005).

Enzymes can modify cellulose fibers in a sustainable and selective way, unlike chemical and physical treatments, giving them novel and multifunctional properties. A great effort is currently being made to characterize these enzymes, due to their great potential for biomodification and valorization of renewable substrates. A new type of cellulosic enzyme, called polysaccharide lytic monooxygenase (LPMO), has recently been identified and characterized. Its mechanism of action, unknown until 2010 (Vaaje-Kolstad et al., 2010), depolymerizes polysaccharides by oxidative breakdown, generating carboxylic groups. This activity has opened a new range of applications due to the functionalization that it confers on the polysaccharide, which differs from the traditional enzymatic hydrolysis.

Currently, we are working with two LPMOs: SamLPMO10C from *Streptomyces ambofaciens*, and LPMOSha10A, from *Streptomyces halstedii*. Two strategies have been used to express these two LPMOs: a homologous expression in *Streptomyces lividans* and an heterologous expression in *Escherichia coli*. Both expression systems have resulted in functional enzymes.

ShaLPMO10A has been identified and chosen for its potential on cellulosic fibers. Through tests carried out on crystalline cellulose, its oxidative activity was verified obtaining oxidized products at carbon 1 of the glucose subunits of the cellulose chains.

In a binding assay to bacterial nanocellulose, it has been observed that both LPMOs bind strongly to the substrate. This is interesting because cellulose can be biomodified by these enzymes, which opens a range of possibilities for the development of cellulose-based products modified by these enzymes.

References

1. Klemm, D., Heublein, B., Fink, H.-P., & Bohn, A. (2005). Cellulose: Fascinating Biopolymer and Sustainable Raw Material. *Angewandte Chemie International Edition*, 44(22), 3358–3393. https://doi.org/10.1002/anie.200460587.
2. Vaaje-Kolstad, G., Westereng, B., Horn, S. J., Liu, Z., Zhai, H., Sørlie, M., & Eijsink, V. G. H. (2010). An Oxidative Enzyme Boosting the Enzymatic Conversion of Recalcitrant Polysaccharides. *Science*, 330(6001), 219–222. https://doi.org/10.1126/science.1192231.

P10
JAMMING INDUCED BY HYDRODYNAMIC INTERACTIONS IN CONFINED FLOW-DRIVEN PARTICLE TRANSPORT

ecereceda@ub.edu

E. Cereceda-López[1,2], D. Lips[3], A. Ortiz-Ambriz[1,2,4], A. Ryabov[5], P. Maas[3], P. Tierno[1,2,4]

[1] Departament de Física de la Matèria Condensada, Universitat de Barcelona, 08028, Barcelona, Spain
[2] Institut de Nanociència i Nanotecnologia, Universitat de Barcelona (IN²UB), 08028, Barcelona, Spain
[3] Universität Osnabrück, Fachbereich Physik, Barbarastraße 7, D-49076 Osnabrück, Germany
[4] University of Barcelona Institute of Complex Systems (UBICS), 08028, Barcelona, Spain
[5] Charles University, Faculty of Mathematics and Physics, Department of Macromolecular Physics, V Holešovickách 2, CZ-18000 Praha 8, Czech Republic

In the present work, we experimentally study the transport of particles in a quasi-one-dimensional (q1D) periodic potential. We compare the experimental results with simulations based on the Brownian Asymmetric Simple Exclusion Process [1, 2], and we discuss the importance of hydrodynamic interactions (HI) in flow-driven particle transport.

The experimental setup consists of 27 time-shared optical tweezers, which create individual Gaussian potential wells, uniformly distributed in a ring-shape confining up to 27 colloidal particles. We rotate the optical traps at constant angular velocity to create a quasi-sinusoidal traveling potential landscape. Varying the number of particles in the potential landscape allows us to measure the fundamental diagram of the system, which is the colloidal current as a function of the particle density. We find that for different potential landscape barrier heights the particle current density decreases after reaching a maximum value.

We compare the experimental results with simulations, and we attribute the decrease of the current density relationship to the jamming produced by the HI between particles. We explain this phenomenon using the equations of motion that include HI and show that the latter enhances the potential barrier in flow-driven systems. This is opposed to previous observations in force-driven systems, which remark the fundamental difference with our flow-driven system.

References
1. D. Lips, A. Ryabov and P. Maass, Brownian Asymmetric Simple Exclusion Process, Phys. Rev. Lett. 121, 160601 (2018).
2. D. Lips, A. Ryabov and P. Maass, Single-_le transport in periodic potentials: The Brownian asymmetric simple exclusion process, Phys. Rev. E 100, 052121 (2019).

P11
ALIGNMENT TRANSITION OF AN ACTIVE NEMATIC IN THE PRESENCE OF MAGNETIC FIELD

olga.b.bantysh@ub.edu

O. Bantysh[1], J. Ignés-Mullol[1,2], F. Sagués Mestre[1,2]

[1] Departament de Química Física, Universitat de Barcelona, 08028 Barcelona, Catalonia, Spain.
[2] Institute of Nanoscience and Nanotechnology, Universitat de Barcelona, 08028 Barcelona, Catalonia, Spain.

It is possible to assemble a biomimetic active material from microscopic components like cells' filaments and protein motors. This material consumes energy and generates continuous motion. Such active systems are capable of self-organization at different length and time scales, often exhibiting turbulent flows and the emergence of long-range orientational order, which is characteristic of active nematics. Previously it was demonstrated that, by bringing into contact a two-dimensional nematic liquid crystal with anisotropic oil that features smectic liquid-crystalline order, it is possible to transform the originally turbulent flow of the active fluid into well-aligned flow ordered by a magnetic field [1].

We attempted to characterize quantitatively the order-disorder transition of active nematic in a simple and intuitive way. We demonstrated that the average projection of active nematic directors on the direction determined by external magnetic field could be used as an order parameter (OP) for this system. The OP could be calculated from fluorescent images, as a projection of the local orientation of bundles of MT filaments on the ordering direction (orthogonal to the magnetic field). This OP allows to discriminate clearly between turbulent and aligned states of the active nematic, and to extract internal properties of this system such as "order oscillations". The last ones probably reflect some internal property of the active nematic and could be related to the relaxation of accumulating distortions.

References
1. P. Guillamat, J. Ignés-Mullol, and F. Sagués, "Control of active liquid crystals with a magnetic field," Proc. Natl. Acad. Sci. U. S. A., vol. 113, no. 20, pp. 5498–5502.

P12
A MATHEMATICAL MODEL OF CHEMOTACTIC ENDOTHELIAL CELL MIGRATION

josep.ferre@fmc.ub.edu

J. Ferré-Torres[1,5], A. Noguera-Monteagudo[2], J. R. Romero-Arias[3], O. Castaño[2], R. A. Barrio[4], A. Hernandez-Machado[1,5]

[1] Condensed Matter Physics Department, Faculty of Physics, University of Barcelona, Spain.
[2] Electronics and Biomedical Engineering Department, University of Barcelona, Spain.
[3] Instituto de Investigaciones en Matemáticas Aplicadas y en Sistemas, Universidad Nacional Autónoma de México, CdMx 01000, México.
[4] Instituto de Física, Universidad Nacional Autónoma de México, 01000 CdMx, México.
[5] Institute for Nanoscience and Nanotechnology of the University of Barcelona (IN²UB), Spain.

The formation of new vasculature from pre-existing blood vessels, or angiogenesis, occurs in numerous physiological and pathological conditions. A standard approach to study angiogenesis is to investigate the underlying cellular mechanisms focusing on endothelial cell (EC) motility in response to proangiogenic molecules such as vascular endothelial growth factor (VEGF). In cultured ECs, VEGF induces directed cell motility and a chemotactic response often described as a drift in the direction of the growth factor gradient.

Here, we present a novel model to describe chemotactic EC migration in response to proangiogenic factors by using the Ginzburg-Landau theory, incorporating the effect of the chemoattractant factor into the system energy. We present the collective migration of ECs in a pore promoted by the influence of a chemotactic factor.

$$\frac{\partial \phi}{\partial t} = M\nabla^2 \left(\underbrace{-\phi + \phi^3 - \epsilon^2 \nabla^2 \phi}_{\text{Surface tension}} + \underbrace{2\phi\epsilon C_0 B_\phi - \epsilon^2 \nabla^2 B_\phi}_{\text{Chemotactic factor effect}} \right)$$

The first three terms of the dynamic equation, the ϕ dependent terms, stand for the cohesion of collective cells by introducing a surface tension into the system. B_ϕ, $B_\phi = \epsilon C_0 (\phi^2 - 1)$, is the effect of the chemotactic factor towards ECs. The first term, B_ϕ^2, stands for the chemotactic response of ECs to chemotactic factors affecting only the outer layers of the endothelium and the second, $\nabla B_\phi \cdot \nabla \phi$ directs migration towards the source of chemotactic factors. This allows us to capture biologically observed phenomena of surface activation in response to VEGF gradients.

By defining a chemotactic factor gradient on the background plus adding gaussian-like distributions of a given chemotactic factor inside the pore, we have been able to describe the dynamics of EC collective migration.

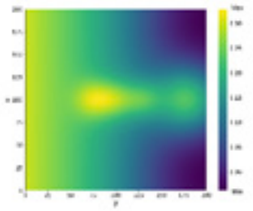

Angiogenic factor distribution

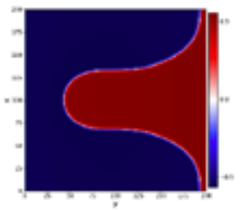

Endothelial cell migration (from right to left)

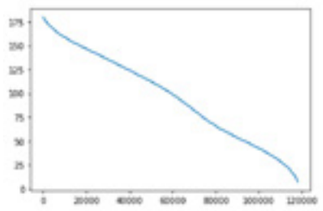

Position of the tip as a function of the time-step (x10³)

P13
NOVEL DECELLULARIZATION METHOD FOR LUNG TISSUE SLICES

mnarciso@ibecbarcelona.eu

M. Narciso[1,3], A. Uldemolins[1], C. Júnior[1,3], J. Otero[1,2,3], D. Navajas[1,2,3], R. Farré[1,2,4], N. Gavara[1,3], I. Almendros[1,2,4*]

[1] Unitat de Biofísica i Bioenginyeria, Facultat de Medicina i Ciències de la Salut, Universitat de Barcelona, Spain.
[2] CIBER de Enfermedades Respiratorias, Madrid Spain.
[3] The Institute for Bioengineering of Catalonia (IBEC), The Barcelona Institute of Science and Technology, Barcelona, Spain.
[4] Institut d'Investigacions Biomèdiques August Pi i Sunyer, Barcelona, Spain.

The decellularization of the lung – the removal of all its cellular material leaving only the extracellular matrix (ECM) scaffold - is essential to the study of pulmonary physiology and physiopathology as well as for regenerative medicine and tissue engineering. Currently, perfusion of detergents and/or enzymes through the trachea and the pulmonary artery is the most common protocol to decellularize whole lungs. However, decellularization of the whole lung is not always the desired endpoint, due to the anticipated procedures to be carried out on the remaining ECM scaffold. Accordingly, an optimal protocol has not yet been established for the decellularization of lung thin slices attached to a glass slide. The aim of this work was to develop a decellularization method for lung tissue slices that preserves their composition and structure, without detachment from a glass slide. To achieve this, we compared different decellularizing agents from past works and tested their effectiveness in removing cellular content while also preserving their ECM. To this end, we assessed the fluorescence intensity of DAPI staining, using a custom image analysis pipeline, as an indicator of the remaining cells. The presence of type I collagen and elastin were also quantified using immunostaining followed by the same fluorescence quantification pipeline. We found that SDC 2 % was the most effective agent for decellularization (93 % decrease in DAPI fluorescence signal when compared to native tissue) and maintenance of ECM lung structures and composition (11 % decrease in collagen I signal and 7 % decrease in elastin signal). Conversely, SDS was effective in cellular removal (99 % decrease in DAPI) but its negative effects on matrix protein content were already widely reported. Other decellularization protocols based on CHAPS, triton and ammonia hydroxide decreased DAPI intensity by 65 %, 53 % and 56 %, respectively, not achieving full cellular removal. The optimal SDC 2 % protocol was further evaluated in porcine, mice and rat lung slices, achieving similar levels of decellularization. In addition, the scaffolds resulting from the optimized protocol were mechanically characterized using AFM and recellularized with mesenchymal stem cells to assess their biocompatibility. The decellularization method presented here has the advantage of not requiring fixation or additional adherence treatments, is fast and can be especially suitable in studies which require the identification of some regions microscopically prior to in situ decellularization or human biopsies.

P14
KINETIC ENERGY SPECTRA OF ACTIVE NEMATIC TURBULENCE

bmartinez@ub.edu

B. Martínez-Prat[1,2], R. Alert[3,4], F. Meng[5,6], J. Ignés-Mullol[1,2], J. F. Joanny[8,9], J. Casademunt[10,11], R. Golestanian[5,12], F. Sagués Mestre[1,2]

[1] Department of Materials Science and Physical Chemistry, Universitat de Barcelona, Barcelona, Catalonia, Spain.
[2] Institute of Nanoscience and Nanotechnology (IN²UB), Universitat de Barcelona, Barcelona, Catalonia, Spain.
[3] Princeton Center for Theoretical Science, Princeton University, Princeton, NJ, USA.
[4] Lewis-Sigler Institute for Integrative Genomics, Princeton University, Princeton, NJ, USA.
[5] Max Planck Institute for Dynamics and Self-Organization (MPIDS), D-37077 Göttingen, Germany
[6] CAS Key Laboratory for Theoretical Physics, Institute of Theoretical Physics, Chinese Academy of Sciences, Beijing 100190, China.
[7] ESPCI Paris, PSL University, Paris, France
[8] Laboratoire PhysicoChimie Curie, Institut Curie, PSL University, Sorbonne Universités, UPMC, Paris, France
[9] Collège de France, Paris, France
[10] Departament de Física de la Matèria Condensada, Universitat de Barcelona, Barcelona, Catalonia, Spain.
[11] Universitat de Barcelona Institute of Complex Systems (UBICS), Universitat de Barcelona, Barcelona, Catalonia, Spain.
[12] Rudolf Peierls Centre for Theoretical Physics, University of Oxford, Oxford OX1 3PU, United Kingdom

The unifying property of active fluids is their ability to flow on their own thanks to the internal stresses produced by their constituents. Bacterial suspensions, sperm, mixtures of cytoskeletal proteins and cell monolayers are typical examples of active fluids. Despite operating at low Reynolds number, where inertia is negligible, these systems can trigger chaotic flows, which have been termed active turbulence due to the visual resemblance with conventional turbulence. Nevertheless, the extent of this similarity remains disputed. Here, we work with an active fluid layer with orientational order, composed by kinesins and microtubules from the cytoskeleton [1] (see Fig. 1), and we demonstrate the existence of scaling regimes with universal exponents, like in inertial turbulence. More precisely, we corroborate experimentally the existence of two theoretically predicted scaling regimes [2,3], and reveal a new one that arises from the coupling of the active layer with the surrounding fluids. We demonstrate that the way kinetic energy of the active material partitions across different scales depends on the viscous coupling with the environment [4].

Figure 1. *Active nematic based on proteins from the cytoskeleton showing active turbulence. Left: Fluorescence micrograph of the AN. Right: Image on the left with the velocity field showing a pattern of swirls. Scale bar is 100 μm*

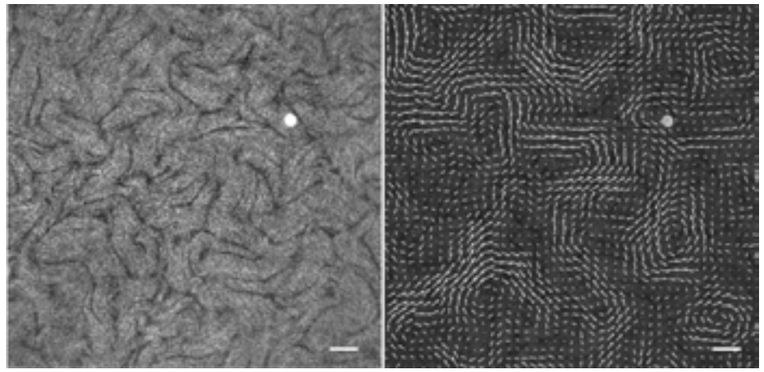

References
1. T. Sanchez, D. T. N. Chen, S. J. Decamp, M. Heymann, and Z. Dogic, Nature, 491, 431–434 (2012)
2. L. Giomi, Phys. Rev. X, 5, 1–11 (2015)
3. R. Alert, J.-F. Joanny, and J. Casademunt, Nat. Phy., 16, 682–688 (2020)
4. B. Martínez-Prat *et al.*, arXiv:2101.11570 (2021)

NanoPharmaMed

P15
EXPLORING A NANOPARTICLE-BASED FORMULATION OF AN IRIDIUM COMPLEX FOR PHOTODYNAMIC THERAPY OF CANCER

ana.caballero@ub.edu

A. B. Caballero[1], E. Ortega[2], G. Vigueras[2], V. Alvarado-Iglesia[1], J. Ruiz[2], P. Gamez[1]

[1] nanoBIC, Departament de Química Inorgànica i Orgànica, Universitat de Barcelona; Institut de Nanociència i Nanotecnologia de la Universitat de Barcelona (IN²UB).
[2] Departamento de Química Inorgánica, Universidad de Murcia.

Photodynamic therapy (PDT) is an approach that is gaining interest in medicine, and most particularly in cancer treatment. This is thanks to its high selectivity, low side effects, lack of drug resistance, non-invasive nature and easy combination with other treatments[1]. PDT requires the simultaneous presence of a photosensitizer, molecular oxygen and light. Upon irradiation and subsequent intersystem crossing, the photosensitizer ends into a long-lived triplet excited state, which reacts with a biomolecule and/or molecular oxygen and releases, respectively, reactive oxygen species (ROS) and/or $^1O_2$. Such species are extremely harmful and will induce severe cellular damages, resulting in necrosis and/or apoptosis[2].

In this work, we present our latest results on the use of cyclometallated Ir(III) complexes as photosensitizers for their application in PDT. Moreover, we describe how the use of drug delivery systems, such as albumin-capped gold nanoparticles, modifies the in vitro biological activity and mechanism of action of the iridium drug in tumor cell lines.

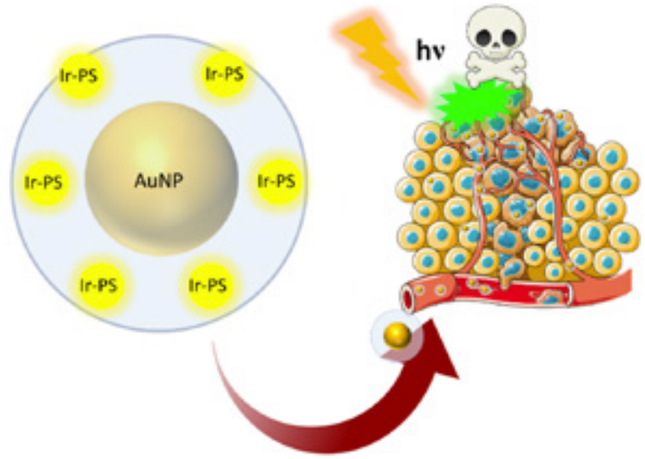

References
1. M. Lan, S. Zhao, W. Liu, C.-S. Lee, W. J. Zhang, P. F. Wang. Adv. *Healthcare Mater*. **2019**, 8, 1900132.
2. C. Imberti, P. Zhang, H. Huang, P. J. Sadler, *Angew. Chem. Int.* Ed. **2020**, 59, 61.

P16

EPIGALLOCATECHIN-3-GALLATE-LOADED PEGYLATED PLGA NANOPARTICLES TO REDUCE THE STRIATAL PATHOLOGY AND MOTOR DEFICITS IN A MICE MODEL OF HUNTINGTON'S DISEASE

acanofernandez@ub.edu

A. Cano[1,2,3], M. Ettcheto[3,4], M. Espina[1,2], E. Sánchez-López[1,2,3], P. Turowski[5], A. Camins[3,4], M.L. García[1,2,3]

[1] Department of Pharmacy, Pharmaceutical Technology and Physical Chemistry, Faculty of Pharmacy and Food Sciences, University of Barcelona, Spain.
[2] Institute of Nanoscience and Nanotechnology (IN²UB), Barcelona, Spain.
[3] Biomedical Research Networking Centre in Neurodegenerative Diseases (CIBERNED), Madrid, Spain.
[4] Department of Pharmacology, Toxicology and Therapeutic Chemistry, Faculty of Pharmacy and Food Sciences, University of Barcelona, Spain.
[5] UCL Institute of Ophthalmology, University College of London, United Kingdom.

Neurodegenerative diseases diseases are increasingly prevalent in developed countries. Huntington's disease (HD), an autosomal neurodegenerative disease, is mainly characterized by a motor dysfunction accompanied by behavioural disturbances ranging from irritability, apathy to depression and cognitive decline (1). Currently, HD affects ca. 5-10/100,000 individuals in developed countries with recent rises potentially linked to an increase in mutation rates.The main cause of its appearance is the incorrect folding of protein Huntingtin. HD is a chronic pathology, with affected individuals expected to survive for 15–20 years after the onset of first symptoms. There are only two drugs currently approved by the *Food and Drug Administration* for the treatment of HD, tetrabenazine and its deuterated derivative SD-809, but they do not cure the disease and lead to serious adverse effects, such as deterioration of pre-existing depressions[1]. For this reason, many efforts have been done to find new treatments for this pathology. Phytochemicals have shown to provide neuroprotection in many neurodegenerative diseases. In this sense, Epigallocatechin-3-gallate (EGCG) has aroused much interest for its multiple beneficial effects in neurological diseases, but its stability and bioavailability problems compromise its therapeutic success[2]. The use of nanomaterials for the development of controlled drug release systems is one of the most interesting alternatives of the last decades for the administration of compounds with these characteristics. Polymeric nanoparticles (NPs) are among the most explored vehicles in nanomedicine, specifically those composed of poly (lactic-co-glycolic acid) (PLGA) matrices. Thus, here we present EGCG-loaded PLGA-PEG NPs (EGCG NPs) to protect the EGCG stability, improve its brain penetration and enhance the symptomatology of HD[1]. For this aim, NPs were prepared by the double emulsion method and a physicochemical study was performed. An *in vitro* and *ex vivo* models of the blood-brain barrier (BBB) were developed to evaluate the penetration of EGCG NPs into the brain[2]. 3-nitropropionic (3-NP) C57BL/6 mice model was used to evaluate the nanocarrier efficacy. Beam-walk and Tail Suspension tests were used as determinant parameters of motor behavior and depressive state, respectively. Immunohistochemistry of glial fibrillary acidic protein (GFAP) were performed to evaluate the neuroinflammation state of study groups. Fluorojade-C and Nissl staining was performed to analyze the neurodegeneration. Obtained results evidenced that EGCG NPs induce tight junction disruption and opened the BBB *in vitro* and *ex vivo*, leading to an increase of EGCG amount in the brain. Treatment of 3-NP mice with free EGCG NPs resulted in a significant improvement in the neurological score, which was close to 0. Likewise, EGCG NPs exhibited a potent antidepressant effect in 3-NP HD-induced mice. In addition, EGCG NPs significantly reduced the motor dysfunctions, neuroinflammation and neurodegeneration of treated mice, more than free drug (2). In summary, the current study adds to increasing evidence of significantly improved pharmacological effectivity of EGCG when loaded into PLGA-PEG NPs. Mechanistically, we propose that stabilisation of EGCG in NPs complexes and a destabilised BBB led to higher therapeutic EGCG concentrations in the brain, which clearly participate in the increased effect of the drug. Indeed, NP encapsulation clearly renders EGCG more robust for in vivo application and thus EGCG/AA NPs will facilitate future pre-clinical studies assessing the effectiveness of this phytochemical in ND. Our data highlight the potential benefits of this novel NPs formulation to manage the neurological symptoms of HD and thus, we propose that EGCG/AA NPs could be a novel and promising adjuvant for the symptomatic treatment of a wide range of ND, and HD in particular.

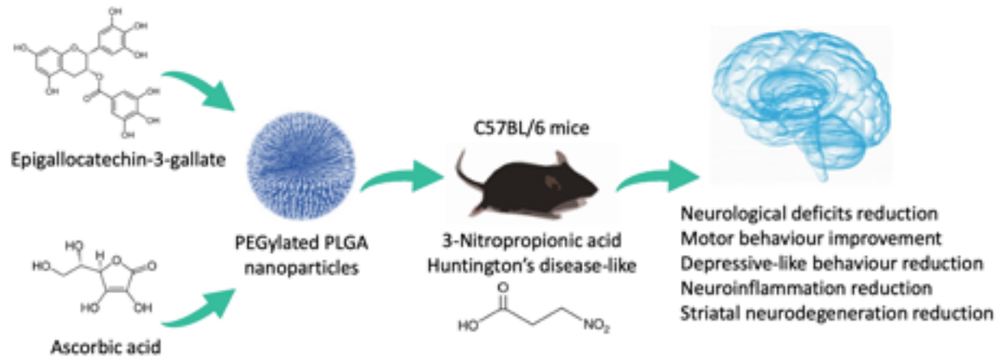

References

1. Cano A, Ettcheto M, Espina M, Auladell C, Folch J, Kühne BA, et al. Epigallocatechin-3-gallate PEGylated poly (lactic-co-glycolic) acid nanoparticles mitigate striatal pathology and motor deficits in 3-nitropropionic acid intoxicated mice. *Nanomedicine (Lond)*. 2021;16(1):19–35.
2. Cano A, Ettcheto M, Chang J, Barroso E, Espina M, Kühne B, et al. Dual-drug loaded nanoparticles of Epigallocatechin-3-gallate (EGCG)/ Ascorbic acid enhance therapeutic efficacy of EGCG in a APPswe / PS1dE9 Alzheimer' s disease mice model. *Journal of Controlled Release*. 2019;301:62–75.

P17
BIODEGRADABLE RILUZOLE NANOPARTICLES WITH THERAPEUTIC POTENTIAL FOR ALZHEIMER'S DISEASE

gesteruelas@ub.edu

G. Esteruelas[1,2*], L. Bonilla1,2, V. Garcia[1], M. Espina[1,2], A. Cano[1,2], E. B. Souto[3], M. L. Garcia[1,2], E. Sánchez-López[1,2]

[1] Department of Pharmacy, and Pharmaceutical Technology and Physical Chemistry. Faculty of Pharmacy and Food Science. University of Barcelona, 08028 Barcelona, Spain
[2] Institute of Nanoscience and Nanotechnology (IN²UB). University of Barcelona; 08028 Barcelona, Spain
[3] Faculty of Pharmacy (FFUC). Department of Pharmaceutical Technology. University of Coimbra, Pólo das Ciências da Saúde, Azinhaga de Santa Comba, 3000-548 Coimbra, Portugal

It is well known that life expectancy has increased significantly. Moreover, the incidence of neurodegenerative diseases such as Alzheimer's disease (AD), constitutes one of the main causes of dementia worldwide, affecting more than 46.8 million people. Despite this high incidence, no treatments are available able to cure AD[1]. In this sense, low drug penetration trough the Blood Brain Barrier (BBB) constitutes a major drawback for AD treatment. Therefore, nanostructured systems may facilitate drug transport across the BBB offering a prolonged and sustained release. Among different types of nanostructured systems, PLGA nanoparticles (NPs) are approved by the FDA and have been widely used for pharmaceutical applications. Moreover, among different strategies, Riluzole (RLZ) is a neuroprotective drug with high potential for AD. However, due to its physicochemical characteristics its transport across the BBB is highly limited. Consequently, in the present study, PLGA nanoparticles (NPs) have been developed encapsulating RLZ.

To carry out the preparation of RLZ loaded NPs, the solvent displacement method was used[2]. In order to optimize the formulation obtaining the maximum information with the minimum number of experiments, a central factorial experimental design was carried out. RLZ NPs were characterized physiochemically by analysing average size, polydispersity index, zeta potential and encapsulation efficiency. RLZ loaded NPs interactions were assessed by means of differential scanning calorimetry (DSC), Fourier transform infrared spectroscopy (FTIR) and X-ray diffraction (XRD). In addition, RLZ loaded NPs were negatively stained and visualized using transmission electron microscope.

In the optimization process of RLZ loaded NPs, significant parameters were studied. In this way, pH was one of the independent variables that highly influenced the physicochemical parameters of RLZ NPs. Moreover, optimized RLZ NPs showed an average size below 200 nm and a monomodal population. In addition, entrapment efficiency was higher than 90 %. Interaction studies (DSC and XRD) showed that RLZ was encapsulated and dispersed within the polymeric matrix. Moreover, FTIR confirmed that no new bonds between RLZ and PLGA were formed. Finally, microscopical images (Figure 1) showed that RLZ NPs possess a spherical shape without any signs of aggregation.

In conclusion, a new drug delivery system based in biodegradable polymeric PLGA NPs able to encapsulate high amount of RLZ has been optimized and physiochemically characterized. In this sense, RLZ NPs could constitute a suitable drug delivery system for the treatment of AD.

Figure 1. *A) Transmission electron microscopy of RLZ NPs, B) XRD profile of RLZ NPs and their components and C) DSC thermograms of RLZ NPs and their components*

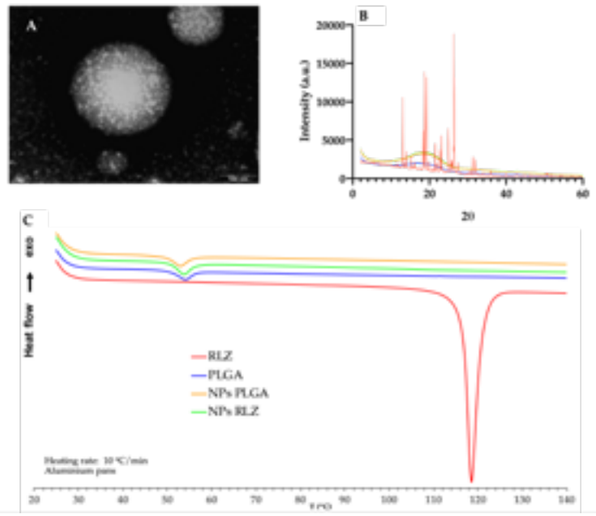

References
1. Mancino R, Martucci A, Cesareo M, Giannini C, Corasaniti MT, Bagetta G, *et al.* Glaucoma and Alzheimer Disease: One Age-Related Neurodegenerative Disease of the Brain. Curr Neuropharmacol. 2017;16(7):971–7.
2. Sánchez-López E, Esteruelas G, Ortiz A, Espina M, Prat J, Muñoz M, *et al.* Article dexibuprofen biodegradable nanoparticles: One step closer towards a better ocular interaction study. Nanomaterials. 2020;10(4):1–24.

P18
MELATONIN LOADED LIPID NANOPARTICLES FOR THE TREATMENT OF OCULAR NEURODEGENERATION

lbonilla95@ub.edu

L. Bonilla[1,2*], G. Esteruelas[1,2], A. Cano[1,2], E. B. Souto[3], M. L. García[1,2], M. Espina[1,2], E. Sánchez-López[1,2]

1 Department of Pharmacy and Pharmaceutical Technology and Physical Chemistry. Faculty of Pharmacy and Food Sciences, University of Barcelona, 08028 Barcelona, Spain.
2 Institute of Nanoscience and Nanotechnology (IN²UB). University of Barcelona, 08028 Barcelona, Spain.
3 Department of Pharmaceutical Technology. Faculty of Pharmacy. University of Coimbra (FFUC). Pólo das Ciências da Saúde, Azinhaga de Santa Comba, 3000-548 Coimbra, Portugal.

Glaucoma is one of the leading causes of blindness worldwide. It constitutes a multifactorial optic neuropathy; which cause is still unknown and its major risk factor is the elevated intraocular pressure (IOP). To date, there is no effective treatment able to cure glaucoma and the majority of the available therapies focus on IOP reduction. In this sense, Melatonin (MEL), is a neurohormone synthesized in the eye, which has been proven highly effective in order to reduce IOP. However, MEL suffers from instability and poor bioavailability in inner tissues when administered topically. Therefore, MEL bioavailability can be improved by developing drug delivery systems such as the last generation of lipid nanoparticles (NLC).

The aim of this work is the encapsulation of MEL into NLC functionalized with a cationic lipid for topical administration in order to reduce IOP [1]. NLC were prepared by hot high-pressure homogenization method and a design of experiments was used to optimize the developed formulation, where a series of independent parameters and their influence on NLC properties were studied. After obtaining an optimized formulation, a cationic lipid was added to increase the retention time on the ocular surface. The morphology of the optimized NLC was determined by transmission electron microscopy (TEM). Moreover, *in vitro* ocular tolerance was carried out performing the HET-CAM® test as described in the INVITTOX n°15 protocol. HET-CAM is based on the observation of the irritant effects (bleeding, vasoconstriction and coagulation) in the chorioallantoic membrane (CAM) of an embryonated egg. Ocular irritation was determined using the ocular irritation index (OII) [2].

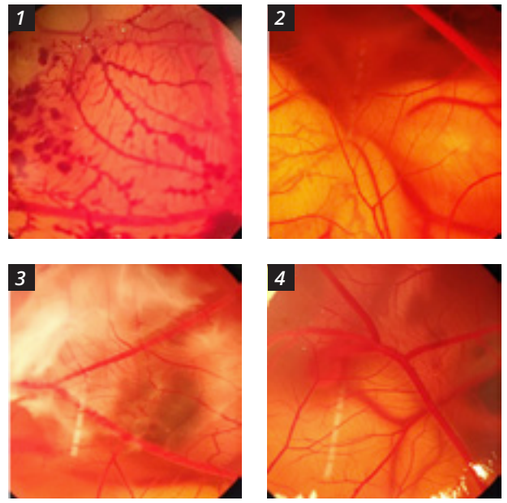

Image 1. *Positive control NaOH 0.1M*
Image 2. *Negative control NaCl 0.9 %*
Image 3. *NLC MEL*
Image 4. *Free MEL*

An optimized formulation coated with a cationic lipid was obtained showing a mean average size below 150 nm and a polydispersity index lower than 0,300. Moreover, zeta potential was around 20 mV which will facilitate NLC internalization. Developed NLCs were able to encapsulate around 50 % of the initial MEL. TEM images demonstrate that MEL NLC were spherical and non-aggregated with an average size that was in agreement with DLS measurements. In vitro ocular tolerance was studied using the HET-CAM test, by applying 300 µl of the substance directly to the CAM. In this sense, NaCl 0.9 % was used as a negative control and NaOH as a positive control (Image 1 and 2 respectively). MEL NLC and free MEL solution, were assessed and their OII was calculated. The results of MEL NLC revealed optimal ocular tolerance during the first 5 min of application being classified as non-irritant (Image 3). Otherwise, free MEL solution was moderately irritating (Image 4). This difference may be due to the fact that NLC are able to release MEL in a prolonged manner avoiding its irritant effects.

In conclusion, cationic MEL loaded NLC were optimized in order to be topically applied for the treatment of glaucoma and showed an optimal ocular tolerance *in vitro*.

References
1. Occhiutto ML, Maranhão RC, Costa VP, Konstas AG. Nanotechnology for Medical and Surgical Glaucoma Therapy—A Review. Adv Ther. 2020;37(1):155-99.
2. Sánchez-López E, Egea MA, Cano A, Espina M, Calpena AC, Ettcheto M, *et al.* PEGylated PLGA nanospheres optimized by design of experiments for ocular administration of dexibuprofen-in vitro, ex vivo and in vivo characterization. Colloids Surfaces B Biointerfaces. 2016;145:241-50.

P19
BIODEGRADABLE NANOPARTICLES AS NANOCARRIERS FOR PROTEIN DELIVERY IN OCULAR INFLAMMATORY DISEASES

alopezmachado@ub.edu

A. López-Machado[1,2], N. Díaz Garrido[3,4,5], A. Cano[1,2,6], M. Espina[1,2], J. Badía[3,4,5], L. Baldomà[3,4,5], E. B. Souto[7,8], M. L. García[1,2,6], E. Sánchez-López[1,2,6]

[1] Department of Pharmacy, Pharmaceutical Technology and Physical Chemistry, Faculty of Pharmacy and Food Sciences, UB, Barcelona, Spain.
[2] Institute of Nanoscience and Nanotechnology (IN²UB), UB, Spain.
[3] Department of Biochemistry & Physiology, Faculty of Pharmacy & Food Sciences, UB, Spain.
[4] Institute of Biomedicine, University of Barcelona (IBUB), Spain.
[5] Institut de Recerca Sant Joan de Deu (IRSJD), Spain
[6] Biomedical Research Networking Centre in Neurodegenerative Diseases (CIBERNED), Spain.
[7] Department of Pharmaceutical Technology, Faculty of Pharmacy, University of Coimbra, Portugal.
[8] CEB—Centre of Biological Engineering, Campus de Gualtar, University of Minho, Braga, Portugal.

One of the most prevalent pathologies in ophthalmology is ocular inflammation. Since conventional treatments such as corticosteroids, cause various side effects, drug alternatives have become an unmet medical need. In this sense, bovine lactoferrin (bLF), an iron-binding glycoprotein, constitutes a promising alternative due to its important antioxidant and anti-inflammatory properties[1].

However, its instability in aqueous solution and nasolacrimal duct drainage compromises its potential effectiveness, resulting in a pre-corneal drug half-life of 1-3 minutes and only a 5% of the dose penetrates the cornea and is able to reach intraocular tissues[2]. To overcome these drawbacks, bLF has been encapsulated into a biodegradable polymer for the development of a colloidal carrier for controlled drug release, aimed to enhance their corneal surface contact and their ocular penetration into the different structures[3].

bLF nanoparticles (NPs) were prepared using the double emulsion method and optimized using the design of experiment (DoE) approach. The optimized formulation showed a monodisperse population with an average size of 130 nm and positive surface charge. Cells culture assays did not show cytotoxic effects on corneal epithelial cells. The ability to inhibit inflammatory response caused by lipopolysaccharide was also evaluated obtaining a significantly decreased in the expression of proinflammatory cytokines, such as IL-8 and TNFα. Moreover, it was evaluated the cellular internalization of bLF-NPs associated to Rhodamine. NPs visualized by confocal fluorescent microscopy were found in the cytoplasm (Figure 1). In addition, the in vivo assay consisted of the ocular uptake of the fluorescent formulation was carried out. bLF-NPs were administered in the right eye of C57BL/6 adult male mice, after 48 h, the sectioned eye was analysed by fluorescence microscopy. Great fluorescence was observed in both the anterior and posterior segment of the eye treated with bLF-NPs.

According to the above studies, we have developed a novel nanotechnological tool in the treatment of ocular inflammation. The development of bLF-NPs could constitute a new non-invasive system for ocular treatment of conditions affecting both the anterior and posterior tissues.

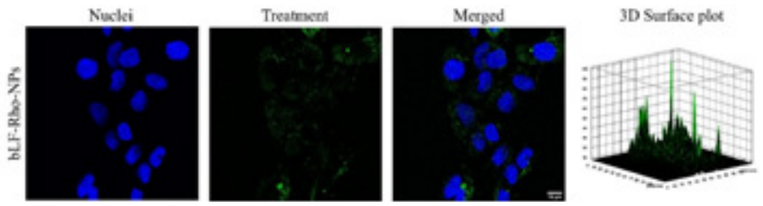

Figure 1. *Cellular uptake of bLF-NPs (dilution 1:50). Images are representative of three independent biological experiments. 3D surface mapping analysis of internalized NPs (green signal)*

References
1. Rageh, A. A. *et al.* Lactoferrin Expresion in Human and Murine Ocular Tissue. *Cur Eye Res* **41**, 883–889 (2017).
2. Sánchez-López, E. *et al.* PEGylated PLGA nanospheres optimized by design of experiments for ocular administration of dexibuprofen-in vitro, ex vivo and in vivo characterization. *Colloids Surfaces B Biointerfaces* **145**, 241–250 (2016).
3. Gonzalez-Pizarro, R. *et al.* Ocular penetration of fluorometholone-loaded PEG-PLGA nanoparticles functionalized with cell-penetrating peptides. *Nanomedicine* **14**, 3089–3104 (2019).

P20
SAFETY AND BIOLOGICAL ACTIVITY OF NANOMATERIALS WITHOUT EXPERIMENTAL ANIMALS: MAIN IN VITRO METHODOLOGIES. AN ETHICAL AND SUSTAINABLE APPROACH

mpvinardellmh@ub.edu

M. P. Vinardell[1,2], M. Mitjans[1,2]

[1] Dept. Bioquímica i Fisiologia, Universitat de Barcelona, Facultat de Farmàcia i Ciències de l'Alimentació. Av. Joan XXIII 27-31 Barcelona (Spain).
[2] Institut de Nanociència i Nanotecnologia (IN²UB), Universitat de Barcelona.

Nanomaterials (NMs) are an emerging class of functional materials with a wide range of applications. Applications of NMs in the field of biomedicine includes from drug delivery systems and platforms to coated medical devices. However, concerns have been expressed about the risks of such materials and whether they can cause adverse effects. Studies of the potential hazards of NMs can be studied without the use of experimental animals. Other research involving nanomaterials is their potential antitumoral effects or its use to enhance the therapeutic efficacy of anticancer drugs. All these in vitro methodologies constitute the research in our group. Here, we present the principal methods and techniques performed in our laboratory and the most significant results obtained.

Thus, in the case of NMS for uses that imply entering blood vessels or contacting blood or blood components, we evaluated their effects on coagulation, haemolysis and complement activation. These studies are performed with human blood and constitute simple and reliable methods following protocols developed for registration purposes. NMs are also found in formulations used in photoprotection. The study of photoprotective activity is also possible to be evaluated by using human derived cells exposed to UV light and studying cell viability, interleukin release and UV-induced DNA damage. Other interesting application is its use as targeted delivery systems to improve the potential antitumor activity by various strategies. In vitro studies allow to assess the cytotoxicity of such nanosystems and compare their efficacy in front of the raw compounds thanks to the use of different cancer cells and non-tumoral cell lines. This strategy must be the first line of preclinical studies not only for scientific reason (better understanding of mechanism for example) but also for ethical and economic reasons.

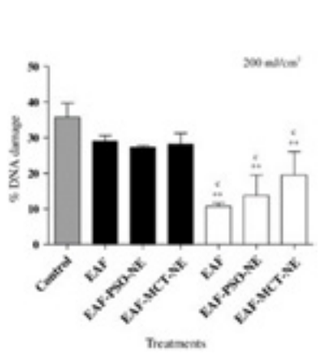

Figure 1. *Photoprotection of free EAF and EAF-loaded P. granatum nanoemulsions against UVB-induced DNA damage [1]*

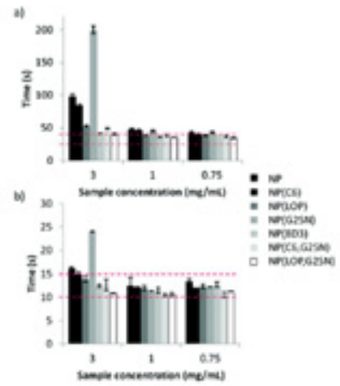

Figure 2. *Coagulation time of different Nanoparticles [2]*

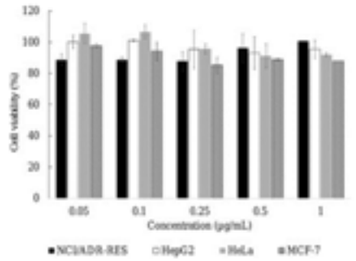

Figure 3. *Unloaded-PLGA-NPs in DOX-sensitive and resistant tumor cell lines by MTT assay [3]*

References
1. Baccarin T, Mitjans M, Ramos D, Lemos-Senna E, Vinardell MP. J Photochem Photobiol B. 153, 127-136 (2015).
2. Fornaguera C, Calderó G, Mitjans M, Vinardell MP, Solans C, Vauthier C. Nanoscale. 7, 6045-58 (2015).
3. Scheeren LE, Nogueira-Librelotto DR, Mathes D, Pillat MM, Macedo LB, Mitjans M, Vinardell MP, Rolim CMB. Toxicol In Vitro. 75,105192 (2021).

P21
ROLE OF EXPERIMENTAL CONDITIONS TO UNDERESTIMATE HEMOLYTIC ACTIVITY OF NANOMATERIALS

montsemitjans@ub.edu

M. Mitjans[1,2], J. J. Piñero[1], L. Marics[1], M. P. Vinardell[1,2]

[1] Departament de Bioquímica I Fisiologia, Facultat de Farmàcia i Ciències de l'Alimentació, Universitat de Barcelona.

[2] Institut de Nanociència i Nanotecnologia de la UB, IN²UB.

Interactions of nanomaterials (NMs) with blood or blood components is a preliminary step to characterize their cytotoxic profile. *In vitro* studies offer the possibility to evaluate such NMs before to address more complex and toxicological preclinical studies. However, the origin of blood, the composition of media or other are fundamental parameters than can lead to erroneous conclusions. Here we study the influence of different parameters on the potential haemolysis induced by commercial ZnO micro and nanoparticles (<50nm and <100 nm). For comparative purposes, some assays also were performed with AlO_3 (raw, nanopower 13 nm and nanowires). Previous studies of our group have determined the hemolytic activity of micro and nanoparticles of ZnO using phosphate buffer solution (PBs, pH7.4) and observed that ZnO particles tend to aggregate. However, when using the physiological solution of NaCl 0.9 % we observed a decrease of hemolytic activity in parallel with increase in ZnO concentration. In this sense, Cho *et al.*, (2013) describe that haemoglobin protein adsorb to ZnO nanoparticles and thus an underestimation of their potential hemolytic activity (1). This adsorption was demonstrated by incubating a haemoglobin solution in different media (PBS, NaCl 0.9 % and Tris-maleate buffer) and at different pH (5.7 and 7.4) in the presence of two metal oxides ZnO and AlO_3 (micro and nano). Results show that only zinc oxide can adsorb the haemoglobin protein in acidic media.

Other important thing is the origin of erythrocyte cells and the conditions of hemolytic assay. For these purposes, we have studied the hemolytic activity of different concentrations of ZnO particles in PBS and in PBS containing 0.5 mg/ml of albumin at room temperature and 37°C (using an incubator). Suspension of rat or human red cells were used for comparative purposes. Results obtained for both cell types at room temperature were inconsistent and with high variability and we attributed this inconsistency the impossibility of maintaining constant room temperature. Related to inclusion of 0.5 mg/ml of albumin, no significant effects were recorded suggesting that protein corona is not formed in this condition. Finally, related to erythrocyte sources, we found higher haemolysis in the case of rat than human origin probably due to by the existence of differences in cellular membrane lipid and protein composition between both species.

In conclusion, a good description of the different conditions related to biological assays to characterize NMs is fundamental to reach reliable and conclusive inferences about their toxicological activity.

References

1. Cho, W.; Duffin, R.; Bradley, M.; Megson, I. L.; Macnee, W.; Lee, J. K.; Jeong, J.; Donaldson, K. Predictive Value of in Vitro Assays Depends on the Mechanism of Toxicity of Metal Oxide Nanoparticles. Part. Fibre Toxicol. 2013, 10 (1), 1.

P22
IN VIVO MODULATION OF THE EXPRESSION OF PROINFLAMMATORY CYTOKINES BY A NATURAL FLAVANONE INCLUDED IN A NANOSTRUCTURED FORMULATION

pbustosa19@alumnes.ub.edu

P. Bustos-Salgado[1], N. Díaz Garrido[2], B. Andrade-Carrera[3], V. Domínguez-Villegas[3], J. Badía[2], L. Baldomà[2], A. C. Calpena-Campmany[1,4], M. L. Garduño-Ramírez[5]

[1] Department of Pharmacy and Pharmaceutical Technology and Physical Chemistry, Faculty of Pharmacy and Food Science, University of Barcelona, Av. Joan XXIII 29-31, Barcelona 08028, Spain. pbustosa19@alumnes.ub.edu (P.B.-S.), anacalpena@ub.edu (A.C.-C.).

[2] Department of Biochemistry and Physiology, Faculty of Pharmacy and Food Sciences, University of Barcelona, 08028 Barcelona, Spain. natalia.diaz.garrido@gmail.com (N.D.-G.), josefabadia@ub.edu (J.B.-P.), lbaldoma@ub.edu (L.B.-L.)

[3] Facultad de Ciencias Químicas e Ingeniería, Universidad Autónoma del Estado de Morelos; Av. Universidad 1001, 62209 Cuernavaca, Morelos, México; valeri.dominguez@uaem.mx (V.D.-V-), bereniceac@uaem.mx (B.A.-C.)

[4] Institute of Nanoscience and Nanotechnology (IN²UB), University of Barcelona, 08007 Barcelona, Spain.

[5] Centro de Investigaciones Químicas, Instituto de Investigación en Ciencias Básicas y Aplicadas, Universidad Autónoma del Estado de Morelos; Av. Universidad 1001, 62209 Cuernavaca, Morelos, México. lgarduno@uaem.mx (M.L.G.-R.)

Skin inflammation is one of the most common skin problems [1,2]. The intensity of inflammation and the time to resolution are critical in avoiding or limiting damage to normal skin tissue. Non-steroidal anti-inflammatory drugs (NSAID) and also glucocorticoids are currently used to treat inflammation, but severe adverse effects make these drugs unsuitable for chronic therapies [3,4]. Plant-derived natural compounds may potentially be suitable in this regard [5,6]. Flavonoids have the potential to inhibit the enzymes involved in the metabolism of arachidonic acid (AA) decreasing the release of the inflammatory mediators derived from this pathway [2]. In addition, the nanostructured systems provide an advantage in improving the delivery of flavanones into the active site [7]. In our previous investigations, we have shown that in vivo, the topic application of the FF**1** produces an anti-inflammatory effect on skin [8]. Based on the above, the aim of this research was the evaluation of IL-1β, IL-6, and TNF-α gene expression in the AA edema rat model after treatment with a flavanone extracted from *E. platycarpa* formulated in a nanostructured system (FF**1**).

Materials and methods

The components of the nanostructured formulation of flavanone **1** ((2S)-5,7-dihydroxy-6-prenylflavanone)) (**FF1**, 5 %w/w) were: Labrasol, Labrafac lipophile, Plurol oleique and propylene glycol. The test AA edema rat model was developed using adult male Sprague Dawley rats. Firstly, an arachidonic acid solution (5 mg/ mL) was applied on both sides of all the animals 'ears (n = 5, 200 - 240 g), except the negative control group (C^-). The animals in the positive control group (C^+) were treated only with an AA solution. The experimental group was treated with 50 µL of FF**1**. In parallel, another group was treated with commercial gel diclofenac sodium 10 mg/g as the reference drug formulation (RdF). Passed 20 min of treatment, the quantification of cytokine mRNA expression was assessed from small sections of rat ear tissue. Total RNA was isolated using TRIZol method following the manufacturer´s protocol. RNA concentration and quality were tested and the RNA integrity was verified. The RNA was reversed transcribed to cDNA using a High Capacity cDNA Reverse Transcription kit. Afterward, qPCR was performed using a Master Mix and specific oligonucleotides for IL-6, TNF-α and IL-1β (Table 1). Relative gene expression of each gene was normalized to β-actin and the $2^{-\Delta\Delta Ct}$ formula was used to calculate fold-change.

Table 1: *Primer sequences used for quantitative RT-qPCR.*

Gene (Rat)	Primer sequences (5´- 3´)	Gene accession number
IL-6	FW: AGAAAAGAGTTGTGCAATGGCA RV: GGCAAATTTCCTGGTTATATCC	NM_012589.2
TNF-α	FW: AAATGGGCTCCCTCTCATCAGTTC RV: TCTGCTTGGTGGTTTGCTACGAC	NM_012675.3
IL-1β	FW: CACCTCTCAAGCAGAGCACAG RV: GGGTTCCATGGTGAAGTCAAC	NM_031512.2

Results

Treatment with FF**1** significantly reduced the expression of TNF-α, IL-6 and IL-1β (Figure 1). For IL-6 expression, the inhibitory activity of FF1 was higher than the reference anti-inflammatory drug formulation (RdF).

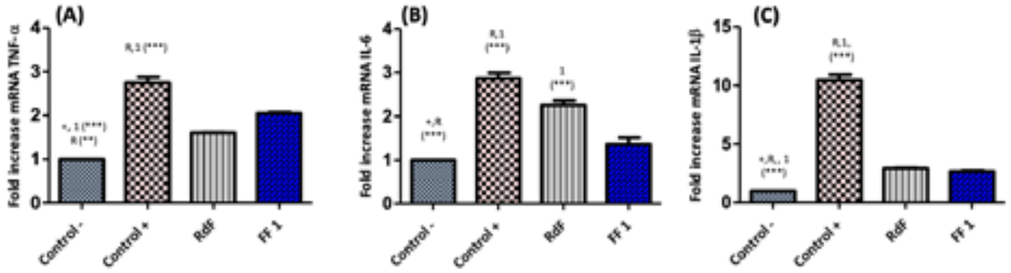

Figure 1. *Relative expression of cytokines: (A): TNF-α; (B): IL-6; (C): IL-1β. Non-treated rats (Control −), rats treated only with AA (Control +), rats treated with diclofenac gel (RdF), rats treated with FF1. Significant difference between Control + (+), RdF (R), FF1 (1) ** p < 0.01, *** p < 0.001 was assessed by non-parametric Tukey's t-test (n = 5)*

Conclusions

Based on the FF1 potential to reduce expression of proinflammatory cytokines, this formulation is a promising therapeutic alternative to treat inflammatory skin conditions.

References

1. Abdel-Mottaleb MM, Try C, Pellenquer Y, Lamprecht A. Nanomedicine Strategies for Targeting Skin Inflammation. *Nanomedicine* 9(11), 1–20 (2014).
2. Maleki SJ, Crespo JF, Cabanillas B. Anti-inflammatory effects of flavonoids. *Food Chem.* 299(July) (2019).
3. Paoletti T, Fallarini S, Gugliesi F, Minassi A, Appendino G, Lombardi G. Anti-inflammatory and vascularprotective properties of 8-prenylapigenin. *Eur. J. Pharmacol.* 620(1–3), 120–130 (2009).
4. Park KE, Qin Y, Bavry AA. Nonsteroidal anti-inflammatory drugs and their effects in the elderly. *Aging health* 8(2), 167–177 (2012).
5. Singh MR, Nag MK, Patel S, Daharwal SJ. Novel Approaches for Dermal and Transdermal Delivery of Herbal Drugs. *J. Pharmacogn. Phytochem.* 5(6), 271–279 (2013).
6. Scheau C, Badarau IA, Mihai L et al. Cannabinoids in the Pathophysiology of Skin Inflammatio. *Molecules* 25(3), 652 (2020).
7. Gopi S, Amalraj A, Haponiuk J, Thomas S. Introduction of Nanotechnology in Herbal Drugs and Nutraceutical: A Review. *J. Nanomedine. Biotherapeutic Discov.* 6(2), 1–8 (2016).
8. Bustos-Salgado P, Andrade-Carrera B, Domínguez-Villegas V et al. Biopharmaceutic study and in vivo efficacy of natural and derivatives flavanones formulations. *Nanomedicine* 16(3), 368 (2021).

P23
NOVEL ANTIFUNGAL DRUG AND NEW FORMULATION FOR THE TREATMENT OF ORAL CANDIDIASIS

elisa.giannone@studio.unibo.it

N. Pérez-González[1], J. A. Morales-Molina[2,3], E. Giannone[4], L. Halbaut-Bellowa[5,6], M. J. Rodríguez-Lagunas[7,8], B. Clares-Naveros[1,3,5], A. C. Calpena-Campmany[5,6]

[1] Department of Pharmacy and Pharmaceutical Technology, Faculty of Pharmacy, University of Granada, Granada, Spain
[2] Pharmacy Department, Torrecardenas Hospital, Almería, Spain
[3] Biomedical Research Institute ibs. Granada, Spain
[4] University of Bologna, Bologna, Italy
[5] Institute of Nanoscience and Nanotechnology (IN²UB), University of Barcelona, 08028 Barcelona, Spain
[6] Department of Pharmacy & Pharmaceutical Technology & Physical Chemistry, Faculty of Pharmacy & Food Sciences, University of Barcelona, 08028, Barcelona, Spain
[7] Department of Biochemistry & Physiology, Faculty of Pharmacy & Food Sciences, University of Barcelona, 08028, Barcelona, Spain
[8] Institute of Biomedicine, University of Barcelona, 08028, Barcelona, Spain

In the last decades, the incidence of fungal infections has increased due to defects in the immune system. A growing emergence of candidiasis oral fungal infections is evident[1]. In recent years, a growing concern about resistance to anti-infective agents has emerged. One of the most common microbial agents is *Candida albicans*. Under certain conditions, *Candida ssp* can cause infections of mucosal tissues. Although patients respond adequately to topical antifungal treatments, new strategies and drugs are needed. Therefore, it is important to investigate new antifungal agents that increase the therapeutic arsenal available to date[2,3].

Purpose

The aim of this work was to develop a hydrogel prepared with Pluronic® F-127 (P407) for the treatment of oral candidiasis.

Methods

The gel CSP-B3 was obtained by the cold method, by keeping the P407 under stirring for 24 hours. The nanometric structure of the gel was determined using a ZetaSizer® Nano ZS (Malvern Instruments Ltd., Malvern, UK), the mean droplet size (Z-ave) and its distribution expressed by polydispersity index (PI) were recorded at 10, 25 and 32°C. The rheological behaviour of the gel was studied using a Haake Rheostress 1 rheometer. Evolutions of biomechanical properties of the buccal tissues such as transmucosal water loss (TMWL, using Tewameter®) and stratum corneum hydration (SCH, using Corneometer® 825) were tested in ex vivo before and after the treatment. Histological analysis of sample and positive and negative control was performed. Moreover, the antifungal activity of the formulation has been investigated by Kirby-Bauer Disk Diffusion Susceptibility Test against *Candida spp*.

Results and Discussions

DLS measurements of CSP-B3 showed Z-ave values of 116.20 ± 13.54, 341.50 ± 10.87 and 75.89 ± 4.69 nm, with PI values of 1.00 ± 0.68, 0.97 ± 0.53 and 0.38 ± 0.33 at 10, 25 and 32°C, respectively. The biomechanical properties of the tissue before and after the treatment is shown in Fig 1. There were no changes in TMWL and SCH values after CSP-B3 application. The rotational analysis shows that CSP-B3 exhibits a behaviour characteristic of a shear thinning system at both 25°C and 32°C. Histological analysis doesn't show a change in the tissues treated with CSP-BE respect control +, then the formulation does not lead alteration in ex-vivo tissues analysis. Moreover, CSP- B3 is totally effective on 4 Candida strains: *C. glabrata, C. albicans, C. tropicalis* and *C. parapsilosis*.

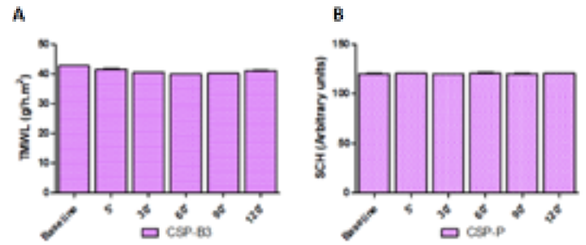

Figure 1. *Biomechanical parameters evolution monitored before and 2 hours after application. Change in TEWL value, A, and Change in SCH value, B*

Conclusion

The formulation shows efficient antifungal activity and does not cause tissues alterations, thus representing a potential new pharmaceutical formulation towards fungal infections of the oral cavity.

References

1. Krishnan, P. A. Fungal Infections of the Oral Mucosa. *Indian J. Dent. Res. Off. Publ. Indian Soc. Dent. Res.* **2012**, 23 (5), 650–659.
2. Letscher-Bru, V. Caspofungin: The First Representative of a New Antifungal Class. *J. Antimicrob. Chemother.* **2003**, 51 (3), 513–521.
3. Walker, L. A.; Munro, C. A. Caspofungin Induced Cell Wall Changes of Candida Species Influences Macrophage Interactions. *Front. Cell. Infect. Microbiol.* **2020**, 10, 164.

P24
DEVELOPMENT AND CHARACTERIZATION OF NEW ANTIFUNGAL FORMULATIONS TO COMBAT OCULAR KERATITIS.

rmohammo31@alumnes.ub.edu

N. Pérez-González[1], J. A. Morales-Molina[2,3], R. Mohammadi-Meyabadi[4], M. J. Montes-López[5], B. Clares-Naveros[1,3,6], A. C. Calpena-Campmany[4,6]

[1] Department of Pharmacy and Pharmaceutical Technology, Faculty of Pharmacy, University of Granada, Granada, Spain.
[2] Pharmacy Department, Torrecardenas Hospital, Almería, Spain.
[3] Biomedical Research Institute ibs.Granada, Spain.
[4] Department of Pharmacy and Pharmaceutical Technology and Physical Chemistry, Faculty of Pharmacy and Food Sciences, University of Barcelona, Barcelona, Spain.
[5] Laboratory of Microbiology, Sanitary Microbiology and Parasitology Department, Division of Health Sciences, Faculty of Pharmacy, University of Barcelona, Joan XXIII Avenue s/n, 08028 Barcelona, Spain.
[6] Institute of Nanoscience and Nanotechnology (IN²UB), University of Barcelona, 08028 Barcelona, Spain.

Fungal keratitis or keratomycosis is an infection of the cornea caused by *Candida, Aspergillus* and *Fusarium spp*. It is very difficult to treat because it does not respond to current antifungal treatments. Surgical intervention may be necessary in some cases. Unfortunately, ocular keratitis has not been successfully treated because the available treatments are very limited[1]. In order to increase therapeutic options, a new group of antifungals active against most *Candida spp* and *Aspergillus spp* is needed. Therefore, it is important to investigate the usefulness of new antifungal agents to augment the topical therapeutic arsenal[2-3].

Purpose

The aim of this work was to develop and characterize different Pluronic® F-127 (P407) formulations for the treatment of fungal keratitis.

Methods

The formulations were made adding P407 at two different concentrations using the cold method with continuous stirring for 24 hours. The formulations were characterized by the following methods: pH and dynamic light scattering (DLS) measurements, scanning electron microscopy (SEM), ocular tolerance by Hen's Egg test (HET-CAM®), microbiological studies and appearance. The pH measurements were carried out at different temperatures, 4, 25 and 37°C, and at predetermined time intervals. The average droplet size (Z-ave) and its distribution (PI) was directly recorded at 25°C using a Zetasizer Nano ZS. The internal structure of the formulations was evaluated using a JEOL J-7100F. The ocular tolerability of the formulations was evaluated using the modified hen's egg chorioallantoic membrane test. The antimicrobial activity was evaluated through a Kirby-Bauer Disk Diffusion Susceptibility Test against *Candida spp*. The physical appearance was studied by visual observation of formulations stored 4, 25 and 37˚C.

Results and Discussion

No significant differences in pH (Table 1) were observed at all time points for three storage conditions and the measured pH was within the range tolerated by human eyes4. DLS measurements of CSP-O1 and CSP-O2 showed Z-ave values of 165.10 ± 15.07 and 447.60 ± 40.13 nm, with PI values of 0.41 ± 0.14 and 0.50 ± 0.22 at 25°C, respectively. Fig. 1 illustrates a network with an interconnected porous structure typical of poloxamer. The in vitro potential irritation was detected by the HET CAM test and coagulation, vascular lysis or hemorrhage were not seen in any way (Fig.2). CSP-O1 and CSP-O2 provide antimicrobial properties against strains of *C. albicans, C. tropicalis, C. glabrata* and *C. parapsilosis*. Signs of precipitation and a yellowish colour change were observed after 14 days at 25 and 37°C. The appearance remained unaltered at 4°C.

Nº of days of storage	CSP-01			CSP-02		
	Value at 4°C	Value at 25°C	Value at 37°C	Value at 4°C	Value at 25°C	Value at 37°C
0	6.73 ± 0.07	6.86 ± 0.02	6.62 ± 0.01	6.56 ± 0.01	6.72 ± 0.05	6.72 ± 0.02
3	6.67 ± 0.02	6.93 ± 0.04	6.50 ± 0.01	6.71 ± 0.01	6.78 ± 0.01	6.94 ± 0.01
7	6.84 ± 0.02	6.78 ± 0.04	6.36 ± 0.01	6.70 ± 0.03	6.75 ± 0.01	6.86 ± 0.02
14	6.88 ± 0.03	6.95 ± 0.04	6.55 ± 0.02	6.69 ± 0.09	6.66 ± 0.01	6.65 ± 0.04
21	6.84 ± 0.01	6.80 ± 0.03	6.31 ± 0.01	6.55 ± 0.01	6.43 ± 0.06	6.48 ± 0.01

Table 1. *pH values in samples stored at 4, 25 and 32°C. Values represent mean ± SD (n = 3).*

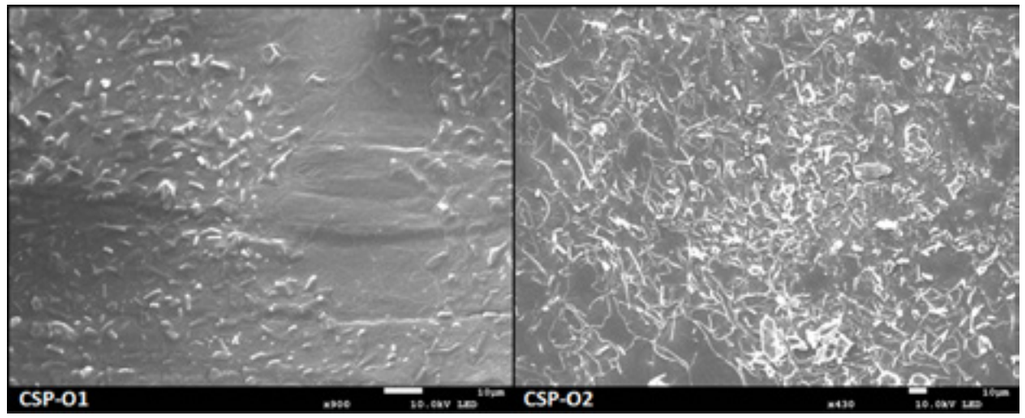

Figure 1. *Scanning Electron Microscopy images of CSP-O1 (x900) and CSP-O2 (x430)*

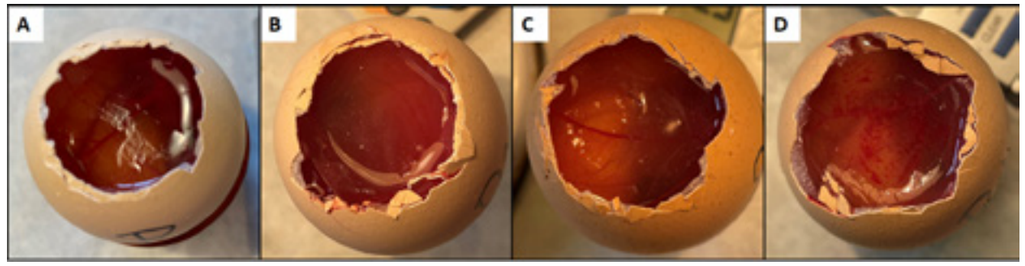

Figure 2. *Tolerance Ocular Assays (HET CAM®). A is the negative control, B is the CSP-O1, C is the CSP-O2 and D is positive control*

Conclusions

Both formulations exhibited non-irritant and significant antimicrobial effects. Thus, these formulations could be proposed as a suitable vehicle for new therapies for ocular keratitis.

References

1. C.F. Neoh, M. Daniell, E. Chan, P.F. Neoh, D.C.M. Kong, Clinical Utility of Caspofungin in Ocular Fungal Infections, in: Adv. Med. Biol., 2015.
2. C. Neoh, J. Jacob, L. Leung, J. Li, A. Stathopoulos, K. Stewart, D.C.M. Kong, Stability of extemporaneously prepared 0.5-percent caspofungin eye drops: A potential cost-savings exercise, Antimicrob. Agents Chemother. (2012). https://doi.org/10.1128/AAC.00060-12
3. C.F. Neoh, M. Daniell, S.C.A. Chen, K. Stewart, D.C.M. Kong, Clinical utility of caspofungin eye drops in fungal keratitis, Int. J. Antimicrob. Agents. 44 (2014). https://doi.org/10.1016/j.ijantimicag.2014.04.008
4. T.H. How, W.Y. Loo, K.L. Yow, L.Y. Lim, E.W. Chan, P.C. Ho, S.Y. Chan, Stability of cefazolin sodium eye drops, J. Clin. Pharm. Ther. 23 (1998). https://doi.org/10.1046/j.1365-2710.1998.00136.x

P25
NEW ANTIFUNGAL FORMULATION FOR THE TREATMENT OF DEMATOMYCOSIS: DESIGN AND EVALUATION

thuanghu8@alumnes.ub.edu

N. Pérez-González[1], J. A. Morales-Molina[2,3], N. Bozal-de Febrer[4], T. Huang[5], B. Clares-Naveros[1,3,6], A. C. Calpena-Campmany[5,6]

[1] Department of Pharmacy and Pharmaceutical Technology, Faculty of Pharmacy, University of Granada, Granada, Spain.
[2] Pharmacy Department, Torrecardenas Hospital, Almería, Spain.
[3] Biomedical Research Institute ibs.Granada, Granada.
[4] Laboratory of Microbiology, Sanitary Microbiology and Parasitology Department, Division of Health Sciences, Faculty of Pharmacy, University of Barcelona, Joan XXIII Avenue s/n, 08028 Barcelona, Spain.
[5] Department of Pharmacy and Pharmaceutical Technology and Physical Chemistry, Faculty of Pharmacy and Food Sciences, University of Barcelona, Barcelona, Spain.
[6] Institute of Nanoscience and Nanotechnology (IN²UB), University of Barcelona, 08028 Barcelona, Spain.

Cutaneous mycosis or dermatomycosis are among the most common and widespread fungal infections in humans. It is estimated that about 15 % of the population has had a fungal skin infection at least once during their lives. Dermatomycosis is an infection caused by fungal species of *Candida*, of which *Candida albicans* is the most common. Although patients respond adequately to topical antifungal treatments, new strategies and drugs are greatly needed. In order to avoid resistance to anti-infective agents, it is important to investigate the usefulness of new antifungals that are effective against strains of *Candida spp* and *Aspergillus spp*[1-3].

Purpose

The aim of this work was to design and evaluate a hydrogel prepared from a physical mixture of two polymers (P407 and CH) containing MK991 for the treatment of dermatomycosis.

Methods

CH was dispersed in acetic acid. The final hydrogel was made by adding P407 and MK991 using the cold method with continuous stirring for 24 hours. This hydrogel was characterized by dynamic light scattering (DLS) measurements, microbiological studies and extensibility test. Furthermore, biomechanical properties of skin, such as trans-epidermal water loss (TEWL) and stratum corneum hydration (SCH), were tested in vivo. TEWL and SCH were determined using a TewameterTM300, and a Corneometer CM 825, respectively. The average droplet size (Z-ave) and its distribution expressed as polydispersity index (PI) was directly recorded at 25 ± 0.5°C using a Zetasizer Nano ZS. The mechanical properties of the hydrogel were evaluated by placing a known weight inside a circle premarked on a glass plate over which a second glass plate was placed, on which force was generated.

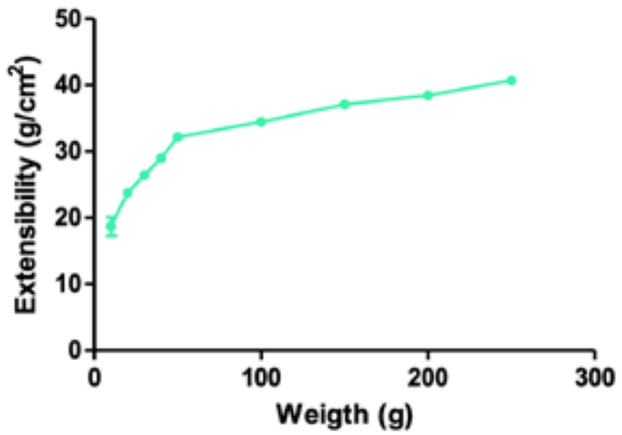

Figure 1. *Extensibility (g/cm2) at room temperature of hydrogel. Values represent mean ± SD (n=3)*

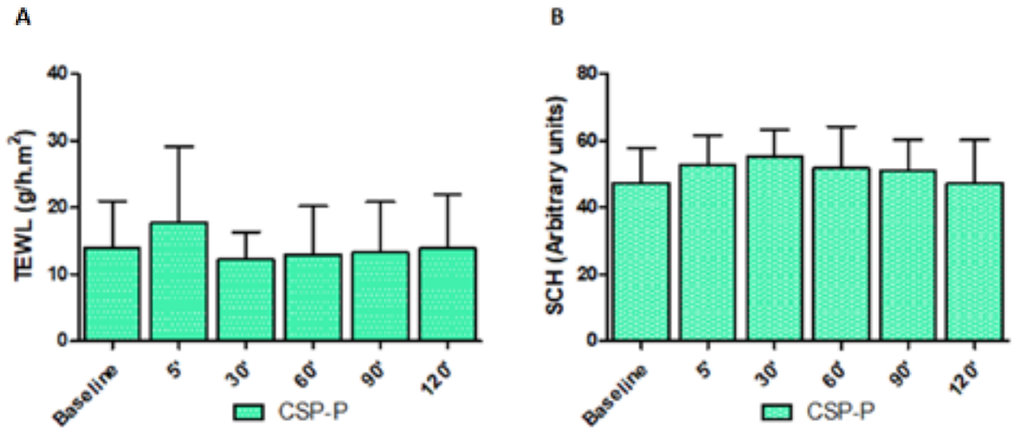

Figure 2. *Biomechanical parameters evolution monitored before and 2 hours after application. Change in TEWL value, A, and Change in SCH value, B. The study was approved by the Ethics Committee of the University of Barcelona*

Results and Discussion

DLS measurements of hydrogel showed Z-ave values of 590.30 ± 42.07 nm with PI values of 0.55 ± 0.21 at 25°C. Extensibility properties of hydrogel are an important factor to evaluate in topical administration. The correct administration dosage depends highly on the spreading. Fig. 1 show the extensibility results of formulation. The evolution of biomechanical parameters (TEWL and SCH) before and after the application of formulations assayed is show in Fig. 2. TEWL values are used as indicators of the integrity of the biological function of the tissue while SCH values indicate the conductance that free water provides to the skin surface. The hydrogel provides antimicrobial properties against strains of *C. albicans, C. tropicalis, C. glabrata* and *C. parapsilosis*.

Conclusions

This formulation could be proposed as a suitable vehicle for new therapies against skin infections by exhibiting biological and antimicrobial effects.

References

1. Micosis cutáneas Diagnóstico y tratamiento. Vicente Crespo-Erchiga a y Vicente Delgado-Florencio b - PDF Free Download, (n.d.). https://docplayer.es/36332420-Micosis-cutaneas-diagnostico-y-tratamiento-vicente-crespo-erchiga-a-y-vicente-delgado-florencio-b.html (accessed June 28, 2021).
2. S.D. Gunaydin, S. Arikan-Akdagli, M. Akova, Fungal infections of the skin and soft tissue, Curr. Opin. Infect. Dis. 33 (2020). https://doi.org/10.1097/QCO.0000000000000630
3. M. Borgers, H. Degreef, G. Cauwenbergh, Fungal Infections of the Skin: Infection Process and Antimycotic Therapy, Curr. Drug Targets. 6 (2005). https://doi.org/10.2174/138945005774912726

P26
DEVELOPMENT AND CHARACTERIZATION OF A THERMOSENSITIVE POLOXAMER-CHITOSAN HYDROGEL FOR THE TREATMENT OF VULVOVAGINAL CANDIDIASIS

noeliaperez93@correo.ugr.es

N. Pérez-González[1], J. A. Morales-Molina[2,3], M. Mallandrich[4,5], L. Halbaut-Bellowa[4,5], M. J. Rodríguez-Lagunas[6,7], B. Clares-Naveros[1,3,5], A. C. Calpena-Campmany[4,5]

[1] Department of Pharmacy and Pharmaceutical Technology, Faculty of Pharmacy, University of Granada, Granada, Spain.
[2] Pharmacy Department, Torrecardenas Hospital, Almería, Spain.
[3] Biomedical Research Institute ibs.Granada., Granada, Spain.
[4] Department of Pharmacy and Pharmaceutical Technology and Physical Chemistry, Faculty of Pharmacy and Food Sciences, University of Barcelona, Barcelona, Spain.
[5] Institute of Nanoscience and Nanotechnology (IN²UB), University of Barcelona, 08028 Barcelona, Spain.
[6] Department of Biochemistry & Physiology, Faculty of Pharmacy & Food Sciences, University of Barcelona, 08028, Barcelona, Spain.
[7] Institute of Biomedicine, University of Barcelona, 08028, Barcelona, Spain.

Vulvovaginal candidiasis (VVC) is one of the most common infections in women. This disease affects approximately 75% of women at least once during their lifetime, and mainly affects young women at childbearing age. Candida albicans accounts for 90-95 % of cases[1-2]. Most patients with VVC respond to topical treatment with antifungal drugs. Although drugs such as amphotericin B or fluconazole have advanced the treatment of fungal infections, mortality rates associated with invasive fungal infections remains high and there has been growing concern about resistance to anti-infective agents. Despite therapeutics advances, new drugs and strategies are greatly needed. Therefore, it is important to investigate the usefulness of new antifungals that are effective against strains of *Candida spp* and *Aspergillus spp*[3].

Purpose

The aim of this work was to develop and characterize a hydrogel prepared from a physical mixture of poloxamer 407 (P407) and chitosan (CH) for the treatment of VVC.

Methods

The physical mixture of P407 and CH was dispersed in water using the cold method with continuous stirring for 24 hours. The hydrogel was characterized by the following methods: rheological and dynamic light scattering (DLS) measurements, histological studies and scanning electron microscopy (SEM). Rheological analyses were carried out with a Haake Rheostress 1 rheometer. The average droplet size (Z-ave) and its distribution expressed as polydispersity index (PI) was directly recorded at 10,25 and 32 ± 0.5°C using a Zetasizer Nano ZS. Vaginal mucosa tissues, as well as, positive and negative controls were histologically evaluated in order to verify if the hydrogel could cause histological changes. Finally, the internal structure of the gel was evaluated using a JEOL J-7100F.

Results and Discussion

The hydrogel was fluid at 10°C and for this reason this system was predominantly viscous (G”>G’). When temperature increased the value of moduli sharply increased at 19°C. A crossover (G’=G”) of 11.25 Pa appeared at 19.5°C (Fig.1). DLS measurements of hydrogel showed Z-ave values of 205.30 ± 14.17, 590.30 ± 42.07 and 115.70 ± 10.31 nm, with PI values of 0.95 ± 0.54, 0.55 ± 0.21 and 0.46 ± 0.12 at 10, 25 and 32°C, respectively. Structural similarities between negative control and treated vaginal mucosa tissues were shown, confirming the tissue integrity. Both samples show the standards mucosa sections: underlying fibrous connective tissue and nonkeratinized stratified epithelium. After treatment, the epithelium maintains its structure with several cellular layers without any discontinuity. Fig. 2 illustrates a network with an interconnected porous structure typical of poloxamer with rough surfaces probably due to chitosan content.

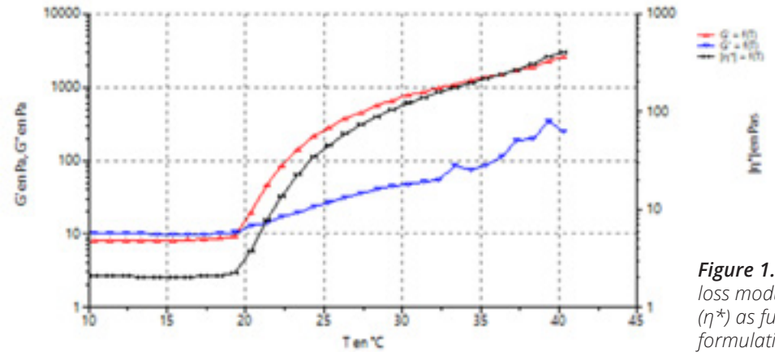

Figure 1. *Storage modulus (G’), loss modulus (G”) and complex viscosity (η*) as function of temperature of the formulation*

Conclusions

The hydrogel has great appeal for the treatment of localized infections and could be proposed as a suitable vehicle for VVC being an alternative therapy.

Figure 2. *Scanning Electron Microscopy images of the hydrogel (x1200)*

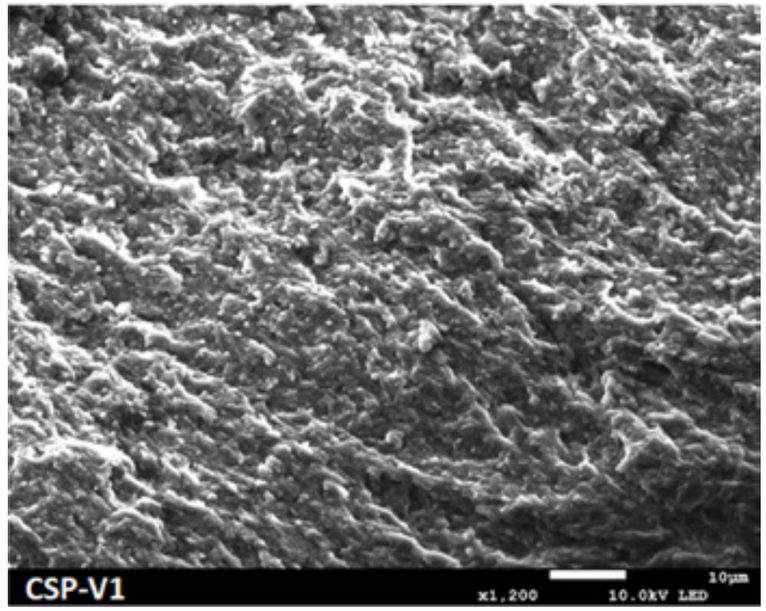

References

1. Sobel, J. D. (2007). Vulvovaginal candidiosis. *Lancet*. https://doi.org/10.1016/S0140-6736(07)60917-9
2. Sustr, V., Foessleitner, P., Kiss, H., & Farr, A. (2020). Vulvovaginal candidosis: Current concepts, challenges and perspectives. *Journal of Fungi*. https://doi.org/10.3390/jof6040267
3. Boucher, H. W., Groll, A. H., Chiou, C. C., & Walsh, T. J. (2004). Newer systemic antifungal agents: Pharmacokinetics, safety and efficacy. *Drugs*. https://doi.org/10.2165/00003495-200464180-00001

P27
DEVELOPMENT OF NEW NANOSTRUCTURED FORMULATIONS FOR FLAVANONE (2S)-5,7-DIHYDROXY-6-METHYL-8-PRENYL-FLAVANONE

karla.gonzalezped@uaem.edu.mx

K. F. González-Pedroza[1,2], A. C. Calpena-Campmany[3,4], M. L. Garduño-Ramírez[2]

[1] Licenciatura en Diseño Molecular y Nanoquímica, Instituto de Investigación en Ciencias Básicas y Aplicadas, Universidad Autónoma del Estado de Morelos, Av. Universidad 1001, 62209 Cuernavaca, Morelos, México karla.gonzalezped@uaem.edu.mx
[2] Centro de Investigaciones Químicas, Instituto de Investigación en Ciencias Básicas y Aplicadas, Universidad Autónoma del Estado de Morelos; Av. Universidad 1001, 62209 Cuernavaca, Morelos, México. lgarduno@uaem.mx
[3] Department of Pharmacy and Pharmaceutical Technology and Physical Chemistry, Faculty of Pharmacy and Food Science, University of Barcelona, Av. Joan XXIII 29-31, Barcelona 08028, Spain; anacalpena@ub.edu
[4] Institute of Nanoscience and Nanotechnology (IN²UB), University of Barcelona, 08007 Barcelona, Spain.

Emulsions are kinetically stabilized and thermodynamically unstable dispersions of two or more immiscible components; those emulsions with a size of 20-200 nm are called miniemulsions or nanoemulsions (NEs), and nanostructured systems are known to provide controlled release and enhanced drug bioavailability, which will depend on the amount and molecular properties of the drug [1,2]. From Eysenhardtia platycarpa, (2S)-5,7-dihydroxy-6-methyl-8-prenyl-flavanone (1) was isolated and evaluated for its anti-inflammatory efficacy in solution and in NE (F1) [3]. To find an improvement in the release of flavanone (1), in the present work two new formulations (F2 and F3) were prepared, in which castor oil and transcutol were used for (F2) and in (F3) plurol oleique and tween 20 replacing the surfactant and co-surfactant: plurol oleique and labrafac of the formulation (F1) already reported and maintaining the rest of the components[3]. With these changes, adequate kinetic stability against sedimentation, flocculation and coalescence is expected.

Materials and methods

For the development of new NEs with flavanone (1), two diferent matrix formulation (F2) and (F3) were prepared in triplicate. (F2B and F3B) are flavanone-free formulations (blank) and (F2F and F3F) contained the 0.5 % flavanone considering the incorporation of the lipophilic as well as hydrophilic components described by Domínguez-Villegas, V. *et al.* [3] Briefly the procedure includes: weighing of components, application of energy with ultrasound, water bath at 32°C, application of ultrasound and freezing at -20°C for 24 h to remove bubbles. The droplet size and polydispersity were determined using Nano-Z-sizer equipment.

Results

Morphometric analysis was performed and the droplet size was determined. Formulations (F2B) and (F2F), were found to be single phase and translucent, indicating adequate incorporation of the components, with an average droplet size of 96.95 □ 32.27 nm and 103.71 □ 38.12 nm, respectively; the increase in droplet size is attributed to the incorporation of flavanone (1); a second population of 9.658 □ 1.845 nm with an intensity of 7.3 was observed, indicating a slight bias in co-surfactant incorporation. The (F3B), was single-phase, translucent and bimodal with distinct populations, one below 10 nm and one above 700 nm due to possible agglomeration of droplets. The (F3F) is monophasic and translucent with three populations of droplets one at 10.99 □ 4.473 nm, another below 2 nm and a third above 700 nm which allows us to assume that it is due to Ostwald ripening.[4]

Conclusions

The physicochemical properties of castor oil, transcutol and the rest of the components favored (F2F) to be of adequate size and could be considered for future therapeutic applications.

References

1. Forgiarini A., Marquez L., Salager J-L. (2006) Nanoemulsiones, 1, Universidad de los Andes, Venezuela, 1 pp.
2. Salager J-L. (2002), Surfactantes Tipos y Usos, 2, Universidad de los Andes, Venezuela, 1-2
3. Domínguez-Villegas, V., *et al.* (2014). Development and characterization of two nano-structured systems for topical application of flavanones isolated from Eysenhardtia platycarpa, Colloids and Surfaces B: Biointerfaces, 116, 183-192
4. Wooster, T.J. *et al.*, (2008) Impact of Oil Type on Nanoemulsion Formation and Ostwald Ripening Stability Langmuir 2008, 24, 12758-12765

P28
EFFICACY EVALUATION OF NANOPARTICLES AND CHITOSAN GEL LOADING KETOROLAC TROMETHAMINE PROPOSED TO ALLEVIATE PAIN ASSOCIATED WITH CONDYLOMA ACUMINATA DURING THE PRE- AND POST-OPERATIVE PERIODS

iabohora7@alumnes.ub.edu

I. Abo Horan[1*], S. El Moussaoui[1*], B. Clares-Naveros[2], C. Alonso[3], L. Coderch[3], M. L. Garduño-Ramirez[4], A. C. Calpena-Campmany[1,6], F. Fernández-Campos[5], M. Mallandrich[1,6]

[1] Department of Pharmacy and Pharmaceutical Technology and Physical-Chemistry. Faculty of Pharmacy. University of Barcelona, Barcelona, Spain.
[2] Department of Pharmacy and Pharmaceutical Technology, School of Pharmacy, University of Granada, Granada, Spain.
[3] Institute of Advanced Chemistry of Catalonia-CSIC (IQAC-CSIC), Barcelona 08034, Spain.
[4] Centro de Investigaciones Químicas, Universidad Autónoma del Estado, de Morelos, Cuernavaca, Morelos, Mexico.
[5] Reig-Jofre Laboratories, Sant Joan Despí, Spain.
[6] Institut de Nanociència i Nanotecnologia IN²UB, Universitat de Barcelona, Barcelona, Spain.
[*] Equally contributed.

Condyloma acuminata (CA) is a human papillomavirus (HPV) infection's clinical manifestation[1]. CA are treated with the primary objective of removing visible lesions and alleviating any pain that may occur[2]. Following the removal of anogenital condylomas,[3] found that KT offers a significant effect as a treatment alternative for alleviating associated pain. Thus, the objective of this study is to propose two alternative formulations containing (KT); KT- loaded NPs (KT-NPS) and KT chitosan hydrogel (KT-CS). The hypothesis is the KT-NPS would be appropriate in the preoperative period as it can be used as a spray, whereas the KT-chitosan hydrogel would be beneficial in the postoperative.

Materials and methods

Formulations: polymeric nanoparticles loading 0.5% KT (138nm; PI 0.066) and chitosan gel 2% KT. The formulations were tested by in vitro permeation test, using Franz cells, to assess their capacity to penetrate and diffuse through human skin. 10 µL of formulation was applied to the skin for 24 hours. At the end of the test, the receptor fluid was collected, and the skin was split into layers. stratum corneum was isolated by the tape-stripping technique, and the epidermis and the dermis were separated by heat treatment. The anti-inflammatory efficacy was also assessed by TPA-induced ear edema in mice. Briefly, TPA was applied to both ears, then, the formulation was applied to one ear. At the end of the experiment and after animals were euthanized, the ears were punched and weighted. The percentage of inhibition of inflammation was calculated according to the following equation:

$$Inhibition\ (\%) = \left(\frac{Weight\ control\ ear - Weight\ treated\ ear}{Weight\ control\ ear}\right) \times 100$$

Results

The permeation experiments indicate that the vast majority of Ketorolac was found on the skin surface, in the residual formulation, for both, the NPs and the CS gel. NPs lead to a higher absorption of KT than the CS gel. In case of NPS, the KT was mainly retained in the epidermis whereas it was in the receptor fluid in the other case (table 1).

Table 1. *Distribution of KT within the skin layers*

%	Nanoparticles	Chitosan gel
S	83.14 ± 3.97	98.52 ± 3.11
SC	0.57 ± 0.81	0.14 ± 0.14
E	4.84 ± 2.17	1.18 ± 0.64
D	0.01 ± 0.01	0.007 ± 0.003
FR	0.13 ± 0.09	1.84 ± 1.74
Total recovery	*88.69 ± 5.72*	*101.68 ± 3.17*
Percutaneous absorption	4.98 ± 2.22	3.02 ± 1.77

b.l.q.: below limit quantification
b.l.d.: below limit detection

The anti-inflammatory efficiency study revealed that the KT-NPs exhibit a higher anti-inflammatory efficacy than KT-CS (Figure 1). Taking into account that KT-NPS exert the anti-inflammatory effect at a lower dose, and they are located in the epidermis, this formulation might be a good option for the pre- and intra-operative period. KT-CS is also located in epidermis. Keeping in mind that Chitosan is known to have antimicrobial properties, the combination KT in a CS gel could be useful for a topical treatment after the surgical removal of the anogenital warts.

Conclusion

It seems that from the obtained results, especially the distribution of KT within the skin and the anti-inflammatory efficacy, the hypothesis could be correct which means that this therapy might be a promising candidate in the management of Condyloma acuminata´s pain.

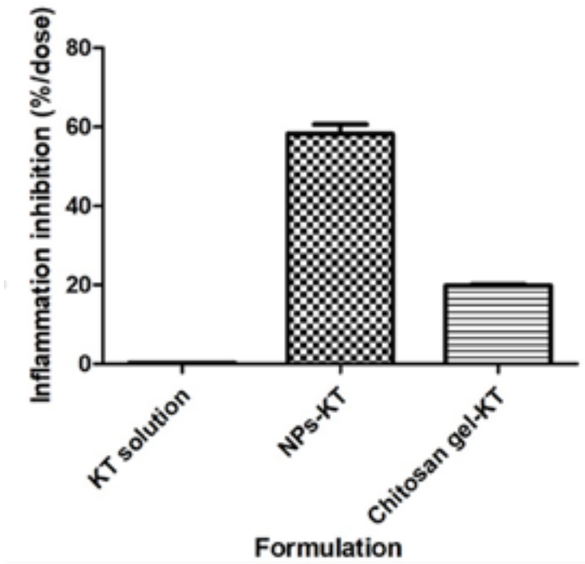

Figure 1. Anti-inflammatory efficacy expressed as a percentage reduction in inflammation when compared to a control

References

1. W. G. Rhea, B. M. Bourgeois, and D. R. Sewell, "Condyloma acuminata: a fatal disease?," *Am. Surg.*, vol. 64, no. 11, pp. 1082–1087, 1998, [Online]. Available: http://europepmc.org/abstract/MED/9798775
2. R. Vender, M. Bourcier, N. Bhatia, and C. Lynde, "Therapeutic options for external genital warts," *J. Cutan. Med. Surg.*, vol. 17 Suppl 2, pp. S61-7, 2013, [Online]. Available: http://europepmc.org/abstract/MED/24388560
3. S. El Moussaoui *et al.*, "Topical Mucoadhesive Alginate-Based Hydrogel Loading Ketorolac for Pain Management after Pharmacotherapy, Ablation, or Surgical Removal in Condyloma Acuminata," *Gels* , vol. 7, no. 1. 2021, doi: 10.3390/gels7010008

P29

CHITOSAN GEL AND NANOSTRUCTURED FORMULATION CONTAINING KETOROLAC TROMETHAMINE AS ANTI-INFLAMMATORY AGENT: PHYSICOCHEMICAL AND BIOPHARMACEUTICAL CHARACTERIZATION

iabohora7@alumnes.ub.edu

I. Abo Horan[1*], S. El Moussaoui[1*], L. Halbaut-Bellowa[1], B. Clares-Naveros[2], M. L. García[1,4], A. C. Calpena-Campmany[1,4], F. Fernández-Campos[3], M. Mallandrich[1,4]

[1] Department of Pharmacy and Pharmaceutical Technology and Physical-Chemistry. Faculty of Pharmacy. University of Barcelona, Barcelona, Spain.
[2] Department of Pharmacy and Pharmaceutical Technology, School of Pharmacy, University of Granada, Granada, Spain.
[3] Reig-Jofre Laboratories, Sant Joan Despí, Spain.
[4] Institut de Nanociència i Nanotecnologia IN²UB, Universitat de Barcelona, Barcelona, Spain.
[*] Equally contributed.

Ketorolac Tromethamine (KT) is a non-steroidal anti-inflammatory drug (NSAID) with a potent and moderate non-opioid analgesic activity. It is administered in eye drops, tablets, and as intramuscular injections for pre- and postoperative pain treatment [1]. Biodegradable Polymeric Nanoparticles (NPs) are widely used to enhance the bioavailability of topically administered drugs. Poly lactic-co-glycolic acid (PLGA) is a biodegradable polymer used due to its biocompatibility, mucoadhesiveness and nonantigenic nature [2,3,4]. Hydrogels are traditional formulations composed of different polymer types -either natural or synthetic ones- which are able to form a 3D network in presence of water [5].

The **purpose** of this work was to prepare and characterize a chitosan gel formulation and a nanostructured formulation containing KT as anti-inflammatory agent.

Materials and methods

The KT-NPS 0.5% were synthesized using the Double Emulsion-Solvent evaporation method [6] and then they were characterized in terms of particle size and polydispersity index (PDI). The KT-CS 2 % was thoroughly characterized in terms of degradation, swelling and the rheological behavior. Besides, the morphology for both formulations was studied by SEM or TEM. And finally, the release profile was investigated by means of Franz cells.

Results

The characterization of the formulations indicate that the NPS have a round-shape structure and the mean particle size was 138 nm, with a PI of 0.066, which indicates a monodisperse system. The chitosan presented a compact structure with small porous (Figure 1).

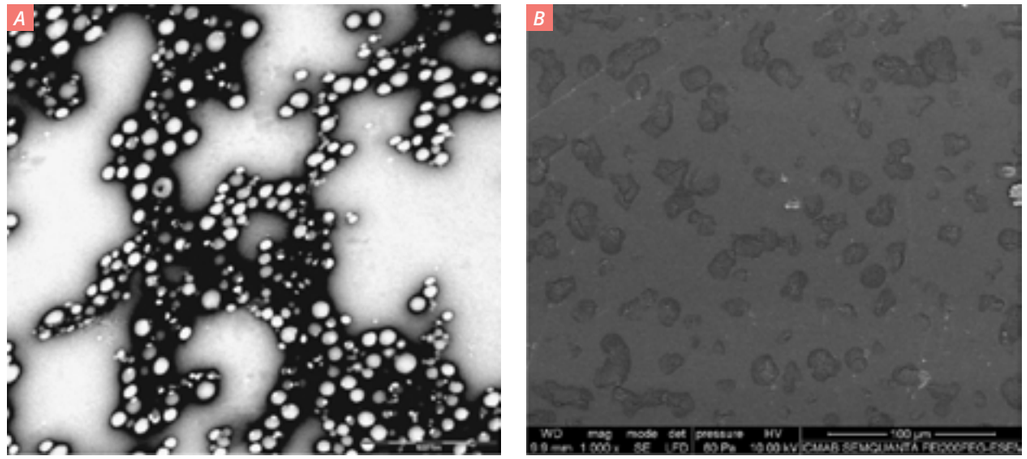

Figure 1. *Morphological analysis of the formulations. Panel A: TEM observation of the KT-NPs and Panel B: SEM observation of the dried KT-CS gel*

The swelling process of the CS gel followed a first order model, the dried gel showed a fast initial uptake of PBS during the first 10 minutes, followed by a slower PBS uptake. The degradation in PBS was within 3.75 hours (figure 2). The fresh chitosan gel showed an initial uptake of PBS followed by a weight loss which fitted to a one phase exponential decay.

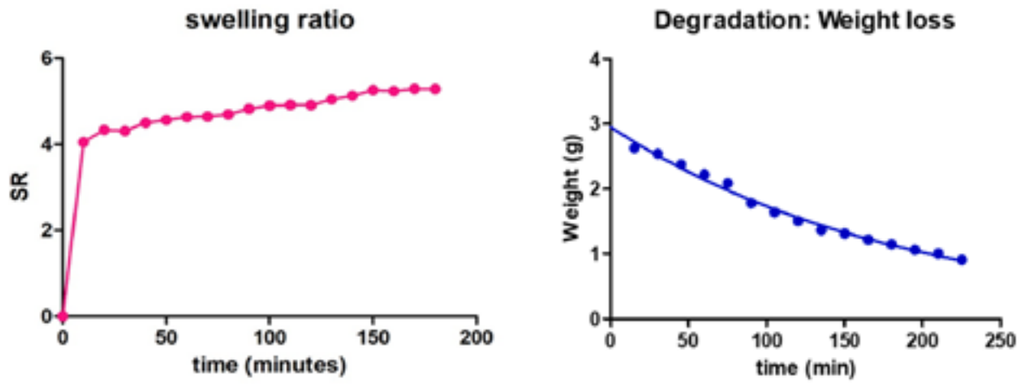

Figure 2. *Swelling and degradation processes of the KT-chitosan gel*

The rheological study (figure 3) revealed that the gel viscosity was 1.431 Pas ± 0.0004. The flow data best fitted to the Herschel-Bulkley model (r2 = 0.9999).

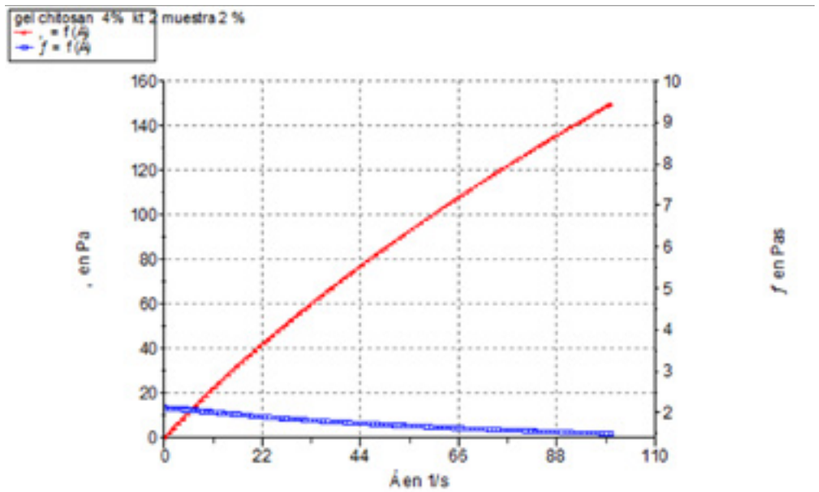

Figure 3. *Rheological profile of the KT-chitosan gel*

According to drug release study, the best fitted model to the experimental data was the first order kinetic equation (figure 4), with K value of 0,901 h-1 for chitosan gel and 1.841 h-1 for the nanoparticles. The nanoparticles allowed a higher release of KT than the chitosan gel.

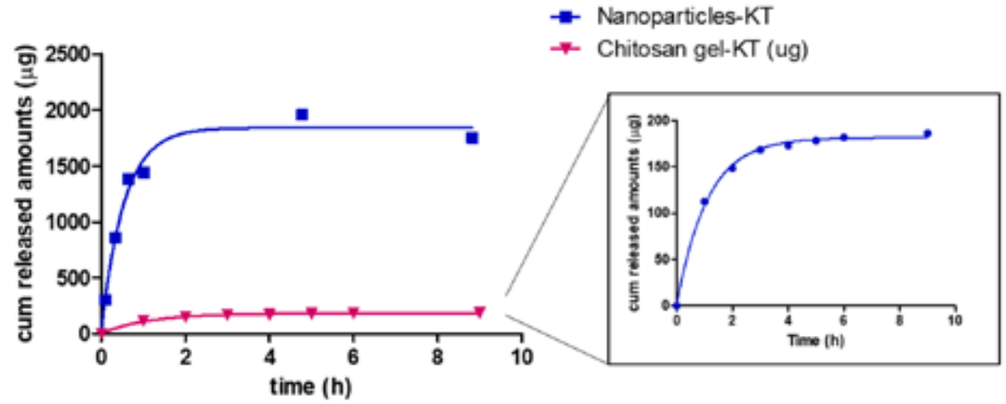

Figure 4. *In vitro release profile of the formulations, KT-NPS and KT-chitosan gel*

Conclusion

Two formulations of Ketorolac were prepared a chitosan gel and polymeric nanoparticles and characterized. The NPs resulted small and released a higher amount of KT than the chitosan gel.

References

1. dos Santos KC, da Silva MFG, Pereira-Filho ER, Fernandes JB, Polikarpov I, Forim MR. Polymeric nanoparticles loaded with the 3,5,3 ´-triiodothyroacetic acid (Triac), a thyroid hormone: Factorial design, characterization, and release kinetics. Nanotechnology, Science and Applications; 5(1):37-48, (2012).
2. Danhier F, Ansorena E, Silva JM, Coco R, Le Breton A, Préat V. PLGA-based nanoparticles: An overview of biomedical applications. J Controlled Release; 161(2):505-522, (2012).
3. Nagarwal RC, Kant S, Singh PN, Maiti P, Pandit JK. Polymeric nanoparticulate system: A potential approach for ocular drug delivery. J Controlled Release; 136(1):2-13, (2009);
4. El-Setouhy DA, El-Ashmony A, Mohy S. Ketorolac trometamol topical formulations: release behaviour, physical characterization, skin permeation, efficacy and gastric safety. J Pharm Pharmacol; 62(1):25-34, (2010).
5. Gorshkova, M.Y.; Volkova, I.F.; Vanchugova, L.V.; Valuev, I.L.; Valuev, L.I. Sodium Alginate Based Mucoadhesive Hydrogels. Appl. Biochem. Microbiol; 55, 371–374, (2019).
6. Mallandrich, M., Calpena, A. C., Clares, B., Parra, A., García, M. L., Soriano, J. L., & Fernández-Campos, F. Nano-engineering of ketorolac tromethamine platforms for ocular treatment of inflammatory disorders. Nanomedicine, 16(5), 401–414, (2021).

NanoMagnetics

P30
A NEW DINUCLEAR EU(III) COMPLEX WITH 2-FLUOROBENZOATE: IMPROVING THE EMISSION QUANTUM YIELD

anniatubau@ub.edu

À. Tubau[1], L. Rodríguez[1], A. Lázaro[1], R. Vicente[1], M. Font-Bardia[2]

[1] Departament de Química Inorgànica i Orgànica, Secció de Química Inorgànica, Universitat de Barcelona, Martí i Franquès 1-11, 08028 Barcelona.

[2] Departament de Mineralogia, Cristallografia i Dipòsits Minerals and Unitat de Difracció de R-X. Centre Científic i Tecnològic de la Universitat de Barcelona (CCiTUB). Universitat de Barcelona. Solé i Sabarís 1-3. 08028 Barcelona.

S. Bräse *et al.*, in a deep study of lanthanide fluorobenzoates coordination compounds searching for the optimal lanthanide and optimal ligand fluorination degree to obtain photo stable, non-toxic and luminescent compounds suitable for their use as bio-probes, have concluded that the europium 2-fluorobenzoate (2FBz) compound $[Eu_2(2FBz)_6(H_2O)_4]$, combined the best properties[1]. Taking into account our experience in the syntheses and luminescence study of 2-fluorobenzoate lanthanide(III) coordination compounds[2] we have synthesized, from a straightforward new room temperature synthetic method, a new europium 2-fluorobenzoate compound of formula $[Eu_2(2FBz)_4(H2FBz)_2(H_2O)_2]$ (**1**), H2FBz = 2-fluorobenzoic acid, to increase the emission quantum yield taking into account that the number of quenching water molecules in the new compound is a half with respect to $[Eu_2(2FBz)_6(H_2O)_4]$.

Compound **1** crystallizes in a triclinic crystal system with a P-1 space group. A partially labelled molecular plot is shown in Fig. 1. Each Eu^{3+} is nonacoordinated. The Eu-O bond length are in the range of 2.348(2) to 2.638(2) Å, the Eu---Eu intramolecular distance is 3.964(3) Å and the O1-Eu-O2 bite angle of the 2FBz ligand in the bidentate chelating coordination mode is 51.69(4)°.

In the emission spectra recorded at excitation wavelength (λ_{ex}) of 274 nm for **1**, Fig. 2, the bands that arise from the *f-f* transitions are assigned to: $^5D_0 \rightarrow {}^7F0$ at 578 nm, $^5D_0 \rightarrow {}^7F_1$ at 591 nm, $^5D_0 \rightarrow {}^7F_2$ at 618 nm, $^5D_0 \rightarrow {}^7F_3$ at 652 nm and $^5D_0 \rightarrow {}^7F_4$ at 701 nm. The red emission colour of the compound can be seen in the naked eye, inset Fig.2.

The overall quantum yield is 27 % for **1**. For the previously published compound of formula $[Eu_2(2FBz)_6(H_2O)_4]$ the quantum yield was 15 %. Compounds **1** is water soluble, with solubility of 7.98 mmol/L. The QY decreases to 0.23 % when **1** dissolved in water, but photoluminescence properties are still present in water solution making 1 a choice for bioanalytical applications.

***Figure 1**. Partially labelled plot of compound 1. H atoms are omitted for clarity*

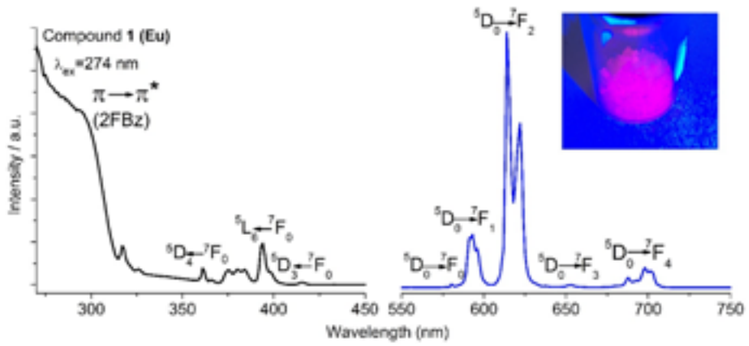

***Figure 2**. Solid state excitation (black) and emission (bue) spectra at r. t. of compound 1. Inset shows the emission colour of 1 under UV lamp radiation*

References

1. A. S. Kalyakina, V. V. Utochnikova, I. S. Bushmarinov, I. M. Le-Deygen, D. Volz, P. Weis, U. Schepers, N. P. Kuzmina, S. Bräse, *Chem. Eur. J.* 2017, 23, 14944-14953
2. B. Casanovas, M. Font-Bardía, S. Speed, M. Salah El Fallah, R. Vicente. *Eur. J. Inorg. Chem.*, 2018, 1928-1937

P31
FACILE SURFACE FUNCTIONALIZATION WITH LUMINESCENT AND MAGNETIC LANTHANOID SCHIFF BASE COMPLEXES

ggabarro@ub.edu

G. Gabarró-Riera[1,2], E. C. Sañudo[1,2]

[1] Departament de Química Inorgànica i Química Orgànica. Secció de Química Inorgànica. Facultat de Química. Universitat de Barcelona.

[2] Institut de Nanociència i Nanotecnologia IN²UB, Barcelona.

The constant evolution of technology requires smaller and more efficient devices. Functional molecules such as single-molecule magnets have been proposed as possible building blocks for the next generation of quantum computers or data storage devices[1]. For this reason, addressing and manipulating single molecules on surfaces is essential and one of the main problems to overcome[2].

In this work, lanthanoid (europium and dysprosium) complexes with Schiff base ligands[3] have been anchored to a silicon substrate with terminal carboxylate groups via a ligand-exchange reaction—thus, through a chemisorption process. In the europium complex, characteristic luminescence is observed in layers thinner than two nanometers. On the other hand, the magnetic properties of the dysprosium compound could be potentially improved due to a better magnetic anisotropy.

Atomic force microscopy allows us to observe the total and homogeneous coverage of samples independent of their size for both europium and dysprosium compounds and the integrity of the molecules is corroborated by matrix-assisted laser desorption/ionization with a time-of-flight detector (MALDI-ToF).

References

1. E. Coronado, Molecular magnetism : from chemical design to spin control in molecules, materials and devices, *Nat. Rev. Mater.*, 2020, **5**, 87–104
2. D. Gatteschi, A. Cornia, M. Mannini and R. Sessoli, Organizing and Addressing Magnetic Molecules, *Inorg. Chem.*, 2009, **48**, 3408–3419
3. S. Gholizadeh Dogaheh, H. Khanmohammadi and E. C. Sañudo, Double-decker luminescent ytterbium and erbium SMMs with symmetric and asymmetric Schiff base ligands, *New J. Chem.*, 2017, **41**, 10101–10111

P32
CONTROLLED SYNTHESIS OF OF Bi_2S_3 NANOPARTICLES FOR COMPUTED TOMOGRAPHY

cmoyaalv@ulb.ac.be

M. Escoda-Torroella[1,2], C. Moya[1-3,*], A. Fraile Rodríguez[1,2], A. Labarta[1,2], X. Batlle[1,2]

1 Departament de Física de la Matèria Condensada, Martí i Franquès 1, 08028 Barcelona, Spain,
2 Institut de Nanociència i Nanotecnologia, Universitat de Barcelona, Martí i Franquès 1, 08028 Barcelona, Spain,
3 Université libre de Bruxelles, Engineering of Molecular Nanosystems, 50 Avenue F.D. Roosevelt, 1050 Bruxelles, Belgium

Computed tomography (CT) is an X-ray based 3D imaging technique widely used to enhance the contrast among human body tissues because it allows deep tissue penetration and high-resolution imaging. Clinically approved CT contrast agents are iodinated molecules or barium suspensions, but their short circulation time and the high doses required limits their efficiency. The use of nanoparticles (NPs) exhibits some advantages in comparison with small molecules such as longer circulation times and the possibility to functionalize the NPs to achieve target imaging and cell-tracking. In particular, Bi_2S_3 NPs are suitable as contrast agents for CT because of the large X-ray attenuation coefficient of Bi. In addition, Bi_2S_3 is less expensive and less toxic than other species with similar X-ray attenuation coefficient such as Au, Pt or Ta.

In this work, Bi_2S_3 NPs with different size and shape have been prepared by hot-injection synthesis of a sulphur precursor by tuning the temperature and the reaction time. On the one hand, when the injection is performed at 105 ºC with short reaction times, 6 nm spheroid-shaped NPs are obtained. As the reaction time is increased, NPs grow anisotropically, leading to needle-shaped particles of 50 nm in length. On the other hand, by injecting at 165 ºC, rod-shaped NPs of 30 nm are obtained regardless of the reaction time. Additionally, High Resolution Transmission Electron Microscopy (HRTEM) and powder X-ray Diffraction (XRD) were performed to study the dependence of the NPs crystal quality on the reaction conditions. Finally, the NPs were stabilized in aqueous media by a silica coating so that they can be combined with other materials to obtain a multifunctional system.

This work was supported by Spanish MCIU and AEI (MAT2015-68772-P; PGC2018-097789-B-I00) and European Union FEDER funds. M.E.T. acknowledges Spanish MCIU for BES-2016-077527.

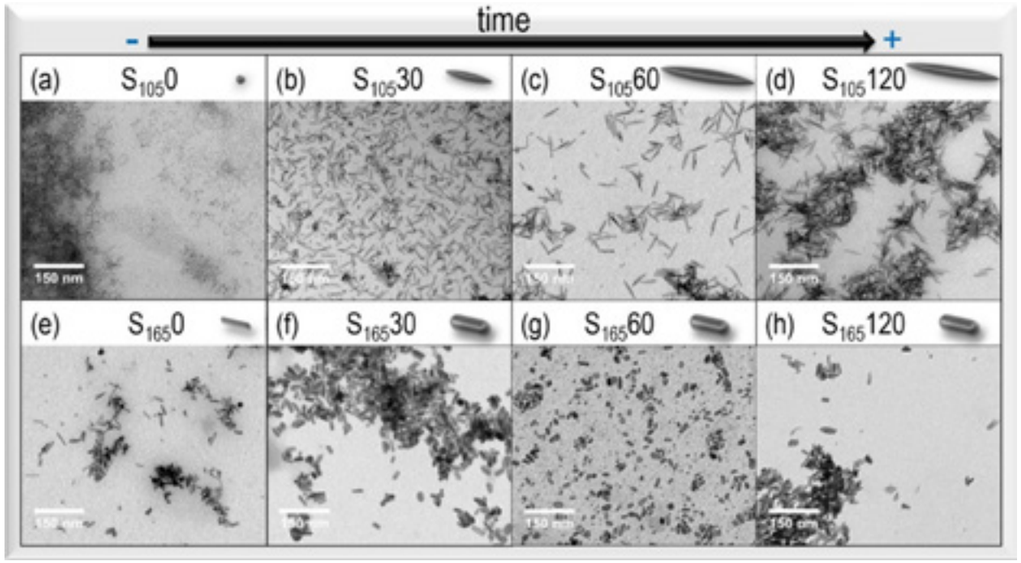

Figure 1. *Gallery of Bi_2S_3 NPs with tuneable morphology from 0 to 120 minutes at 105 and 165ºC. (a-d) Series of nanoneedles, and (e-h) Series of nanorods*

P33
AN INSIGHT ON THE STRUCTURAL AND MAGNETIC PROPERTIES OF IRON OXIDE NANOFLOWERS

mariona.escoda@ub.edu

M. Escoda-Torroella[1,2,*], C. Moya[2,3], M. P. Morales[4], P. Bender[5], E. Martín Jefremovas[6], L. Fernández Barquín[6], A. Fraile Rodríguez[1,2], A. Labarta[1,2], X. Batlle[1,2]

1 Departament de Física de la Matèria Condensada, Martí i Franquès 1, 08028 Barcelona, Spain.
2 Institut de Nanociència i Nanotecnologia, Universitat de Barcelona, Martí i Franquès 1, 08028 Barcelona, Spain.
3 Université libre de Bruxelles, Engineering of Molecular Nanosystems, 1050 Bruxelles, Belgium.
4 Instituto de Ciencia de Materiales de Madrid, ICMM/CSIC, 28049 Madrid, Spain.
5 Heinz Maier-Leibnitz Zentrum, Technische Universität München, D-85748 Garching, Germany.
6 Departamento CITIMAC, Faculty of Science, University of Cantabria, 39005 Santander, Spain.

Single-core magnetite/maghemite nanoparticles have been extensively studied because of their outstanding properties for biomedical and environmental applications[1,2]. Recently, a great interest has been focused on multicore nanoparticles, which are formed of aggregates arranged in a nanoflower (NF) shape. Nevertheless, there is a lot to understand of its structure and magnetic properties to achieve good control over their performance in applications. In this work, three different samples synthesized by the polyol method were studied. The size of the NFs was determined by transmission electron microscopy (TEM), obtaining values of 37 ± 9 nm, 121 ± 13 nm, and 186 ± 28 nm. To gain insight into their internal structure, the size of the cores was determined by both TEM and X-ray diffraction. We found that the crystal size was higher than the size of the cores measured by TEM, showing a crystallographic correlation that extends beyond the individual cores. In addition, selected area electron diffraction patterns also showed a preferred orientation of the crystals inside the NF. These complex structures led to an interesting magnetic performance with high values of saturation magnetization, around 80 emu/g, and low values of the coercive field at 300K. This may be related to a vortex-like arrangement of the core spins corresponding to almost zero remnant magnetization when no field is applied, even when the NF are as large as 100 nm in diameter. Further insight into this complex magnetic structure was gained by performing small-angle neutron scattering experiments to determine the magnetic correlations among the spin cores within the NFs.3 The understanding of the internal structure and the consequent magnetic behavior is essential for the optimization of the NF for medical or environmental applications.

The work was supported by Spanish MCIU and AEI (MAT2015-68772-P; PGC2018-097789-B-I00) and European Union FEDER funds. M.E-T. acknowledges Spanish MCIU for BES-2016-077527.

References
1. Lartigue, L. *et al. ACS Nano* **6**, 10935–10949 (2012)
2. Hugounenq, P. *et al. J. Phys. Chem.* C **116**, 15702–15712 (2012)
3. Bender, P. *et al. Appl. Phys. Lett.* **115**, 132406 (2019)

P34
THE PURSUIT OF NEW MULTIFUNCTIONAL MATERIALS: NEW SUPRAMOLECULAR HELICATES OF Fe(II) AND Co(II). TEMPLATE EFFECT BY ENCAPSULATED SPECIES

leoni.barrios@ub.edu

L. A. Barrios Moreno[1,2], N. Capó Serrano[1], M. Darawsheh[1], O. Roubeau[3,4], S. J. Teat[5], G. Aromí[1,2]

[1] Departament de Química Inorgànica i Orgànica, Universitat de Barcelona, Barcelona, Spain
[2] Institut de Nanociència i Nanotecnologia de la Universitat de Barcelona, Barcelona, Spain
[3] Instituto de Ciencias de Materiales de Aragón (ICMA), Zaragoza, Spain
[4] Universidad de Zaragoza, Zaragoza, Spain
[5] Advanced Light Source Laboratory, Berkeley, USA

Inspired by nature, we pursuit the design and the effective synthesis of organic moieties capable to produce new molecular functional assembles incorporating several functions that can interact synergistically or being addressed by external stimuli.

The versatility of the new bis-(pyrazol-pyridyl) organic ligands, allow the synthesis of several novel metallo-supramolecular triple stranded helicates encapsulating anionic species, such as ClO^{4-}, SiF_6^{2-}, $Cr(Oxalate)_3^{3-}$, $Fe(Oxalate)_3^{3-}$ among others.

The encapsulation of SiF_6^{2-} shows an evident template effect guiding the reaction to form exclusively the heteroleptic helicate with formula $(SiF_6@[M(L1)(LX)2])(PF_6)_2$ (where M= Fe(II) or Co(II), L1= $C_{22}H_{16}N_6$; LX= L2, $C_{28}H_{20}N_6$ or L3, $C_{30}H_{26}N_6$).

The influence of the ratio of L/LX has been studied against the nature of the encapsulated species, and this ratio does not affect the stoichiometry of the above-mentioned complex.

This new family of host-guest molecular systems can offer different properties, depending on the metal centers involved and the nature of the guest.

***Figure 1**. Representation of the multifunctional $Cr(Oxalate)_3@[Fe_2(L2)_3]$ host-guest system[1] (left) and the template effect of the anion SiF_6^{2-} (right) forming the $SiF_6@[Co2(L1)(L3)2](PF_6)_2$ helicate*

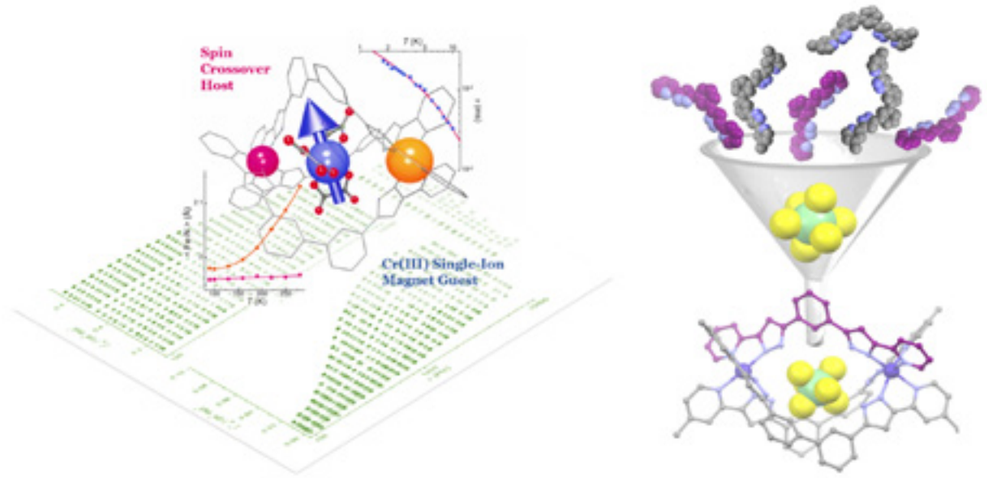

References
1. *Angew. Chem. Int. Ed.*, **2018**, 57, 13509-13513

P35
SURFACE ACOUSTIC WAVES CONTROL OF MAGNETIC MODES IN NANODEVICES

ferran.macia@ub.edu

F. Macià, B. Casals, W. Kaliq, J. M. Hernàndez, A. García-Santiago
Department of Condensed Matter Physics, University of Barcelona, 08028 Barcelona, Spain

Spin waves in magnetic materials are coherent dispersive waves, typically in the low GHz frequency regime and with wavelengths of hundreds of nanometers. Interest in spin waves is motivated by the possibility of its integration into nano-scale devices for high-speed and low-power signal processing. However, generation of spin waves with high amplitudes—and their detection—is challenging due to the mismatch of wavelengths with electromagnetic waves in free space, which is of the order of several centimeters.

In this talk I will review some recent experiments on the coupling of surface acoustic waves (SAW) and spin waves using X-ray Photo-Emission Electron Microscope (XPEEM). The main observations are: i) the control of SAW interference patterns [1], ii) the SAW generation of large amplitude spin waves (up to 25 degrees) over large distances (up to several millimeters) [2], iii) the induced delays on the SAW compared to the SW [3], and the iv) the possibility of moving magnetic domains at the SAW velocity [4,5]. Additionally, I will also show the effect of a periodical spatial strain in the reversing process of a magnetic thin film besides the reduction of the nucleation energy [6].

References
1. Journal of Synchrotron Radiation 26, 184-193 (2019)
2. Phys Rev. Lett. 124, 137202 (2020)
3. In preparation
4. Nature Commun. 8, 407 (2017)
5. MRS bulletin 43, 854 (2018)
6 In preparation

P36
CRUCIAL ROLE OF THE Co CATIONS ON THE DESTABILIZATION OF THE FERRIMAGNETIC ALIGNMENT IN Co-FERRITE NANOPARTICLES WITH TUNABLE STRUCTURAL DEFECTS

arantxa.fraile@ub.edu

C. Moya[1,2,3], A. Fraile Rodríguez[1,2], M. Escoda-Torroella[1,2], M. García del Muro[1,2], S. R. V. Avula[4], C. Piamonteze[4], X. Batlle[1,2], A. Labarta[1,2]

[1] Departament de Física de la Matèria Condensada, Universitat de Barcelona, 08028 Barcelona, Spain.
[2] Institut de Nanociència i Nanotecnologia (IN²UB), Universitat de Barcelona, 08028 Barcelona, Spain.
[3] Université Libre de Bruxelles (ULB), Engineering of Molecular Nanosystems, 1050 Bruxelles, Belgium.
[4] Swiss Light Source, Paul Scherrer Institut, CH 5232 Villigen PSI, Switzerland.

Cobalt ferrite nanoparticles (NP) are competitive candidates in nanomedicine and biomedical applications due to a suitable combination of excellent chemical and magnetic characteristics, such as a high chemical stability, surface active sites, and ease of synthesis and functionalization, together with a high anisotropy constant, a high coercivity, and a moderate saturation magnetization. However, in order to control the functional response of cobalt ferrite NP, one of the biggest challenges is to quantitatively disentangle the dependence on the overall magnetic response of the composition, structure, or surface chemistry.

In our work, by combining an advanced chemical synthesis approach with a broad set of world-class complementary local probes, we have unravelled the key role played by the Co^{2+} cations on the destabilization of the collinear ferrimagnetism in Co ferrite NP through the selective incorporation of structural defects. A set of samples of monodispersed, 8 nm Co ferrite NP of similar stoichiometry but with a progressive inclusion of structural defects was prepared [1,2]. Synchrotron-based, element-, valence- and site- specific X-ray spectroscopy and magnetometry on ensembles of NP was combined with high-resolution transmission microscopy of selected, individual NP [3]. The analysis of element-specific X-ray Magnetic Circular Dichroism (XMCD) spectra and hysteresis loops for all cationic sites reveals that the collinear alignment of the Co^{2+} cations in octahedral sites is significantly more affected by the structural disorder than in any other cation. This is due to the local anisotropy axes induced by the strain associated with the structural defects, giving rise to Co^{2+} spin canting via spin-orbit coupling due to the relatively large Co^{2+} orbital momentum. As the number of structural defects increases, the rest of the cations are progressively dragged off the ferrimagnetic alignment, being the Fe^{3+} cations in tetrahedral sites the last ones to be affected by the disorder [3].

Our work highlights the importance of combining a great control over the NP microstructural features, by employing suitable synthesis methods, with the use of advanced complementary local probes in order to disentangle and quantify the effect of every cation and the local environment into the final magnetic response of cobalt ferrite NP, which is essential to tailor and boost their performance for targeted biomedical applications.

References
1. C. Moya, M. P. Morales, X. Battle and A. Labarta, *Phys. Chem. Chem. Phys.* 17, 13143 (2015)
2. C. Moya, G. Salas, M. P. Morales, X. Batlle and A. Labarta, *J. Mater. Chem.* C 3, 4522 (2015)
3. C. Moya, A. Fraile Rodríguez, M. Escoda-Torroella, M. García del Muro, *et al.*, *J. Phys. Chem C* 125, 691 (2021)

P37
DRIVING MAGNETIC DOMAINS AT THE NANOSCALE BY STRAIN-INDUCED PROXIMITY

arantxa.fraile@ub.edu

A. Fraile Rodríguez[1,2], J. Rodriguez-Alvarez[1,2], I. Valmianski[3], M. García del Muro[1,2], C. Wolowiec[3], F. Kronast[4], J. G. Ramirez[5], I. K. Schuller[3], A. Labarta[1,2], X. Batlle[1,2]

1 Departament de Física de la Matèria Condensada, Universitat de Barcelona, 08028 Barcelona, Spain.
2 Institut de Nanociència i Nanotecnologia (IN²UB),Universitat de Barcelona, 08028 Barcelona, Spain.
3 Department of Physics and Center for Advanced Nanoscience, University of California San Diego, La Jolla, CA 92093, USA.
4 Helmholtz-Zentrum Berlin für Materialien und Energie GmbH, 12489 Berlin, Germany
5 Department of Physics, Universidad de los Andes, Bogotá 111711, Colombia.

Coupling of lattice and spin degrees of freedom without the use of external magnetic fields allows for energy-efficient spintronic devices. In this context, hybrid materials composed of an oxide layer undergoing a first-order, structural phase transition (e.g. V_2O_3) and a ferromagnetic layer (e.g. Ni) coupled by proximity through the inverse magnetoelastic effect offer a promising alternative to voltage-controlled magnetism or other switching mechanisms without a magnetic field.

Here we show by direct imaging of the thermal evolution of the Ni spin structure that the magnetic domains can be tuned in both size and magnetic anisotropy upon crossing the structural phase transition (SPT) of the proximal V_2O_3 layer[1]. We find a drastic temperature-driven reorientation of the Ni magnetic domains across the SPT, which is responsible for an abrupt increase in the coercive field (up to 500 %). By synchrotron-based photoemission electron microscopy (PEEM) combined with X-ray magnetic circular dichroism (XMCD) we show a reconfiguration of the ferromagnetic domain pattern in the Ni layer across the V_2O_3 SPT together with changes in magnitude and direction of the effective uniaxial magnetic anisotropy. These observations are in good agreement with both angular dependent ferromagnetic resonance measurements and micromagnetic simulations. Following a simple model of strain-dependent magnetic anisotropies, our simulations replicate both the change in the coercivity and the reorientation of the magnetization of the Ni domains as well as exhibit a phase coexistence of different magnetic domains across the SPT in the V_2O_3. Direct observations of the lateral correlation length of the Ni domains show an increase of almost an order of magnitude at the SPT compared to room temperature as well as a broad spatial distribution of the local transition temperatures. This corroborates the phase coexistence of Ni anisotropies due to the V_2O_3 structural domains coexistence across the SPT. Our data reveal that the reorientation of Ni domains is controlled by the reconfiguration of the structural domains of the oxide layer across the SPT[2,3] due to strain induced proximity. Our findings reveal a novel pathway to control magnetic domains without a magnetic field through proximity to a material undergoing a first-order structural phase transition, which allows for engineering of coercive fields for novel device concepts based on “straintronics”.

References
1. Valmianski, I., Fraile Rodríguez. A., Rodriguez-Alvarez, J., *et al., Nanoscale* 13, 4985 (2021)
2. McLeod, A. S., Van Heumen, E., Ramirez, J. G., *et al. Nat. Phys.* 13, 80 (2017)
3. Gilbert, D. A., Ramírez, J. G., Saerbeck, T., *et al., Sci. Rep.* 7 13471 (2017)

P38

EXPLORATION OF THE H_2L2 COORDINATION CHEMISTRY. THE DISCORY OF [FE9] SQUARED GRIDS

rdiegocreixenti@ub.edu

R. Diego[1,2], L. A. Barrios Moreno[1,2], L. Parkins[1], O. Roubeau[3], J. Ribas-Ariño[4], S. J. Teat[5], G. Aromí*[1,2]

[1] Departament de Química Inorgànica i Orgànica, Universitat de Barcelona,Diagonal 645, 08028 Barcelona, Spain.
[2] Institut of Nanoscience and Nanotechnology of the University of Barcelona (IN²UB), Barcelona, Spain.
[3] Instituto de Ciencia de Materiales de Aragón (ICMA), CSIC and Universidad de Zaragoza, Plaza San Francisco s/n, 50009, Zaragoza, Spain.
[4] Departament de Química Física, Universitat de Barcelona, Diagonal 645, 08028 Barcelona, Spain.
[5] A dvanced Light Source, Berkeley Laboratory, 1 Cyclotron Road, Berkeley, California 94720, USA.

The coordination chemistry exploration of ligand H_2L2 with different iron (II) sources, solvents and atmospheric conditions allowed the obtaining of three triple-stranded helicates[1,2] with the formula $Fe(C_2O_4)_3$@$[Fe_2(H_2L2)_3](X)\cdot S$ (X:BF_4, S:5(C_2H_3N), CH_4O, 3(H_2O) for 1, X:BF_4, S: 3(CH_4O), 4.75(H_2O) for 2 and X: ClO_4 and S: (H_2O) for 3) displaying different spin-state pairs, and the discovery of a new fascinating supramolecular clusters based on a planar iron nanosheet. The two new $[Fe_9]$ squared grids are composed by hydroxo(oxo) bridges in between the metal ions with the formula $[Fe_9O_4(OH)_8]^{7+}$ (4) and $[Fe_9O_4(OH)_8]^{10+}$ (5). The main differences of both coordination clusters are the occupation of the remaining axial positions of the metal centres regarding the plane ferric O^{2-}/OH^- core. Thus, based on the crystalline structure, charge balance, the valence bond sum (VBS), the elemental analysis (EA) and magnetometry, the whole compounds are formulated as $[Fe_9O_4(OH)_{10}(H_2L2)_6(H_2O)_4](BF_4)_5$ (4) and $[Fe_9O_4CL_6(OH)_8(H_2L2)_6]4(Cl)$ (5). These unprecedented complexes displaying nearly planar sheet of irons have an interesting magnetic behaviour.

References
1. Darawsheh, M.; Barrios, L. A.; Roubeau, O.; Teat, S. J.; Aromí. *Chem. - A Eur. J.* 2016, 22, 8635–8645
2. Aromi, G.; Darawsheh, M.; Barrios, L. A.; Roubeau, O.; Teat, S. J. *Angew. Chemie Int.* Ed. 2018, 57, 13509–13513

NanoPhotoElectro

P39

A HIGHLY SENSITIVE REFRACTIVE INDEX SENSOR BASED ON AN INVERTED HONEYCOMB PLASMONIC LATTICE

javier.rodriguez@ub.edu

J. Rodríguez-Álvarez[1,2], L. Gnoatto[1], M. Martinez-Castells[1], A. Guerrero[3], X. Borrisé[4], A. Fraile Rodríguez[1,2], X. Batlle[1,2], A. Labarta[1,2]

[1] Departament de Física de la Matèria Condensada, Universitat de Barcelona, 08028 Barcelona, Spain.
[2] Institut de Nanociència i Nanotecnologia (IN²UB), Barcelona, 08028, Spain.
[3] Institut de Microelectrónica de Barcelona (IMB-CNM, CSIC), Bellaterra, 08193, Spain.
[4] Catalan Institute of Nanoscience and Nanotechnology (ICN2), CSIC and The Barcelona Institute of Science and Technology, Campus UAB, Bellaterra, 08193 Barcelona, Spain.

In this work, we present a highly efficient refractive index sensor based on the excitation of collective excitations in a plasmonic lattice [1]. This kind of sensors exploit the fact that the wavelength of the plasmonic resonances is highly dependent on the features of the surrounding medium. In our case, we propose a heterostructure based on an Au inverted honeycomb lattice as shown in Fig. 1a. Numerical simulations revealed that this structure yields large enhancements of the intensity of the excited electric field hundreds of nanometers away from the structure, maximizing the sensing volume and sensitivity [1]. To test the performance of the system, simulations changing the value of the refractive index of a thin layer laying on top of the structure were carried out, mimicking the situation in which biomolecules are adsorbed on top of an Au layer. The results showed high sensitivity values ranging from 99 to 395 nm/RIU (RIU stands for refractive index unit) for relatively thin layers of test materials within 50 and 200 nm. In addition, the sensor was also capable of detecting slight changes of the refractive index of a water medium at a fixed wavelength as small as 0.002 RIU [1], showing its potential for high molecular specificity.

As an experimental proof of concept, the heterostructure was manufactured by a simple method based on electron beam lithography and the measured optical response agreed with the simulations. This work paves the way for increasing the sensitivity and specificity of plasmonic sensors as well as improving the signal of some enhanced surface spectroscopies.

Figure 1. *(a) Schematic representation of the studied structure. The inset shows a cross-sectional view. (b) Resonant wavelength corresponding to the surface lattice resonance as a function of the refractive index for three values of the test layer thickness*

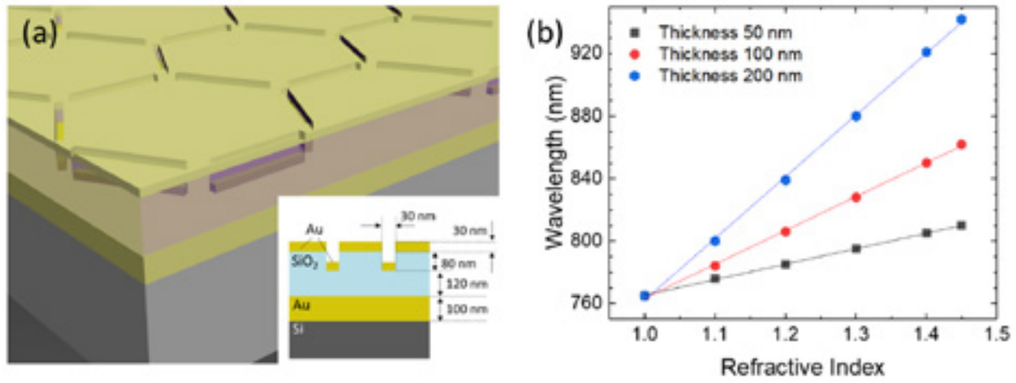

References
1. J. Rodríguez-Álvarez *et al.*, "An inverted honeycomb plasmonic lattice as an efficient refractive index sensor," *Nanomaterials*, vol. 11, no. 5, pp. 1–12, 2021

P40
HIGHLY TUNABLE CIRCULAR DICHROISM THROUGH COUPLED MODES IN TRISKELIA NANOSTRUCTURES

javier.rodriguez@ub.edu

J. Rodríguez-Álvarez[1,2], A. García-Martín[4], A. Fraile Rodríguez[1,2], X. Batlle[1,2], A. Labarta[1,2]

[1] Departament de Física de la Matèria Condensada, Universitat de Barcelona, 08028 Barcelona, Spain.
[2] Institut de Nanociència i Nanotecnologia (IN²UB), Barcelona, 08028, Spain.
[3] Institut de Microelectrónica de Barcelona (IMB-CNM, CSIC), Bellaterra, 08193, Spain.
[4] Instituto de Micro y Nanotecnología IMN-CNM, CSIC, CEI UAM+CSIC, Isaac Newton 8, E28760 Tres Cantos, Madrid, Spain.

Even though planar chiral structures can induce a polarization-dependent absorption of the incident radiation [1], only three-dimensional systems can exhibit a measurable difference in the total optical loss, that is, circular dichroism (CD). Our work is focused on the design and simulation of a simple 3D structure that presents large CD in the near-Infrared (NIR) and optical ranges that can be easily tuned by adjusting its geometrical parameters[2].

The building block used in this work, so-called "triskelion", shows a three-fold rotational symmetry and has chiral nature (Figure 1c). A single triskelion shows significant dichroism in both the absorption and scattering (Figure 1a and 1b). However, the two dichroic signals cancel each other owing to its planar nature [1]. On the contrary, when two triskelia are stacked together to form a non-planar structure (Figure 1f), we found a remarkable dichroism in the extinction spectrum due to new resonances arising from the interaction between the two triskelia. This geometric arrangement provides a simple platform to finely control the CD of the system by adjusting the distance between the triskelia and their relative rotation angle, two parameters that can be easily tuned in the manufacturing process.

Further simulations of the near-field distribution of the electric field for several values of the relative rotation angle have been performed too, providing deeper insight into the effect of the nanostructure symmetry on the CD in the total optical loss.

Figure 1. *Absorption (a) and scattering (b) cross-section spectra for a single triskelion, and (d) and (e) two triskelia with a relative rotation angle of 30° and 30 nm of separation. Right panels (c) and (f) show schematic representations of a single triskelion and two triskelia, respectively*

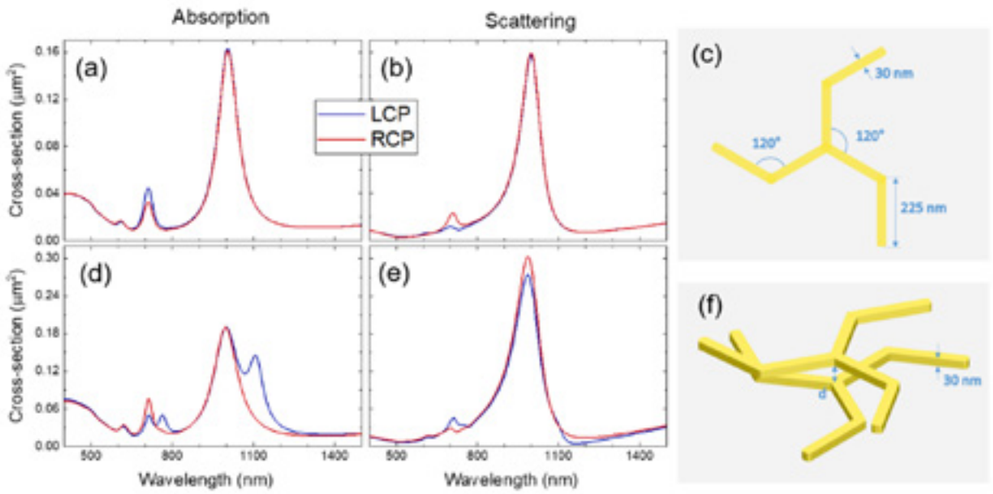

References

1. B. Hopkins, A. N. Poddubny, A. E. Miroshnichenko, and Y. S. Kivshar, "Circular dichroism induced by Fano resonances in planar chiral oligomers," *Laser Photonics Rev.*, vol. 10, n°1, pp. 137–146, 2016
2. J. Rodríguez-Álvarez *et al.*, "Highly Tunable Circular Dichroism through Coupled Optical Modes in Triskelia Nanostructures," *in preparation*, 2021

P41
SILICON-BASED OPTOMECHANICAL CRYSTALS FOR ROOM-TEMPERATURE APPLICATIONS

dnavarro@ub.edu

D. Navarro-Urrios[1], N. E. Capuj[2], J. Gomis-Bresco[3]

[1] MIND-IN²UB, Departament d'Enginyeria Electrónica i Biomédica, Facultat de Física, Universitat de Barcelona, Martí Franqués 1, 08028 Barcelona, Spain.
[2] Depto. Física, Universidad de La Laguna, 38200 San Cristóbal de La Laguna, Spain.
[3] ENPHOCAMAT-IN²UB, Departament de Física Aplicada, Facultat de Física, Universitat de Barcelona, Martí Franqués 1, 08028 Barcelona, Spain.

The paradigmatic setup in cavity optomechanics is an optical cavity with an end mirror that can vibrate. This kind of setup appeared already several decades ago in theoretical considerations and basic experiments, starting with Vladimir Braginsky's work at the end of the 60s. Since then, the advances of fabrication techniques have made available the successful demonstration of a wide variety of high-quality optomechanical (OM) devices, i.e., high-Q mechanical resonators that are efficiently coupled to high-Q optical cavities. All those architectures, which span a huge range of vibration frequencies and effective masses, are described by the same physical formalism and allow, for instance, testing quantum mechanics even on objects of macroscopic scales [1].

In this work we will place our specific research interests in this wide context, which aims to find applications at ambient operation conditions. We will review our progresses using Silicon-based optomechanical photonic crystals (OMCs), which are at the same time photonic crystals cavities in the near IR range (~200 THz) and phononic crystals cavities in the GHz range (see Figure 1). We will summarise our experimental studies on the non-linear dynamical regimes that can be triggered at high intracavity photon numbers both on single OMCs and on pairs of coupled OMCs. Those are mechanical lasing, phase locking to external RF references, chaos and mechanical synchronization [2-4], among other interesting regimes. Finally, we will discuss their possible use as OM sensors of different sorts of submicrometric analytes [5] and of magnetic fields. [6]

Figure 1. *Finite element methods simulation of a photonic and a phononic cavity modes (panels a and b respectively) of a trapezoidal silicon-based optomechanical crystal*

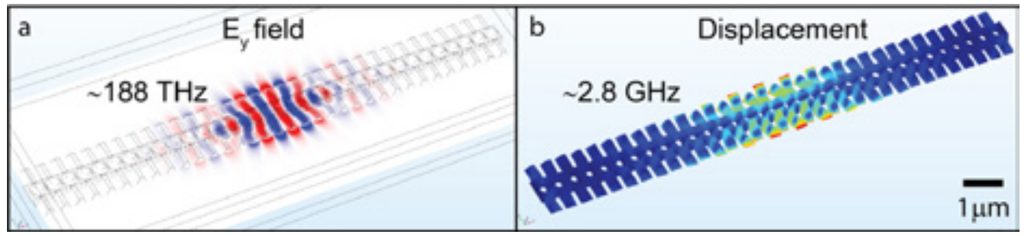

References

1. M. Aspelmeyer, T. J. Kippenberg, and F. Marquardt, "Cavity optomechanics", Rev. Mod. Phys. 86, 1391 (2014).
2. D. Navarro-Urrios, N. Capuj, M. Colombano, P. D. Garcia, M. Sledzinska, F. Alzina, A. Griol, A. Martinez, C. M. Sotomayor-Torres, "Nonlinear dynamics and chaos in an optomechanical beam", Nature Communications, 8, 14965 (2017)
3. M. F. Colombano, G. Arregui, N. E Capuj, A. Pitanti, J. Maire, A. Griol, B. Garrido, A. Martínez, C. M. Sotomayor-Torres, D. Navarro-Urrios, "Synchronization of Optomechanical Nanobeams by Mechanical Interaction", Physical Review Letters 123 (1), 017402 (2019)
4. G. Arregui, M. F. Colombano, J. Maire, A. Pitanti, N. E. Capuj, A. Griol, A. Martínez, C. M. Sotomayor -Torres, D. Navarro-Urrios, "Injection locking in an optomechanical coherent phonon source", Nanophotonics, 10(4): 1319–1327 (2021)
5. D. Navarro-Urrios, E. Kang, P. Xiao, M. F. Colombano, G. Arregui, B. Graczykowski, N. E. Capuj, M. Sledzinska, C. M. Sotomayor-Torres and G. Fytas, "Optomechanical Crystals for Spatial Sensing of Submicron Sized Particles", Scientific Reports, 11 (1), 7829, (2021).
6. M. F. Colombano, G. Arregui, F. Bonell, N. E. Capuj, E. Chavez-Angel, A. Pitanti, S.O. Valenzuela, C. M. Sotomayor-Torres, D. Navarro-Urrios, M. V. Costache, "Ferromagnetic resonance assisted optomechanical magnetometer", Physical Review Letters, 125, 147201 (2020)

P42
STUDY OF PHOTONIC CRYSTALS FOR MECHANICAL BIOSENSOR DEVELOPMENT

elenalopez@ub.edu

E. Lopez-Aymerich[1,2], M. Dimaki[3], S. Hernández[1,2], D. Navarro-Urrios[1,2], M. Moreno[1,2], F. Serras[4], W. E. Svendsen[3], A. Romano-Rodriguez[1,2]

[1] Institute of Nanoscience and Nanotechnology of the University of Barcelona (IN²UB), Universitat de Barcelona.
[2] Department of Electronics and Biomedical Engineering, Universitat de Barcelona.
[3] Department of Biotechnology and Biomedicine, Technical University of Denmark.
[4] Department of Genetics, Microbiology and Statistics and Institute of Biomedicine, Universitat de Barcelona.

The scope of this work is the development of a mechanical biosensor to detect stresses exerted by epithelia during their processes of growth or regeneration. This system will be based on a silicon nanopillar array, triangularly distributed, behaving as a photonic crystal, whose interpillar medium will be water.

Photonic crystals are periodic distributions of two dielectric materials that show the presence of a forbidden band for photons [1]. The behaviour of photons through the structure is driven by the dispersion diagram, or band diagram. If the difference in dielectric permittivity between the two materials is large enough, complete photonic band gaps can be opened, banning the light transmission for a specific light frequency range and polarisation in any direction of the structure. The position and width of these band apertures will be strongly driven by the geometry of the system, in our case the nanopillar's radius and the interpillar distance (or pitch). Taking advantage of these band gaps the introduction of linear and point defects allows the light propagation through the structure in a controlled manner [2].

In this work we present the design, fabrication and characterisation of these photonic crystals, with and without defects. The design has been carried out using simulation methods as the finite-difference time-domain (FDTD) [3] and eigenfrequency solvers. Using the gap-to-midgap ratio as a figure of merit to evaluate the efficiency of the structure, it has been found that for our system the best radius and pitch values are 100 and 500nm, respectively (Fig.1). Three dimensional simulations have shown that pillars with lengths up to 1µm still sustain the desired band gaps, as predicted in literature [4]. The introduction of defects has been simulated too. The results prove that the reduction of the radius of one line of pillars can rise modes from the bottom bands into the photonic band gap: the smaller the radius, the deeper the introduction of the mode. Point defects have proven their behaviour as resonance cavities in the system, giving the rise of sharp transmission peaks in the band gap (Fig.2).

The fabrication of these structures has been carried out in advanced clean room facilities. A sequence of different techniques starting by an electron beam lithography (EBL), followed by a metal deposition and lift-off and finalising with an anisotropic dry etch. The optimisation of this process flow has allowed the successful fabrication of the structures of almost perfect cylindrical pillars with radii from 100nm down to 60nm (Fig.3). It must be pointed out that silicon-on-insulator (SOI) substrates have been used during the nanofabrication. The use of SOI substrates ensure the correct vertical confinement of light thanks to the total internal reflection, preventing the light diffusion towards the substrate. In addition, in order to simplify the light coupling and decoupling into and out of the photonic crystal a grating structure and a waveguide have been nanofabricated.

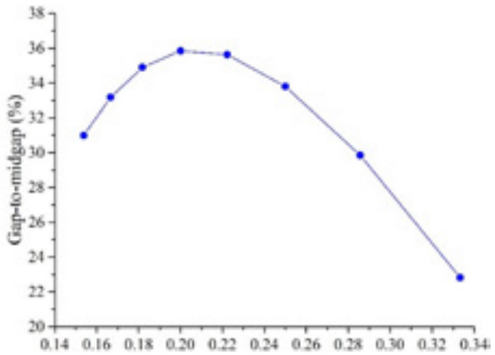

Figure 1. *Gap-to-midgap evolution depending on the radius-to-pitch ratio*

Figure 2. *Projected band diagram of the structure. A single mode in the photonic band gap can be observed (green line). The transmission spectrum of the structure can be seen as well in red*

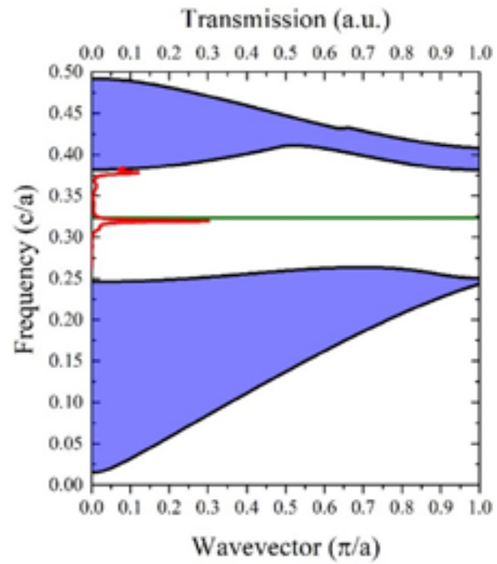

Figure 3. *Scanning electron microscope image of one of the photonic crystals nanofabricated. A waveguide and a cavity in it can be observed*

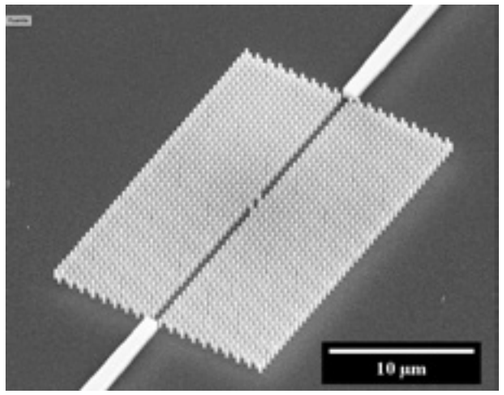

References

1. J.D. Joannopoulos, S.G. Johnson, J.N. Win and R.D. Meade (2017 November, 13). *Photonic crystals: Molding the Flow of Light* (2nd Edition). Available: http://ab-initio.mit.edu/book/photonic-crystals-book.pdf
2. S. G. Johnson, P. R. Villeneuve, S. Fan and J. D. Joannopoulos, "Linear waveguides in photonic-crystal slabs", *Physical Review B*, vol. 62 (12), pp.8212-8222, 2000
3. A. F. Oskooi, D. Roundy, M. Ibanescu, P. Bermel, J. D. Joannopoulos and S. G. Johnson, "MEEP: A flexible free-software package for electromagnetic simulations by the FDTD method", *Computer Physics Communications*, vol. 181, pp.687-792, 2010
4. S. G. Johnson, S. Fan, P. R. Villeneuve and J. D. Joannopoulos, "Guided modes in photonic crystal slabs", *Physical Review B*, vol. 60 (8), pp. 5751-5758, 1999

NanosMat

P43

ALLYL-PALLADIUM(II) HOMO- AND HETEROMETALLACYCLIC STRUCTURES CONTAINING CHIRAL DIPHOSPHANE LIGANDS

montse.ferrer@ub.edu

M. Ferrer[1,2], A. Gallen[1], M. Martínez[1,2], M. Rocamora[1], R. Puttreddy[3], K. Rissanen[3]

[1] Departament de Química Inorgànica i Orgànica, Secció de Química Inorgànica, Universitat de Barcelona, Martí i Franquès, 1-11, E-08028, Barcelona, Spain.

[2] Institut de Nanociència i Nanotecnologia (IN²UB). Universitat de Barcelona, 08028 Barcelona, Spain.

[3] Department of Chemistry, University of Jyväskylä, POB 35, 40014 Jyväskylä, Finland.

New chiral tetranuclear square-like homo- and heterometallamacrocycles containing allyl-palladium and either Pd(P–P)* or Pt(P–P)* optically pure moieties (P–P* = (+)-2,3-O-isopropylidene-2,3-dihydroxy-1,4-bis(diphenylphosphino)butane or (S,S)-DIOP and (1S,3S)-1,3-Dimethyl-1,3-propanediyl]bis(diphenylphosphine) or (S,S)-BDPP) have been obtained from the self-assembly of {Pd(η^3-2-Me-C_3H_4)}$^+$, {M(P–P)*}$^{2+}$ and 4-PPh_2py building blocks in a 1:1:2 molar ratio[1,2,3]. The prepared supramolecular assemblies [{Pd(η^3-2-Me-C_3H_4)}$_2$(4-PPh_2py)$_4${M(P–P)*}$_2$](CF_3SO_3)$_6$ (M = Pd, Pt) have been fully characterised by multinuclear NMR spectroscopy and ESI-MS spectrometry and display remarkable differences on its dynamic behaviour in solution that depend on the phosphane and the labitlity of M-py bonds. Furthermore, the structural features of the new metallamacrocyles have been unambiguously established by X-ray analysis. These species have been assayed as catalytic precursors in the palladium catalysed asymmetric allylic alkylation of rac-3-acetoxy-1,3-diphenyl-1-propene.

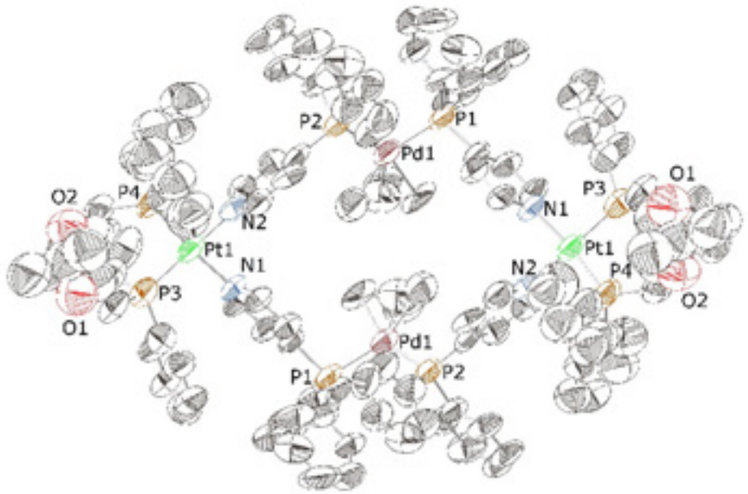

References

1. I. Angurell, M. Ferrer, A. Gutiérrez, M. Martinez, L. Rodríguez, O. Rossell and M. Engeser, *Chem.-Eur. J.*, 2010, **16**, 13960-13964
2. I. Angurell, M. Ferrer, A. Gutiérrez, M. Martínez, M. Rocamora, L. Rodríguez, O. Rossell, Y. Lorenz and M. Engeser, *Chem.-Eur. J.*, 2014, **20**, 14473-14487
3. M. Ferrer, A. Gallen, A. Gutiérrez, M. Martínez, E. Ruiz, Y. Lorenz and M. Engeser, *Chem.– Eur. J.*, 2020, **26**, 7847-7860

P44

PRUSSIANBLUEANALOG MOLECULAR Fe^{II}/Co^{III} CUBES, CONFINEMENT/ EXCHANGE OF WATER AND ALKALINE CATIONS IN WATER SOLUTION

manel.martinez@ub.edu

P. V. Bernhardt[1], M. Font-Bardia[2], M. A. Gonzálvez[1,3], A. Gallen[3], J. Jover[3], M. Ferrer[3], M. Martínez[3,*]

[1] School of Chemistry and Molecular Biosciences, University of Queensland, Brisbane, Queensland 4072, Australia.

[2] Unitat de Difracció de Raigs-X. Centre Científic i Tecnològic de la Universitat de Barcelona. Universitat de Barcelona and Departament de Cristal·lografia, Mineralogia i Dipòsits Minerals. Facultat de Geologia, 08028 Barcelona, Spain.

[3] Secció de Química Inorgànica, Departament de Química Inorgànica i Orgànica and Institute of Nanoscience and Nanotechnology (IN²UB), Universitat de Barcelona, 08028 Barcelona, Spain.

The lithium, sodium, potassium and rubidium salts of the [{$Co^{III}(Me_3$-Tacn)}$_4${$Fe^{II}(CN)_6$}$_4$]$^{4-}$ mixed valence cubic-cage structure have been prepared using a well-developed mechanistically directed self-assembly process described for 2D structures[1-9]. In all cases the preparations have been conducted by reaction of the {$Co^{III}(Me_3$-Tacn)} moiety, in the form of [$Co^{III}(Me_3$-Tacn)Cl_3], with the desired $[Fe^{II}(CN)_6]^{4-}$ salt in aqueous solution at pH 8-9 and 50°C.

The compounds have been characterised by multinuclear (^{1}H, ^{13}C, ^{23}Na, ^{7}Li) NMR spectroscopy and XRD for the sodium salt. The exchange of the internal encapsulated cations is seen to occur slowly and is found to be independent of the self-assembly processes. A comprehensive kinetico-mechanistic study indicates that the process is driven by the distinct solvation processes of the cations inside and outside the cage.

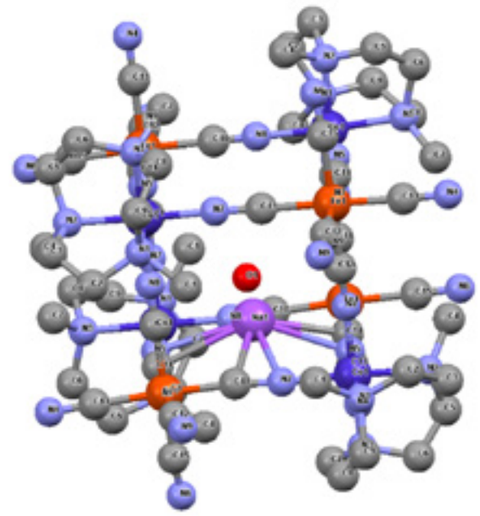

References

1. P. V. Bernhardt, F. Bozoglián, B. P. Macpherson and M. Martínez, *Coord. Chem. Rev*, 2005, 249, 1902-1916
2. P. V. Bernhardt, F. Bozoglián, G. González, M. Martínez, B. P. Macpherson and B. Sienra, *Inorg. Chem*, 2006, 45, 74-82
3. P. V. Bernhardt, B. P. Macpherson and M. Martínez, *Inorg. Chem*, 2000, 39, 5203-5208
4. P. V. Bernhardt and M. Martínez, *Inorg. Chem*, 1999, 38, 424-425
5. L. Alcázar, P. V. Bernhardt, M. Ferrer, M. Font-Bardia, A. Gallen, J. s. Jover, M. Martínez, J. Peters and T. J. Zerk, I*norganic Chemistry*, 2018, 57, 8465-8475
6. M. G. Basallote, P. V. Bernhardt, T. Calvet, C. E. Castillo, M. Font-Bardía, M. Martínez and C. Rodríguez, *Dalton Trans*, 2009, 9567-9577
7. P. V. Bernhardt, M. Martínez and C. Rodríguez, *Eur. J. Inorg. Chem*, 2010, 5621-5629
8. P. V. Bernhardt, M. Martínez and C. Rodríguez, *Inorg. Chem*, 2009, 48, 4787-4797
9. M. A. Gonzálvez, A. Gallen, M. Ferrer and M. Martínez, *Inorganic Chemistry*, 2020, 59, 1582-1587

P45
SYNTHESIS OF GOLD-SILVER CHALCOGENIDE HYBRID SYSTEMS THROUGH A NEW SYNTHETIC APPROACH

mengxi.lin@qi.ub.es

M. Lin[1,2], A. Figuerola[1,2], J. Blanco-Portals[2,3], Ll. Yedra Cardona[2,3], S. Estradé[2,3], F. Peiró[2,3]

[1] Departament de Química Inorgànica i Orgànica, Secció de Química Inorgànica, Universitat de Barcelona, Martí i Franquès 1-11, 08028 Barcelona, Spain.
[2] Institut de Nanociència i Nanotecnologia (IN²UB).
[3] Laboratory of Electron Nanoscopies (LENS)-MIND/IN²UB, Departament d'Electrònica, Universitat de Barcelona, Martí i Franquès 1-11, 08028 Barcelona, Spain.

Developing alternative synthetic route for achieving nanoscale heterostructures can offer more structural and compositional diversities in the system, rather than those obtained by using traditional bottom-up approaches. In this work, a new synthetic route was developed for the synthesis of both Au-Ag_2Se and Au-Ag_2S hybrid systems by directly mixing Au and silver chalcogenides nanoparticles, instead of adding surfactant -Au(III) complexes[1,2] into Ag_2Se and Ag_2S nanostructured semiconductors. The results showed that the Au has partially fused with initial Ag_2Se and Ag_2S, resulting in the formation of two ternary interfaces ($AuAg_3Se_2$ and $AuAg_3S_2$) in between the metallic domain of Au and the initial Ag_2Se and Ag_2S, respectively. Their structures, chemical compositions and optical properties have been studied by electron microscopic techniques, X-ray diffraction and UV/vis spectroscopy.

References
1. *Chem. Mater.* **2016**, 28, 7017−7028
2. *Chem. Mater.* **2018**, 30, 6893−6902

P46
PIANO-STOOL RUTHENIUM(II)-ARENE COMPLEXES WITH 1-PYRENYLPHOSPHANES PRESENTING A DELAYED CYTOTOXIC ACTIVITY

arnald.grabulosa@ub.edu

A. Grabulosa[1,2] L. Rafols[1], D. Josa[1,2], P. Gamez[1,2,3]

[1] Departament de Química Inorgànica i Orgànica, Secció de Química Inorgànica, Universitat de Barcelona, 08028, Barcelona, Spain.
[2] Institut de Nanociència i Nanotecnologia (IN²UB), 08028 Barcelona, Spain.
[3] Institut Català de Recerca i Estudis Avançats (ICREA), 08010, Barcelona, Spain.

The remarkable chemotherapeutic properties of cisplatin, discovered long ago, were the starting point of an intense research field devoted to find more efficient and less toxic drugs based on other transition metals. In this aspect, ruthenium is one of the most studied elements.

Two decades ago, Dyson described that Ru(II) complexes with η^6-coordinated arenes bearing a PTA phosphane showed a potent antimetastatic effect, with RAPTA-C being the most well-known example[1]. Inspired by this research, a few years ago we uncovered a family of Ru(II)-arene complexes with 1-pyrenylphosphane ligands[2a]. These complexes are very cytotoxic against several tumor cell lines and clear Structure Activity Relationships (SARs) were elucidated. More recently, the synthesis of other 1-pyrenylphosphanes and their derived complexes has been expanded[2b] but the active species have remained elusive.

In this contribution we present details on the synthesis of ligands and several types of Ru(II)-arene complexes, including tethered and cyclometallated systems. In addition, the evolution of the complexes in solution, forming the active species, is discussed.

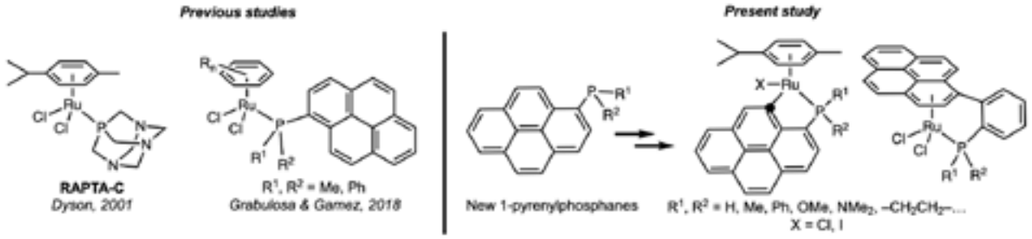

References
1. C. S. Allardyce, P. J. Dyson, D. J. Ellis and S. L. Heath, *Chem. Commun.*, **2001**, 1396
2. (a) R. F. Brissos, P. Clavero, A. Gallen, A. Grabulosa, L. A. Barrios Moreno, A. B. Caballero, L. Korrodi-Gregório, R. Pérez-Tomás, G. Muller, V. Soto-Cerrato and P. Gamez, *Inorg. Chem.*, **2018**, 57, 14786
(b) L. Rafols, S. Torrente, D. Aguilà, V. Soto-Cerrato, R. Pérez-Tomás, P. Gamez and A. Grabulosa, *Organometallics*, **2020**, 39, 2959
(c) L. Rafols, D. Josa, D. Aguilà, L. A. Barrios Moreno, O. Roubeau, J. Cirera, V. Soto-Cerrato, R. Pérez-Tomás, M. Martínez, A. Grabulosa and P. Gamez, *Inorg. Chem.*, **2021**, 60, 7974

P47
CYCLOMETALLATED RU(II) AND OS(II) COMPLEXES WITH A BULKY PHOSPHANE AS ANTITUMORAL AGENTS

dana.josa@ub.edu

D. Josa[1,2], P. Gamez[1,2,3], A. Grabulosa[1,2]

[1] Departament de Química Inorgànica i Orgànica, Secció de Química Inorgànica, Universitat de Barcelona, 08028, Barcelona, Spain.
[2] Institut de Nanociència i Nanotecnologia (IN²UB), 08028 Barcelona, Spain.
[3] Institut Català de Recerca i Estudis Avançats (ICREA), 08010, Barcelona, Spain.

More than 50 years after the discovery of the antitumoral activity of cisplatin, the scrutiny of complexes and organometallic compounds of transition metals as antitumor agents continues at fast pace. Ruthenium[1a] and more recently osmium[1b] have emerged as two of the most promising metals because they often show reduced general toxicity compared to platinum, increased selectivity for cancerous tissues and potential antimetastatic activity, thanks to a variety of action mechanisms they present.

At the beginning of the present century, Dyson and coworkers[1c] uncovered that a family of Ru(II) complexes with η^6-coordinated arenes and the PTA phosphane was particularly active, RAPTA-C being the most well-known member. These results inspired our own research in the area and recently we described a family of Ru(II)-arene complexes with a 1-pyrenylphosphane ligand[2a]. These complexes were very cytotoxic against several tumor cell lines and clear Structure Activity Relationships (SARs) were elucidated.

In this contribution we disclose a novel family of cyclometallated ruthenium (**A**) and osmium (**B**) compounds with 1-pyrenylphosphanes[2b]. Synthesis and biological studies of this complexes against tumor cells are presented.

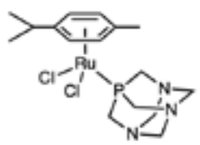

RAPTA-C
Dyson, 2001

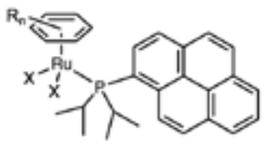

Grabulosa & Gamez, 2021

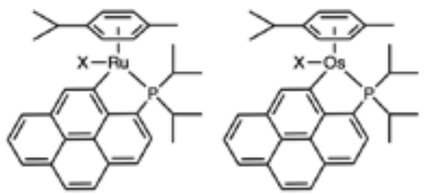

A **B**

References

1. (a) A. Bergamo and G. Sava, *Dalton Trans.*, **2011**, 40, 7817
   (b) P. Zhang and H. Huang, *Dalton Trans.*, **2018**, 47, 14841
   (c) C. S. Allardyce, P. J. Dyson, D. J. Ellis and S. L. Heath, *Chem. Commun.*, **2001**, 1396
2. (a) R. F. Brissos, P. Clavero, A. Gallen, A. Grabulosa, L. A. Barrios Moreno, A. B. Caballero, L. Korrodi-Gregório, R. Pérez-Tomás, G. Muller, V. Soto-Cerrato and P. Gamez, *Inorg. Chem.*, 2018, 57, 14786
   (b) L. Rafols, D. Josa, D. Aguilà, L. A. Barrios Moreno, O. Roubeau, J. Cirera, V. Soto-Cerrato, R. Pérez-Tomás, M. Martínez, A. Grabulosa and P. Gamez, *Inorg. Chem.*, **2021**, 60, 7974

P48
DIRECT GROWTH OF CARBON NANOTUBES ON STAINLESS STEEL BY PLASMA ENHANCED CHEMICAL VAPOUR DEPOSITION

iralshaikh@ub.edu

I. Alshaikh[1,2], R. Amade-Rovira[1,2], E. Bertran-Serra[1,2]

[1] ENPHOCAMAT (FEMAN) group, Department of Applied Physics, Universitat de Barcelona, Spain.
[2] Institute of Nanoscience and Nanotechnology (IN²UB), Universitat de Barcelona.

Direct growth of vertically aligned carbon nanotubes (VACNTs) on a conducting metal substrate is becoming a necessary for energy storage applications, which has been a challenge for a long time. Most of the previous studies investigated the growth of carbon nanotubes (CNTs) over stainless steel (SS) using a diffusion barrier to prevent the diffusion of the catalyst inside the substrate. Some late studies worked on the growth of CNTs directly on different alloys of SS substrate using the Fe, Ni, and Cr inside the SS as a catalyst after the reduction process at high temperature to remove the oxides and to keep chemically stable surface where the surface reduction and CNTs growth were done separately.

In this study, SS-310S0 alloy of 100 μm thickness was used as a substrate to directly grow the CNTs by radiofrequency plasma enhanced chemical vapour deposition (RF-PECVD) using the catalyst particles of the SS-310S0 alloy itself. The conditions were optimized to start the PECVD process directly after the reduction in a continuous process. For reduction, 50 W RF-plasma of H2 at 680 °C weas applied. Different annealing ramp times and PECVD temperatures were used to be optimized using Box-Wilson experimental design (Fig. 1). In this experimental design, we have studied the length, diameter and density of CNTs on the SS-310S0 substrate where the goal is to obtain long, small diameter and high density CNTs. The optimum conditions we obtained (Fig. 2), in the range of the selected parameters, were at annealing ramp time of 1040 s and PECVD temperature of 700 °C when we fix all the other parameters.

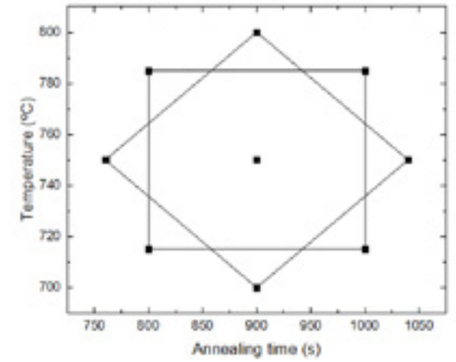

Figure 1. *Box-Wilson experimental design to optimize the CNTs growth conditions over SS 310S0 alloy*

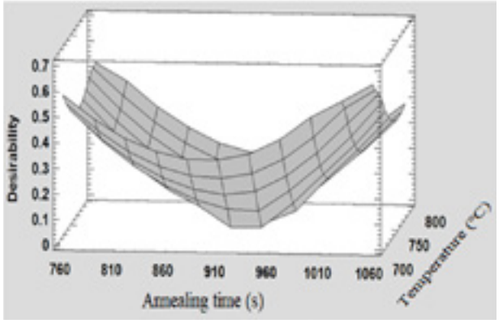

Figure 2. *The conditions desirability for the growth of CNTs*

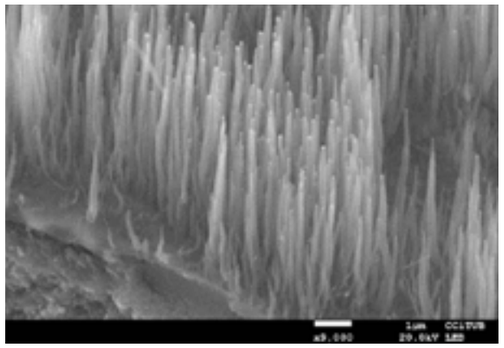

Figure 3. *SEM image of the obtained CNTs obtained by the desired conditions*

References

1. Hashempour, *Carbon*, 63 (2013), 330-347
2. Sun, *Chemical Papers*, 73 (2019), 2143-2151
3. Thapa, *Diamond & Related Materials*, 90 (2018), 144-153
4. Masarapu, *Langmuir*, 23 (2007), 9046-9049
5. Lobo, *Nanomaterials*, 11 (2021), 143

NanoEnergy

P49
TI-CONTAINING HYBRID MESOPOROUS ORGANOSILICAS AS PHOTOCATALYSTS FOR H_2 PRODUCTION FROM ETHANOL

pilar.piscina@qi.ub.es

Y. Wang[1], N. Homs[1,2], P. Ramírez de la Piscina[2]

[1] Departament de Química Inorgànica i Orgànica, secció de Química Inorgànica & Institut de Nanociència i Nanotecnologia (IN²UB), Universitat de Barcelona, Martí i Franquès 1, 08028 Barcelona, Spain.

[2] Catalonia Institute for Energy Research (IREC), Jardins de les Dones de Negre 1, 08930 Barcelona, Spain.

Nowadays there is a severe concern regarding climate change and the use of fossil fuels in the energy scenario. This has attracted considerable interest in both the use of renewable sources, including biomass, and the development of new energy vectors, such as H_2. In this context, the photocatalytic production of hydrogen from biomass-derived alcohols is considered a highly desirable source for renewable H_2 production[1]. Research for efficient photocatalytic systems is a hot topic under continuous progress; diverse semiconductor materials, mainly those based on TiO_2, have been widely studied as photocatalysts for hydrogen production[2].

The high surface area, uniform porous array and long-range structure of ordered mesoporous materials make them interesting candidates to be used as photocatalysts. In this work, a series of complex organic-inorganic mesoporous materials were successfully synthesized by a microwave-assisted method that allowed the preparation of periodic mesoporous organosilicas (PMOs) with Ti (IV) forming part of the structure (Ti-PMO). Ti-PMOs showed a better photocatalytic behavior than PMO and this is related with the presence of tetrahedral Ti(IV) in the PMOs network. Ti-PMOs displayed a lower barrier for the electron transfer and a more efficient charge separation than PMO. The highest H2 production was obtained with Ti20-PMO photocatalyst; after 4 hours of irradiation, 2042 μmol H_2 g_{cat}^{-1} were obtained, which was about 20 times higher than that obtained with a reference commercial TiO_2 (P25).

References

1. A. C. Sola, P. Ramírez de la Piscina, N. Homs, *Catal*. Today, 341 (2020) 13-20
2. 7-N.S. Ibrahim, W.L. Leaw, D. Mohamad, S.H. Aliasc, H. Nur, *Int. J. Hydrogen Energy*, 45 (2020) 28553-28565

P50
ALUMINA REINFORCED PHOTOPOLYMER FOR VAT POLYMERIZATION ADDITIVE MANUFACTURING

xuriguera@ub.edu

P. Barcelona[1], J. A. Padilla[1], X. Ramis[2], J. Bonada[3], E. Xuriguera[1]

[1] IN²UB – Material Science and Physical Chemistry, Universitat de Barcelona, Martí i Franquès 1, 08028 Barcelona, Spain.

[2] Thermodynamics Laboratory, ETSEIB, Universitat Politècnica de Catalunya, Avda. Diagonal 647, 08028 Barcelona, Spain.

[3] Strength of Materials and Structural Engineering Department, Universitat Politècnica de Catalunya, Avda. Diagonal 647, 08028 Barcelona, Spain.

In recent years, many materials have been developed and optimized for additive manufacturing. The range of commercial materials for additive manufacturing technologies is growing quickly. Despite this, most of the polymeric materials available have limited mechanical properties, which means that they cannot be widely used for functional parts[1]. Materials of vat photopolymerization based techniques is a common example. In these technologies, a liquid material sensitive to a light source is cured layer by layer to form the three-dimensional object.

In order to improve the mechanical properties of the polymeric material, alumina micro and nanoparticles were added[2]. To obtain the most stable and homogeneous material, a complete characterization of the rheological behaviour of the reinforced resin has been carried out, as well as its photoreactive behaviour. The chemical stability over time has been determined with calorimetric tests, as well as the stability of the suspension with sedimentation and rheological tests. Furthermore, to improve the mechanical properties and homogeneity of the printed material, a dual acrylic / epoxy resin was used as base material. The polymerization of the acrylic part is produced by the radiation of the light from the printing system, and the epoxy part cures by a post-processing thermal activation[3].

The work was financially supported by Catalan Government with the project BASE 3D (001-P-001646).

References

1. S. C. Ligon, R. Liska, J. Stampfl, M. Gurr, and R.f Mülhaupt. Polymers for 3D Printing and Customized Additive Manufacturing, *Chemical Reviews*, **2017**, 117 (15), 10212-10290
2. J. Bonada, E. Xuriguera, A. Muguruza, J. Gonçalves, P. Barcelona, J.M. Pons, J. Minguella, R. Uceda. Reinforced photocurable materials for an Additive Manufacturing process based on Mask Image Projection, *Procedia Manufacturing*, **2019**, 41, pp. 531–538
3. O. Konuray, A. Altet, J. Bonada, A. Tercjak, X. Fernández-Francos, X. Ramis. Epoxy Doped, Nano-scale Phase-separated Poly-Acrylates with Potential in 3D Printing, *Macromolecular Materials and Engineering*, **2021**, 306 (3), 2000558

P51
3D PRINTING OF ALUMINA BY DIRECT INK WRITING FROM INORGANIC SALT PRECURSORS

japadilla@ub.edu

J. A. Padilla[1], P. Barcelona[1], M. Martínez[1], M. Segarra[1], E. Xuriguera[1]

[1] Materials Science and Physical Chemistry Department, Universitat de Barcelona, C/ Martí i Franquès 1-11, 08028 Barcelona, Spain.

The use of additive manufacturing (AM) techniques is being increasingly implemented due to the possibility of manufacturing parts with high geometric complexity, which cannot be manufactured by traditional processes. Direct Ink Writing (DIW) is the AM technique that has been used in this work. It is a versatile technology that allows the printing of 3D objects layer by layer by extrusion of ink[1]. The main properties of the inks used in DIW are good homogeneity, the absence of bubbles, and shear thinning behaviour.

Usually, the printing of ceramics by DIW requires inks with a high solid load of ceramics, commonly above 40 vol%. The high content of ceramic powder entails the use of additives that prevent agglomeration and/or sedimentation, ensuring the homogeneity and stability of the suspension, with a proper viscosity and workability[2].

An alternative strategy to ceramic powder in the preparation of printing inks is the use of ceramic precursors. In the case of ceramics such as SiO_2, SiC, Si_3N_4, SiCN, etc.,[3] the precursors are based on polymeric compounds such as polysiloxanes. One of the advantages of using ceramic precursors is the aim of obtaining small size pieces with micro details and/or with high porosity.

The present work shows the preparation of inks for DIW technology based on ceramic precursors, specifically inorganic aluminum salts. $AlCl_3$-$6H_2O$ and $AlCl_3$ are the two inorganic salts studied as a precursor to obtaining Al_2O_3 ceramic pieces. Inks are based water and the gelling agent to obtain the proper rheological behaviour is Pluronic F-127.

A complete rheological characterization of the inks has been carried out to ensure printability for DIW. TGA/DTA experiments were performed to study the thermal decomposition and determine the parameters for the thermal treatments need it to obtain alumina after the printing. The evolution of the crystalline phases was studied by XRD and IR, and microstructural characterization by SEM.

References

1. Z. Chen *et al.*, "3D printing of ceramics: A review," *J. Eur. Ceram. Soc.*, vol. 39, no. 4, pp. 661–687, 2019
2. E. Feilden, D. Glymond, E. Saiz, and L. Vandeperre, "High temperature strength of an ultra high temperature ceramic produced by additive manufacturing," *Ceram. Int.*, vol. 45, no. 15, pp. 18210–18214, 2019
3. A. Zocca *et al.*, "Direct Ink Writing of a Preceramic Polymer and Fillers to Produce Hardystonite ($Ca_2ZnSi_2O_7$) Bioceramic Scaffolds," *J. Am. Ceram. Soc.*, vol. 99, no. 6, pp. 1960–1967, 2016

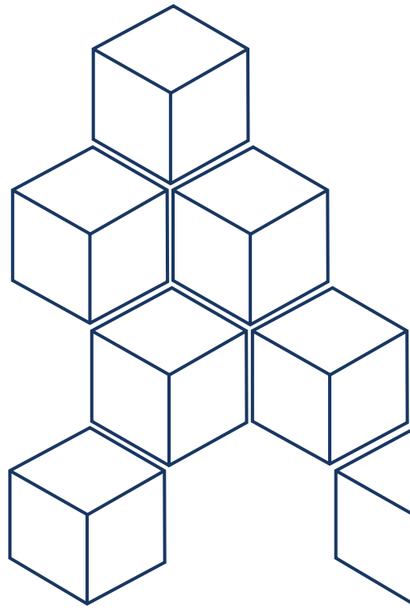

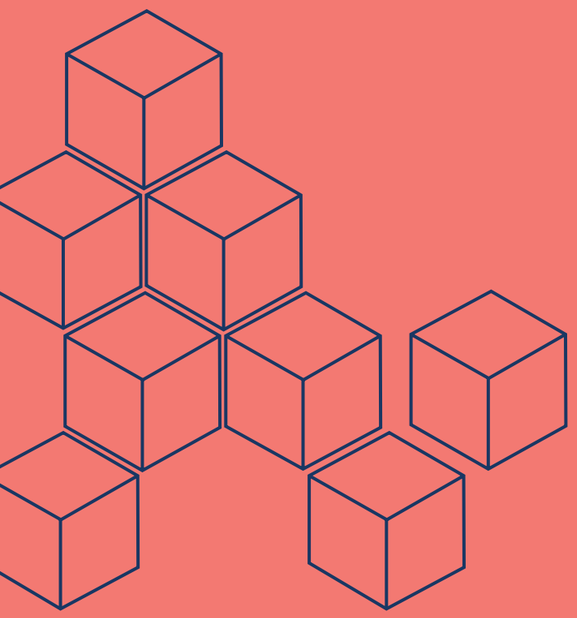

AUTHOR INDEX

AUTHOR INDEX


Institut de Nanociència
i Nanotecnologia
UNIVERSITAT DE
BARCELONA

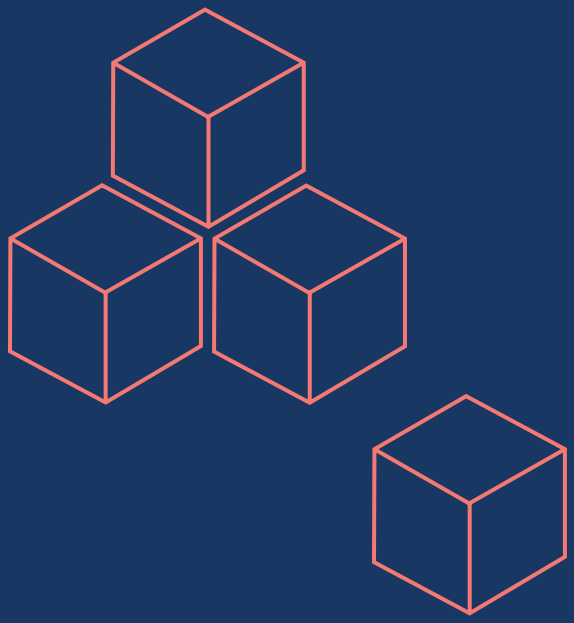

UNIVERSITAT DE BARCELONA
in²ub | Institut de Nanociència i Nanotecnologia

email: in2ub@ub.edu
www.ub.edu/in2ub

Institut de Nanociència i Nanotecnologia

UNIVERSITAT DE BARCELONA